1988-12

Performance of radar receivers in the presence of noise and intentional interference

Mavropoulos, Panagiotis G.

Monterey, California. Naval Postgraduate School

NAVAL POSTGRADUATE SCHOOL
Monterey, California

THESIS

PERFORMANCE OF RADAR RECEIVERS IN THE PRESENCE OF NOISE AND INTENTIONAL INTERFERENCE.

by

Panagiotis G. Mavropoulos

December 1988

Thesis Advisor Daniel C. Bukofzer

REPORT DOCUMENTATION PAGE

1a Report Security Classification Unclassified		1b Restrictive Markings	
2a Security Classification Authority		3 Distribution Availability of Report	
2b Declassification Downgrading Schedule		Approved for public release; distribution is unlimited.	
4 Performing Organization Report Number(s)		5 Monitoring Organization Report Number(s)	
6a Name of Performing Organization Naval Postgraduate School	6b Office Symbol *(if applicable)* 32	7a Name of Monitoring Organization Naval Postgraduate School	
6c Address *(city, state, and ZIP code)* Monterey, CA 93943-5000		7b Address *(city, state, and ZIP code)* Monterey, CA 93943-5000	
8a Name of Funding Sponsoring Organization	8b Office Symbol *(if applicable)*	9 Procurement Instrument Identification Number	
8c Address *(city, state, and ZIP code)*		10 Source of Funding Numbers	
		Program Element No / Project No / Task No / Work Unit Accession No	

11 Title *(include security classification)*
PERFORMANCE OF RADAR RECEIVERS IN THE PRESENCE OF NOISE AND INTENTIONAL INTERFERENCE.

12 Personal Author(s) Panagiotis G. Mavropoulos

13a Type of Report	13b Time Covered	14 Date of Report *(year, month, day)*	15 Page Count
Master's Thesis	From To	December 1988	117

16 Supplementary Notation The views expressed in this thesis are those of the author and do not reflect the official policy or position of the Department of Defense or the U.S. Government.

17 Cosati Codes			18 Subject Terms *(continue on reverse if necessary and identify by block number)*
Field	Group	Subgroup	Radar receivers' performance

19 Abstract *(continue on reverse if necessary and identify by block number)*

This thesis is devoted to analyzing the problem of masking a reflected radar signal, in order to degrade the radar receiver's performance. This is to be accomplished by appropriately choosing the Power Spectral Density (PSD) of a power constrained colored noise interference to be generated either by the target itself or by pre-positioned "friendly" noise makers. The goal in either case is to generate interference signals that result in decreased receiver probability of detection, P_D, for a given receiver probability of false alarm, P_F. Efforts to identify appropriate PSD's of the power constrained interference were carried out by evaluating the receivers' P_D as a function of P_F for two specific target models. The performance results for the various receivers investigated demonstrate that the noise interference generated by the noise makers can achieve significant levels of degradation, while the target generated noise interference tends to improve rather than degrade the radar receiver's performance. In all cases considered, the sinc squared shaped noise interference PSD is more effective at degrading the receiver performance than any other kind of PSD analyzed.

20 Distribution Availability of Abstract	21 Abstract Security Classification	
☒ unclassified unlimited ☐ same as report ☐ DTIC users	Unclassified	
22a Name of Responsible Individual Daniel C. Bukofzer	22b Telephone *(include Area code)* (408) 646-2859	22c Office Symbol 62Bh

Approved for public release; distribution is unlimited.

Performance of RADAR Receivers in the Presence of Noise and Intentional Interference.

by

Panagiotis G. Mavropoulos
Captain, Hellenic Army
B.S., Hellenic Army Academy, 1978

Submitted in partial fulfillment of the
requirements for the degrees of

MASTER OF SCIENCE IN ELECTRICAL ENGINEERING
and
ELECTRICAL ENGINEER

from the

NAVAL POSTGRADUATE SCHOOL
December 1988

ABSTRACT

This thesis is devoted to analyzing the problem of masking a reflected radar signal, in order to degrade the radar receiver's performance. This is to be accomplished by appropriately choosing the Power Spectral Density (PSD) of a power constrained colored noise interference to be generated either by the target itself or by pre-positioned "friendly" noise makers. The goal in either case is to generate interference signals that result in decreased receiver probability of detection, P_D, for a given receiver probability of false alarm, P_F. Efforts to identify appropriate PSD's of the power constrained interference were carried out by evaluating the receivers' P_D as a function of P_F for two specific target models. The performance results for the various receivers investigated demonstrate that the noise interference generated by the noise makers can achieve significant levels of degradation, while the target generated noise interference tends to improve rather than degrade the radar receiver's performance. In all cases considered, the sinc squared shaped noise interference PSD is more effective at degrading the receiver performance than any other kind of PSD analyzed.

TABLE OF CONTENTS

LIST OF TABLES

LIST OF FIGURES

I. INTRODUCTION.

Two of the interesting practical problems dealing with the degradation of radar receivers used for detecting targets in the presence of additive noise interference are investigated in this thesis and described below in greater detail.

The first problem is pictorially described in Figure 1 on page 2. A target, recognizing that it is being illuminated by a radar, generates and transmits a colored noise interference signal, which is received in conjuction with the radar echo and the background noise as well as the thermal noise interference by the radar receiver. Henceforth this problem will be referred to as "Problem 1". This would be done in order to help the target hide its presence by effectively degrading the receiver performance, namely by decreasing the receiver's probability of detection (P_D). The target clearly cannot produce a noise interference with unbounded total power. Thus, the choice of noise interference that minimizes the radar receiver's P_D , subject to a total interference power constraint, is an important practical problem.

The second problem is pictorially shown in Figure 2 on page 3. Assuming that the area where the target is likely to be detected by a radar has been penetrated by near stationary "friendly" noise makers just prior to the target entering the zone of radar detection, the basic question becomes, what interference produced by the friendly noise makers will most effectively minimize the receiver's P_D, subject again to a total power constraint. Therefore, on the basis that the friendly noise makers do not have the ability to produce noise interference with unbounded total power, the choice of noise interference subject to a total power constraint that maximally degrades the radar receiver's performance in order to mask the presence of the target is a practical problem. Henceforth, the problem described above and shown in Figure 2 on page 3 will be referred to as "Problem 2".

It is clear that it would be difficult for the target or the noise makers to decide about the kind of noise interference that must be generated in order to best mask the target without any prior knowledge of the type of receiver that is being used for radar detection. In any case, it must be assumed that the receiver has been optimized for its target detection function under the assumption of no masking signal present. While not completely realistic, it is also of interest to analyze these two problems under the assumption of complete knowledge on the part of the radar receiver about the masking

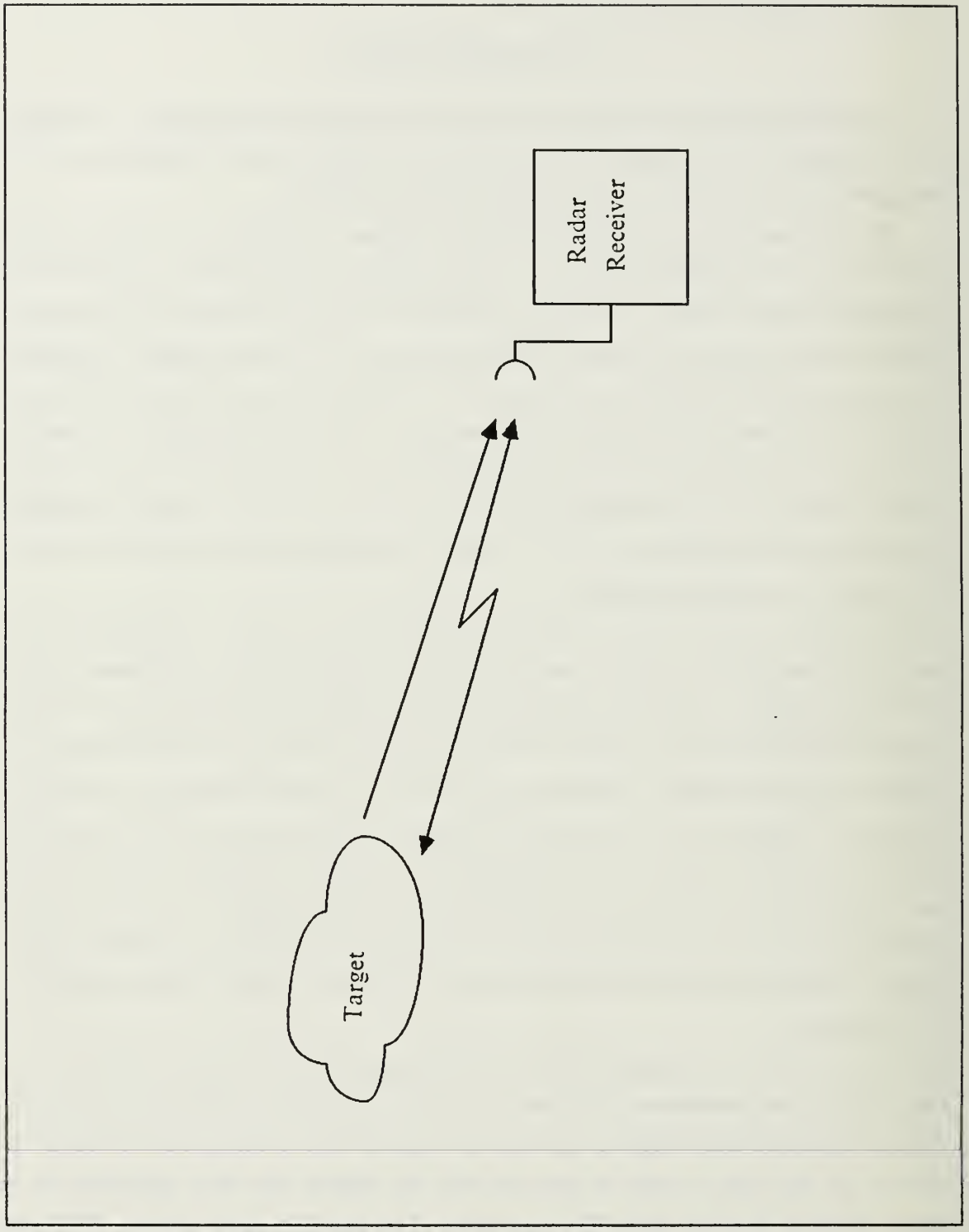

Figure 1. Target Transmits Noise Interference.

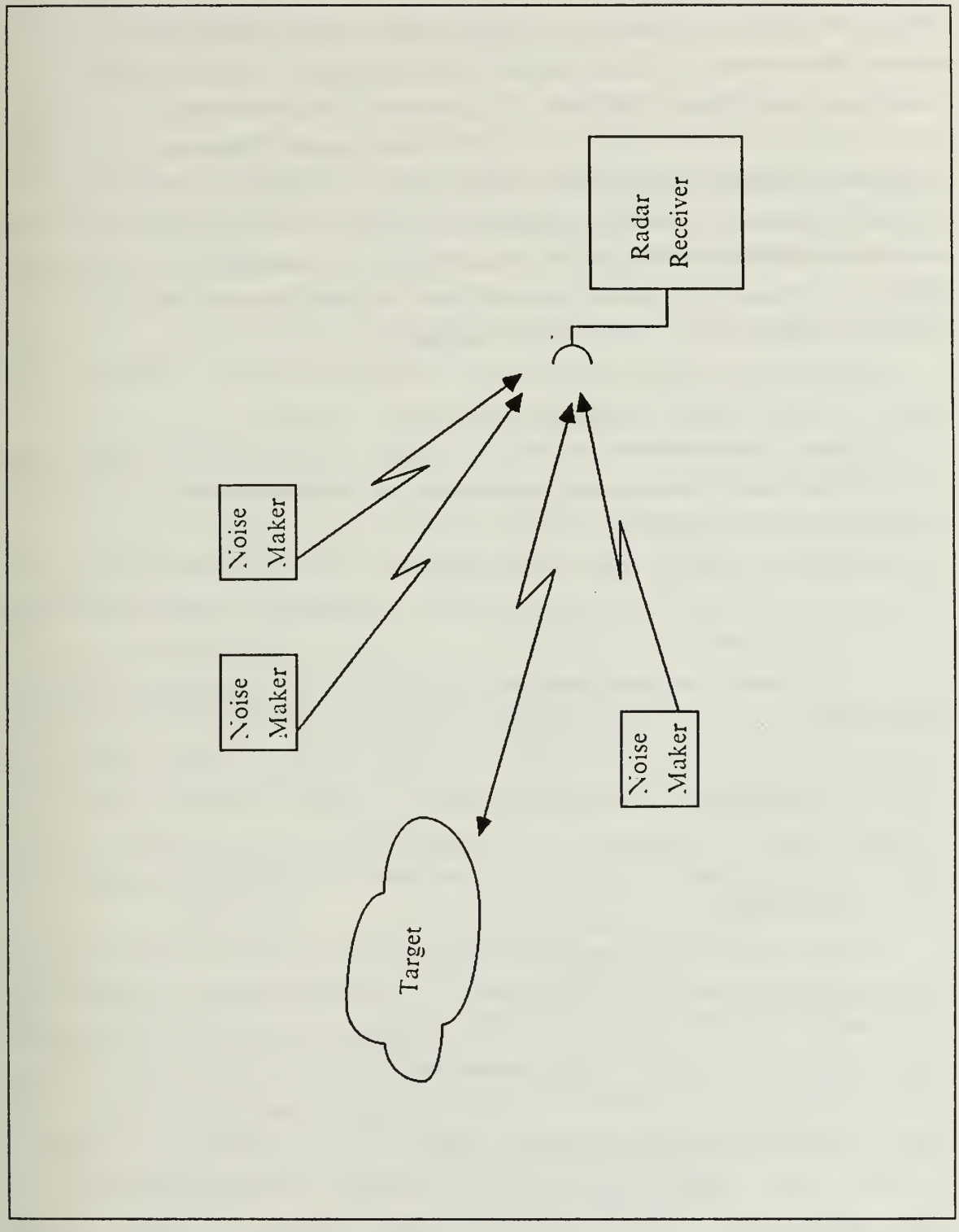

Figure 2. Noise Makers Transmit Noise Interference.

(interference) signal being produced. The results would then yield a minimum level of effectiveness that can be expected to be gained by using masking (interference) techniques. The case in which knowledge exists about the type of receiver implemented is the only one considered in this thesis. Yet the results have demonstrated that there are situations when the target-produced noise interference (i.e., problem 1), instead of hiding its presence by degrading the receiver performance (i.e., reducing P_D), actually improves it. The transmission of the noise interference by the target itself is not effective, and can be rather harmful in essentially all the cases investigated. In constrast, the transmission of noise interference by noise makers, in all cases analyzed, proved to be effective and to cause significant receiver performance degradation.

The analysis and results associated with investigation of the above described problems are presented in the five subsequent chapters.

In Chapter 2, the basic information that already exists in the literature pertaining to the problem under discussion here is presented, along with a mathematical description of the problem to be considered in chapters 3 and 4.

In Chapter 3, a simple target model, which from now on will be referred to as "Target Model A", is used to investigate the effect of various kinds of noise interference generated by the target (i.e., Problem 1). For this particular target model, the situation in which noise makers generate interference (i.e., Problem 2) has been investigated by Bukofzer [Ref. 1], so that pertinent results are presented in this chapter for completeness sake. However, the case where the noise is transmitted by the target when realizing that it has been illuminated by a radar (corresponding to Problem 1 described above) is investigated in detail. The performance of the receiver, which is optimum under conditions to be stated in the sequel, is obtained and presented in terms of the Receiver Operating Characteristics (ROC's).

Chapter 4 is devoted to analyzing the basic problems previously described, assuming a more sophisticated target model is applicable. The so-called Slowly Fluctuating Point Target model, where the reflected radar signal is modeled as a complex Gaussian random process whose envelope is a Rayleigh random variable, which henceforth will be referred to as "Target Model B", is utilized to investigate two specific cases. The first such case involves a receiver designed to be optimum for detecting targets observed in the presence of Additive White Gaussian Noise (AWGN) interference. The performance of this receiver, operating under the scenarios shown in Figure 1 on page 2 and Figure 2 on page 3, is investigated and evaluated in terms of the ROC's under various interference conditions generated either by the target itself, or the prepositioned noise makers. The second

case considered assumes that the receiver has prior knowledge of the kind of noise interference produced by the target or noise makers and therefore is designed to operate optimally in the presence of such noise interference. For such a receiver its performance under the scenarios shown in Figure 1 on page 2 and Figure 2 on page 3 is investigated and results are presented in terms of the ROC's.

In Chapter 5, based on the results presented as mathematical expressions of P_D as a function of P_F in Chapters 3 and 4, the performance of the receiver analyzed in each case is evaluated using numerical methods and various signal and noise power parameters. The effect of the masking signal on the receiver's detection probability P_D is displayed for representative values of the Signal-to-Noise Ratio and the Jamming-to-Signal Ratio.

A summary of the results obtained and the conclusions that can be drawn from these are presented in Chapter 6. Additionally some of the mathematical manipulations that are necessary to the derivation of certain results are presented in the appendices.

A descriptive summary of the problems investigated and described above, is shown in Table 1 below where ACGN and PSD stand for additive colored Gaussian noise and power spectral density, respectively.

Table 1. SUMMARY OF PROBLEMS INVESTIGATED

		TARGET MODELS	
		A	B
PROBLEMS	#1	Quadrature Correlator (Analyzed)	I. Correlator Receiver Optimum for AWGN Interference II. Correlator Receiver Optimum for ACGN Interference a.Bandlimited Constant Amplitude PSD b.Sinc Squared Shaped PSD c.Butterworth Shaped PSD d.Triangular Shaped PSD
	#2	Analyzed in [Ref.2]	I. Correlator Receiver Optimum for AWGN Interference Optimum specrum II. Correlator Receiver Optimum for ACGN Interference a.Bandlimited Constant Amplitude PSD b.Sinc Squared Shaped PSD c.Butterworth Shaped PSD d.Triangular Shaped PSD

II. MATHEMATICAL PRELIMINARIES

A. GENERAL

A conventional pulsed radar transmits a signal which consists of a sequence of pulses. If a target is present, part of the transmitted signal is reflected. Depending on the type of target model assumed, some of the characteristics, such as amplitude, frequency, or phase of the reflected signal will change with respect to those of the transmitted signal.

The basic radar detection problem involves examining the reflected signal in the presence of noise and other forms of interference, and deciding whether or not a target is present . The source of uncertainty inherent in the problem, stems from the fact that the radar receiver does not know a-priori whether or not a target is present, and from the fact that depending on the type of target present, reflected signal parameters such as amplitude. phase, and frequency, may not be known to the receiver either. The simplest possible radar detection problem involves a target modeled as producing a completely known signal return. received in the presence of additive white Gaussian noise (AWGN) interference.

B. TARGET MODEL A.

The first simple target model treats the reflected signal as a sinusoid of known amplitude and frequency, but having a random phase. This radar detection problem has been addressed extensively in the literature under various assumptions of additive noise interference.

1. Additive White Gaussian Noise (AWGN) Under Both Hypotheses.

Van Trees [Ref. 3] provides an extensive intoduction to the principles of radar detection, treated as a hypothesis testing problem. Defining H_1 as the hypothesis that the target is present and H_0 as the hypothesis that the target is absent, the above described problem is mathematically expressed as

$$\begin{aligned} H_1 &: r(t) = \sqrt{2E_r} f(t) \cos[\omega_c t + \phi(t) + \theta] + w(t) \qquad 0 \le t \le T \\ H_0 &: r(t) = w(t) \end{aligned} \tag{2.1}$$

where E_r is the actual received signal energy, θ is a random variable (r.v.) uniformly distributed over $[0, 2\pi]$, and $w(t)$ is a sample function of a zero mean white Gaussian noise process with power spectral density (PSD) $S_w(\omega) = N_0/2$. The amplitude and phase modulations, $f(t)$ and $\phi(t)$, respectively, are deterministic and $f(t)$ is assumed to satisfy

$$\int_0^T |f(t)|^2 \, dt = 1 \tag{2.2}$$

It is demonstrated in Van Trees [Ref. 3] that decisions about two hypotheses are optimally given by the threshold test

$$L \underset{H_0}{\overset{H_1}{\gtrless}} \gamma \tag{2.3}$$

where

$$L \equiv L_c^2 + L_s^2 \tag{2.4}$$

and

$$L_c = \int_0^T \sqrt{2}\, r(t) f(t) \cos[\omega_c t + \phi(t)] \, dt \tag{2.5}$$

$$L_s = \int_0^T \sqrt{2}\, r(t) f(t) \sin[\omega_c t + \phi(t)] \, dt \tag{2.6}$$

The threshold of the test, denoted by γ in Equation 2.3, is normally set by specifying an operating value for P_F, the probability of false alarm.

There are two kinds of errors which can be made. If the receiver decides a signal (i.e., target) is present when in fact it is not, an *error of the first kind* is made. That is, we choose H_1 when H_0 is actually true. Denote this probability $P(D_1/H_0)$, which in the radar terminology corresponds to P_F, the *probability of false alarm* , and it is mathematically expressed as

$$P_F = P(D_1/H_0) = \int_\gamma^\infty f_{l/H_0}(L/H_0) \, dL \tag{2.7}$$

where $f_{l/H_0}(L/H_0)$ is the probability density function of the r.v. L, conditioned on the hypothesis that H_0 is true.

On the other hand, if H_0 is chosen when H_1 is actually true, an *error of the second kind* is made. The probability of an error of second kind denoted as $P(D_0/H_1)$, in the radar terminology is called the *probability of a miss*, and is mathematically expressed as

$$P_M = P(D_0/H_1) = \int_{-\infty}^{\gamma} f_{l/H_1}(L/H_1)\, dL \tag{2.8}$$

Often P_D is used, which is the probability of choosing H_1 when H_1 is actually true. This corresponds to $1 - P(D_0/H_1)$, and in the radar terminology is called the *probability of detection*. Mathematically it is expressed as

$$P_D = P(D_1/H_1) = \int_{\gamma}^{\infty} f_{l/H_1}(L/H_1)\, dL \tag{2.9}$$

The realization of the optimum receiver for the hypothesis testing problem discused above is shown in Figure 3 on page 9, and it is known as a quadrature correlator receiver.

The performance of this receiver, in terms of P_D and P_F is given by

$$\begin{aligned} P_F &= \exp\left(-\frac{\gamma}{N_0}\right) \\ P_D &= Q\left(\sqrt{\frac{2E_r}{N_0}}, \sqrt{\frac{2\gamma}{N_0}}\right) \end{aligned} \tag{2.10}$$

where γ and E_r have been defined above, and

$$Q(\alpha, \beta) = \int_{\beta}^{\infty} z \exp\left(-\frac{z^2 + \alpha^2}{2}\right) I_0(\alpha z)\, dz \tag{2.11}$$

is the so-called Marcum's Q function. The $I_0(x)$ function is defined by

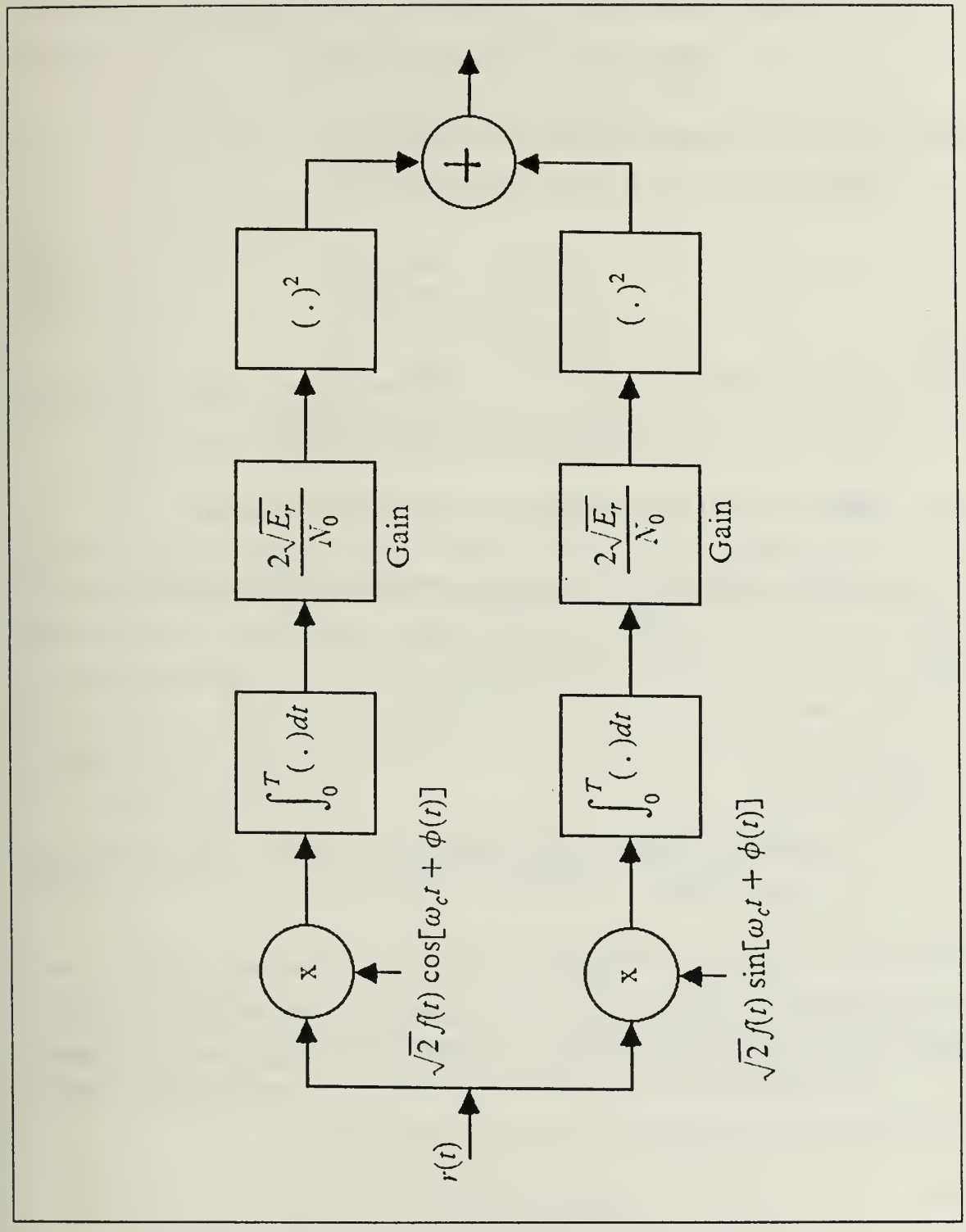

Figure 3. Optimum Quadrature Correlator Receiver.

$$I_0(x) = \frac{1}{2\pi}\int_0^{2\pi} \exp[x\cos(\varepsilon - \varepsilon_0)]d\varepsilon \tag{2.12}$$

and it is known as the modified Bessel function of zero order.

Observe that P_D can be written in terms of P_F as

$$P_D = Q\left(\sqrt{\frac{2E_r}{N_0}}\ ,\ \sqrt{2\ln\frac{1}{P_F}}\right) \tag{2.13}$$

so that P_D can be plotted as a function of P_F for different values of E_r/N_0. Such a plot results in the so called Receiver Operating Characteristics (ROC's).

2. Additive Colored Gaussian Noise (ACGN) Under Both Hypotheses.

The performance of the optimum receiver shown in Figure 3 on page 9, which has been designed for the signal and noise model of Equation 2.1, can be evaluated when an additional source of interference is present, namely additive colored Gaussian noise (ACGN), that is statistically independent of the AWGN $w(t)$. It is obvious that this receiver is no longer optimum for the assumed signal and noise model. Bukofzer [Ref. 2] has investigated this problem which can be mathematically expressed as the hypothesis testing problem

$$\begin{aligned} H_1 &: r(t) = \sqrt{2E_r}f(t)\cos[\omega_c t + \phi(t) + \theta] + n_c(t) + w(t) \qquad 0 \le t \le T \\ H_0 &: r(t) = n_c(t) + w(t) \end{aligned} \tag{2.14}$$

where again E_r is the actual received signal energy, θ is a random variable (r.v.) uniformly distributed over $[0, 2\pi]$ and $n_c(t)$ and $w(t)$ are zero mean independent Gaussian random processes with PSD $S_{n_c}(\omega)$ (as yet unspecified) and $S_w(\omega) = N_0/2$, respectively.

The performance of the receiver shown in Figure 3 on page 9, under the above stated hypotheses and the assumption that $\phi(t) \equiv 0$, is given as

$$\begin{aligned} P_F &= \exp\left(-\frac{\gamma}{2\sigma^2}\right) \\ P_D &= Q\left(\frac{\sqrt{E_r}}{\sigma}\ ,\ \frac{\sqrt{\gamma}}{\sigma}\right) \end{aligned} \tag{2.15}$$

where, using the notation $Var\{\,.\,/\,.\,\}$ to denote the conditioned variance of a r.v.,

$$\begin{aligned}\sigma^2 &\equiv Var\{L_s/H_1\,,\,\theta\} \;=\; Var\{L_c/H_1\,,\,\theta\} \\ &= Var\{L_s/H_0\} \;=\; Var\{L_c/H_0\} \\ &= \frac{N_0}{2} + \sigma_{n_c}^2\end{aligned} \tag{2.16}$$

with

$$\sigma_{n_c}^2 \;=\; \frac{1}{2\pi}\int_{-\infty}^{\infty} S_{n_c}(\omega)\,|F_c(\omega)|^2 d\omega \tag{2.17}$$

Also $F_c(\omega)$ is the Fourier Transform of $f_c(t)$, where

$$f_c(t) \;\equiv\; f(t)\cos\omega_c t \tag{2.18}$$

A direct relationship between P_D and P_F can be obtained, namely

$$P_D \;=\; Q\left(\sqrt{\frac{E_r}{\frac{N_0}{2}+\sigma_{n_c}^2}}\,,\sqrt{2\ln\frac{1}{P_F}}\right) \tag{2.19}$$

C. TARGET MODEL B.

Van Trees [Ref. 1] derives analytically the target model for this particular case, with the assumption that the radar transmits a continuous cosine wave

$$s_t(t) \;=\; \sqrt{2P_t}\,\cos\omega_c t \;=\; \sqrt{2}\,Re\left\{\sqrt{P_t}\,\exp(j\omega_c t)\right\} \qquad -\infty \le t \le \infty \tag{2.20}$$

Assuming that there is a zero-velocity target at some range R from the transmitter, whose physical structure consists of several reflecting surfaces, then the reflected signal can be written as

$$s_r(t) \;=\; \sqrt{2}\,Re\left\{\sqrt{P_t}\sum_{i=1}^{K} g_i \exp[j\omega_c(t-\tau)+\theta_i]\right\} \tag{2.21}$$

where g_i represents the attenuation of the signal due to the two-way path loss, the radar cross section of the i-th reflecting surface while also including the effects of transmitting

and receiving antenna gains, θ_i is a random phase angle introduced by the reflection process, and τ is the signal round trip delay time to and from the target.

Assuming that all θ_i are statistically independent, that the g_i have equal magnitudes and that K is sufficiently large, and then using the central limit theorem, one obtains

$$s_r(t) = \sqrt{2}\, Re\left\{\sqrt{P_t}\,\tilde{b}\, \exp[j\omega_c(t-\tau)]\right\} \tag{2.22}$$

where $\tilde{b}$ is a complex Gaussian random variable. The envelope, $|\,\tilde{b}\,|$, is a Rayleigh random variable, whose moments are

$$E\{\,|\,\tilde{b}\,|\,\} = \sqrt{\frac{\pi}{2}}\,\sigma_b \tag{2.23}$$

and

$$E\{\,|\,\tilde{b}\,|^2\} = 2\sigma_b^2 \tag{2.24}$$

The value of σ_b^2 includes the antenna gains, path losses, and radar cross section of the target.

The reflection process associated with this target model is assumed to be *frequency-independent* and *linear*. That is, if

$$s_t(t) = \sqrt{2}\, Re\left\{\sqrt{P_t}\, \exp(j\omega_c t + j\omega t)\right\} \tag{2.25}$$

is transmitted,

$$s_r(t) = \sqrt{2}\, Re\left\{\sqrt{P_t}\,\tilde{b}\, \exp[j(\omega_c + \omega)(t-\tau)]\right\} \tag{2.26}$$

is received, while if

$$s_t(t) = \sqrt{2}\, Re\left\{\sqrt{E_t}\,\tilde{f}\,(t) \exp(j\omega_c t)\right\} \tag{2.27}$$

is transmitted,

$$s_r(t) = \sqrt{2}\, Re\left\{\sqrt{E_t}\,\tilde{b}\, \exp[j\omega_c(t-\tau)]\tilde{f}\,(t-\tau)\right\} \tag{2.28}$$

is received. Since $\tilde{b}$ has a uniform phase, the $\exp(j\omega_c\tau)$ term, can be absorbed into the phase, so that

$$s_r(t) = \sqrt{2}\, Re\left\{\sqrt{E_t}\,\tilde{b}\tilde{f}(t-\tau)\exp(j\omega_c t)\right\} \tag{2.29}$$

where the function $\tilde{f}(t)$ is the complex envelope of the transmitted signal, which is assumed to be normalized, in the sense that

$$\int_{-\infty}^{\infty} \left|\tilde{f}(t)\right|^2 dt = 1 \tag{2.30}$$

Thus, from Equation 2.27, the transmitted signal energy is E_t and the expected value of the received signal energy is

$$\overline{E}_r \equiv 2E_t\sigma_b^2 \tag{2.31}$$

Considering now a target with constant radial velocity v, the target range $R(t)$ can be written as

$$R(t) = R_0 - vt \tag{2.32}$$

where R_0 is the target range at $t = 0$.

Under these conditions and assuming that the transmitted signal is the one given in Equation 2.27, the reflected signal becomes

$$s_r(t) = \sqrt{2}\, Re\left\{\sqrt{E_t}\,\tilde{b}\tilde{f}(t-\tau+\tfrac{2v}{c}t)\exp\left[j\omega_c(t+\tfrac{2v}{c}t)\right]\right\} \tag{2.33}$$

where c is the velocity of the light. Furthermore, from the assumption

$$\frac{2vT}{c} \ll \frac{1}{W} \tag{2.34}$$

where W is the bandwidth of $\tilde{f}(t)$, the reflected radar signal can be mathematically described as

$$s_r(t) = \sqrt{2}\, Re\left\{\sqrt{E_t}\;\tilde{b}\,\tilde{f}(t-\tau)\;\exp(j\omega_c t + j\omega_D t)\right\} \qquad 0 \le t \le T \tag{2.35}$$

where

$$\omega_D \equiv \omega_c\left(\frac{2v}{c}\right) \tag{2.36}$$

is the shift in the carrier frequency called *Doppler Shift* .

Then, the total received waveform, in which additive Gaussian noise is accounted for, can be written as

$$r(t) = \sqrt{2}\, Re\left\{\sqrt{E_t}\ \tilde{b}\,\tilde{f}(t-\tau)\exp[j\omega_c t + j\omega_D t]\right\} + \sqrt{2}\, Re\{\tilde{n}(t)\exp[j\omega_c t]\} \tag{2.37}$$

or more compactly

$$r(t) = \sqrt{2}\, Re\{\tilde{r}(t)\exp[j\omega_c t]\} \tag{2.38}$$

where

$$\tilde{r}(t) = \tilde{b}\sqrt{E_t}\tilde{f}(t-\tau)\exp[j\omega_D t] + \tilde{n}(t) \tag{2.39}$$

The total noise interference $n(t)$ can be expressed as

$$n(t) \equiv \sqrt{2}\, Re\{\tilde{n}(t)\exp[j\omega_c t]\} \tag{2.40}$$

which represents the actual Gaussian noise that is added to the received signal. Since the detection problem in this case is limited to a particular value of range and Doppler shift, the corresponding parameters τ and ω_D without loss of generality can be set to zero for algebraic simplicity, and the binary hypothesis testing problem can be mathematically described as

$$\begin{aligned} H_1 &: r(t) = \sqrt{2}\, Re\left\{\left[\tilde{b}\sqrt{E_t}\tilde{f}(t) + \tilde{n}(t)\right]\exp[j\omega_c t]\right\} \quad 0 \le t \le T \\ H_0 &: r(t) = \sqrt{2}\, Re\{\tilde{n}(t)\exp[j\omega_c t]\} \end{aligned} \tag{2.41}$$

so that the detection problem can be explicitely formulated for the two different kinds of additive Gaussian noise.

1. Additive White Gaussian Noise (AWGN) Under Both Hypotheses.

In this case, the complex envelopes of the received waveform under the two hypotheses are

$$
\begin{aligned}
H_1 &: \tilde{r}(t) = \sqrt{E_t}\ \tilde{b}\ \tilde{f}(t) + \tilde{w}(t) \qquad 0 \le t \le T \\
H_0 &: \tilde{r}(t) = \tilde{w}(t)
\end{aligned}
\tag{2.42}
$$

where $\tilde{w}(t)$ is a zero mean white complex Gaussian random process with

$$
E[\tilde{w}(t)\tilde{w}^{*}(u)] = N_0\delta(t-u) \tag{2.43}
$$

Thus the transmitted signal energy is E_t and the expected value of the received signal energy is

$$
\overline{E}_r = 2E_t\sigma_b^2 \tag{2.44}
$$

Van Trees [Ref. 2] proves that optimal decisions about the two hypotheses in Equation 2.42 are given by the threshold test

$$
|\tilde{R}_1|^2 \underset{H_0}{\overset{H_1}{\gtrless}} \frac{N_0(N_0 + 2\sigma_b^2 E_t)}{2\sigma_b^2 E_t}\{\ln\eta + \ln(1 + \frac{2\sigma_b^2 E_t}{N_0})\} \equiv \gamma \tag{2.45}
$$

where $\tilde{r}_1$ is a sufficient statistic given by

$$
\tilde{r}_1 \equiv \int_0^T \tilde{r}(t)\tilde{f}^{*}(t)dt \tag{2.46}
$$

which is implemented by the receiver shown in Figure 4 on page 16 (see point labeled 1), or equivalently, by the receiver shown in Figure 5 on page 17 (actual receiver). Note that the test threshold γ depends on η, which itself depends on the prior probabilities of the two alternative hypotheses and the decision costs.

The performance of these receivers has been evaluated in [Ref. 2], in terms of P_D and P_F and demonstrated to be given by

$$
\begin{aligned}
P_F &= \exp(-\frac{\gamma}{N_0}) \\
P_D &= \exp\left(-\frac{\gamma}{\overline{E}_r + N_0}\right)
\end{aligned}
\tag{2.47}
$$

In terms of ROC's, the performance of the optimum receiver is given by

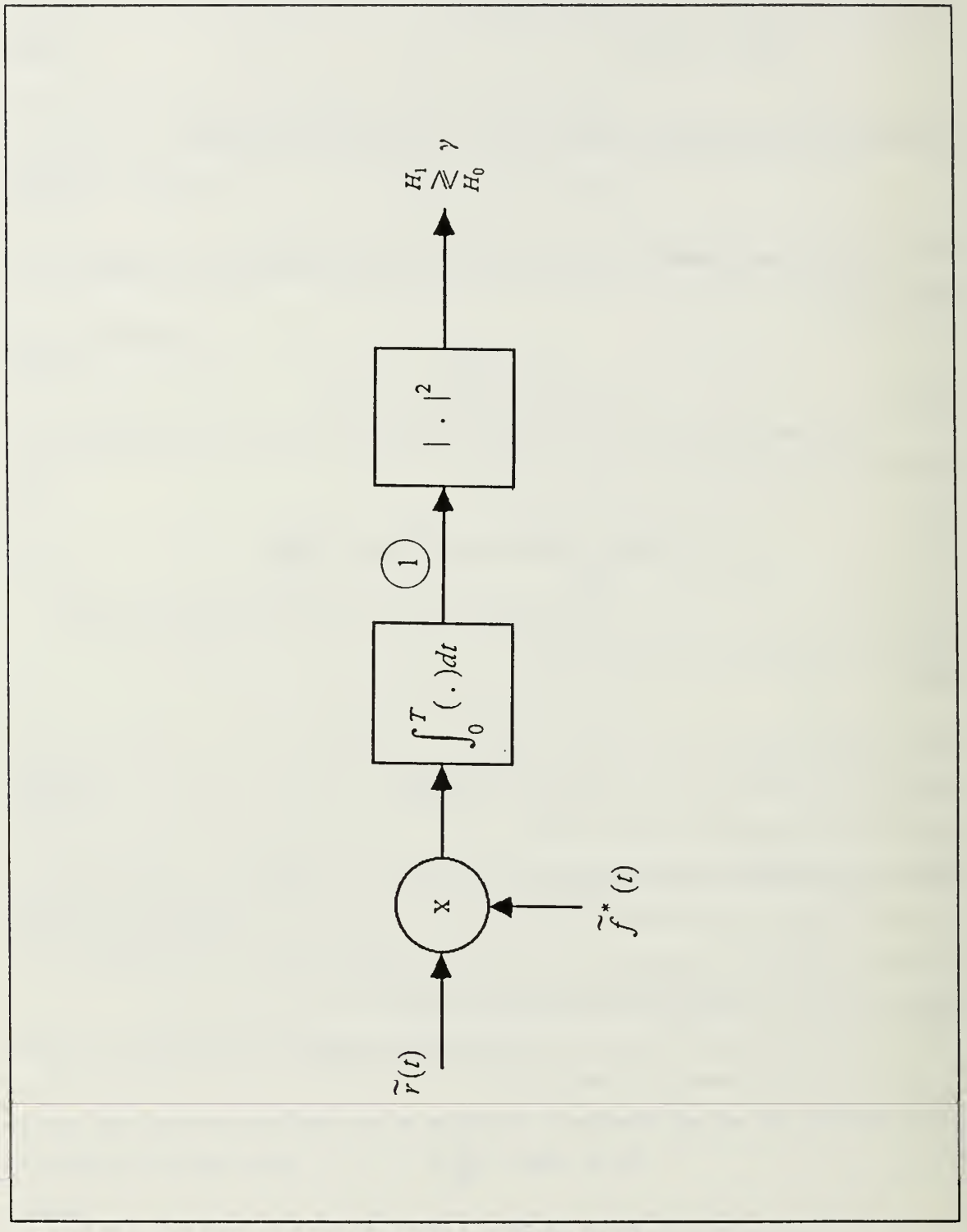

Figure 4. Correlation Receiver Using Complex Signals.

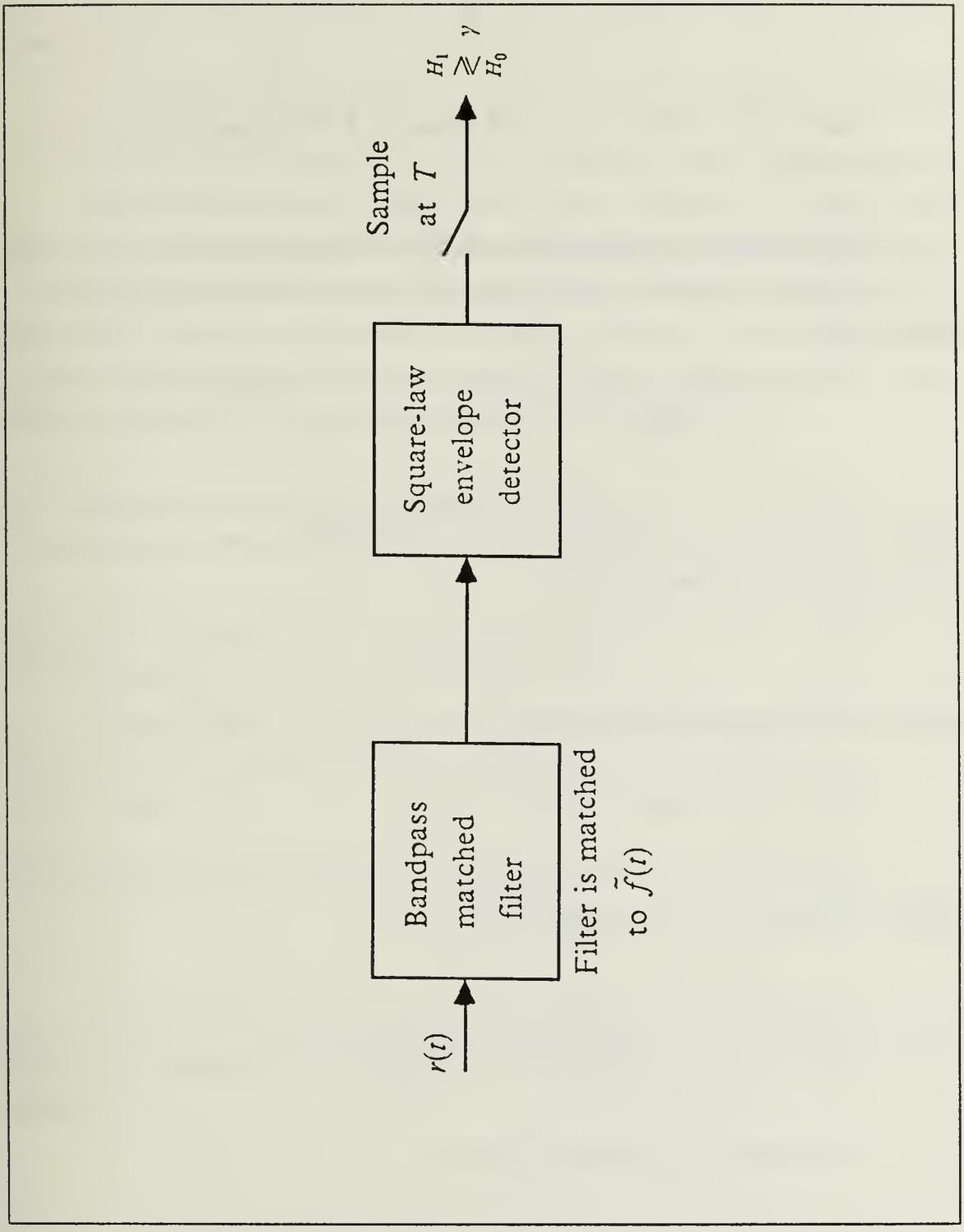

Figure 5. Optimum Receiver (Actual Implementation).

$$\Delta = \frac{\overline{E_r}}{N_0} \tag{2.49}$$

From Equation 2.48 it is clear that increasing Δ always improves the performance of the receiver in the sense that for fixed P_F, P_D increases as Δ increases.

2. Additive Colored Gaussian Noise (ACGN) Under Both Hypotheses.

In this case, the complex envelopes of the received signal under the two hypotheses are

$$\begin{aligned} H_1 &: \tilde{r}(t) = \sqrt{E_t}\ \tilde{b}\,\tilde{f}(t) + \tilde{n}(t) \qquad 0 \le t \le T \\ H_0 &: \tilde{r}(t) = \tilde{n}(t) \end{aligned} \tag{2.50}$$

The additive noise $\tilde{n}(t)$ is a sample function from a zero mean nonwhite complex Gaussian process. It is assumed here that $\tilde{n}(t)$ contains two statistically independent Gaussian components, namely

$$\tilde{n}(t) = \tilde{n}_c(t) + \tilde{w}(t) \tag{2.51}$$

where the covariance of $\tilde{n}(t)$ is given by

$$E[\tilde{n}(t)\tilde{n}^*(u)] \equiv \tilde{K}_{\tilde{n}}(t,u) = \tilde{K}_{\tilde{n}_c}(t,u) + N_0\delta(t-u) \qquad 0 \le t, u \le T \tag{2.52}$$

Van Trees [Ref. 2] derives the optimum threshold test for the hypothesis testing problem of Equation 2.50, which is given by

$$\left| \int_0^T \tilde{r}(z)\tilde{g}^*(z)dz \right|^2 \underset{H_0}{\overset{H_1}{\gtrless}} \gamma \tag{2.53}$$

where $\tilde{g}(t)$ is the solution to the integral equation

$$\tilde{f}(t) = \int_0^T \tilde{K}_{\tilde{n}_c}(t)\,\tilde{g}(u)\,du + N_0\,\tilde{g}(t) \qquad 0 \le t, u \le T \tag{2.54}$$

$$\tilde{f}(t) = \int_0^T \tilde{K}_{\tilde{n}_c}(t)\,\tilde{g}(u)\,du + N_0\,\tilde{g}(t) \qquad 0 \le t, u \le T \tag{2.54}$$

The optimum receivers for this case are shown in Figure 6 on page 20 (conceptual operation using complex signals) and in Figure 7 on page 21 (actual receiver).

A particularly simple solution to this problem is obtained when $\tilde{n}_c(t)$ can be modeled as a stationary process and the observation interval is nearly infinite, leading to the so-called Stationary Process, Long Observation Time, or SPLOT problem. Then Fourier Transforms can be used to solve Equation 2.54, to yield

$$\tilde{G}_\infty(\omega) = \frac{\tilde{F}(\omega)}{\tilde{S}_{\tilde{n}}(\omega)} = \frac{\tilde{F}(\omega)}{N_0 + \tilde{S}_{\tilde{n}_c}(\omega)} \tag{2.55}$$

where $\tilde{F}(\omega)$, $\tilde{S}_{\tilde{n}}(\omega)$ and $\tilde{S}_{\tilde{n}_c}(\omega)$ are the Fourier Transforms of $\tilde{f}(t)$, $\tilde{K}_{\tilde{n}}(t,u)$ and $\tilde{K}_{\tilde{n}_c}(t,u)$ respectively.

The performance of the optimum receiver in terms of ROC's is also given by the functional form of Equation 2.48, which in this case can be expressed as

$$\Delta = \overline{E}_r \int_0^T \tilde{f}(t)\tilde{g}^{\,*}(t)dt \tag{2.56}$$

For the SPLOT problem, Δ can be evaluated by using the inverse Fourier Transform of Equation 2.55 in Equation 2.56, while allowing $T \to \infty$ for computational simplicity.

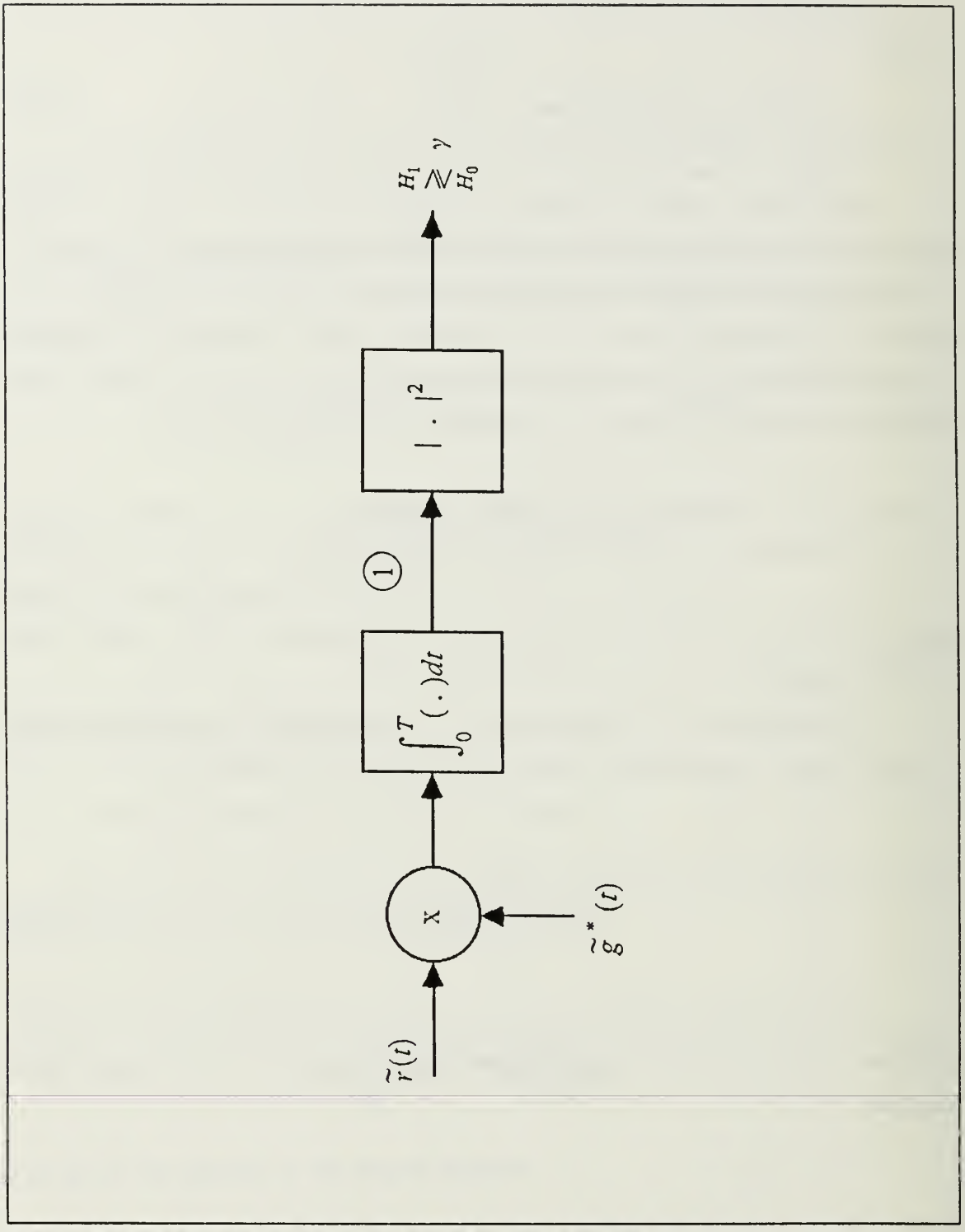

Figure 6. Correlation Receiver Using Complex Signals.

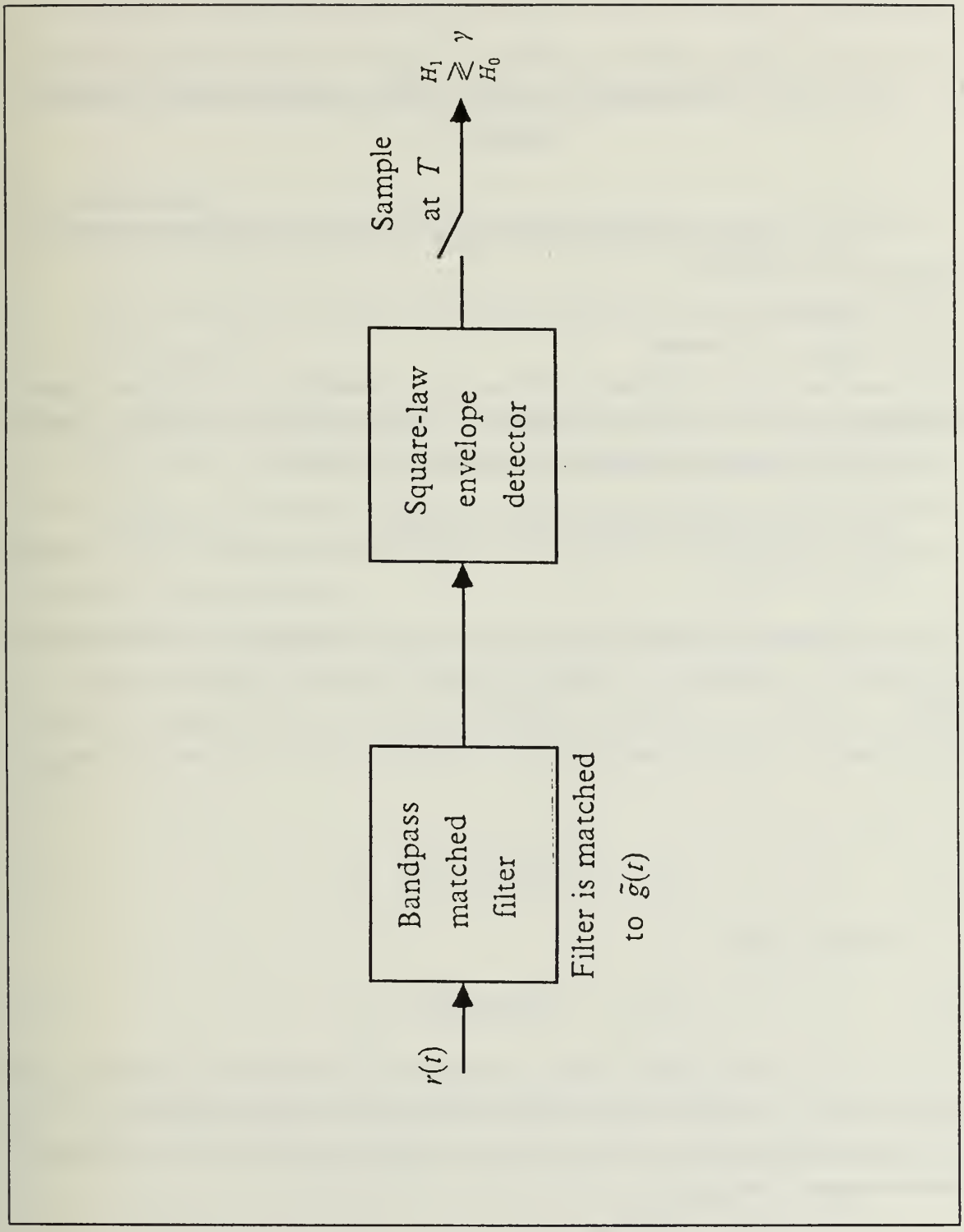

Figure 7. Optimum Receiver (Actual Implementation).

III. RECEIVER PERFORMANCE ANALYSIS BASED ON THE TARGET MODEL A.

The binary detection problem addressed in this chapter involves discriminating between the two alternatives

H_1 : Signal is present

H_0 : Signal is not present

under somewhat more complicated conditions due to uncertainty in the received signal, expressed by a random phase angle imposed on the signal during the reflection process.

The hypothesis testing problem is mathematically described as

$$\begin{aligned} H_1 &: r(t) = \sqrt{2E_r} f(t) \cos[\omega_c t + \phi(t) + \theta] + n(t) \qquad 0 \le t \le T \\ H_0 &: r(t) = n(t) \end{aligned} \tag{3.1}$$

where E_r is the received signal energy, $n(t)$ is a sample function of a zero mean white Gaussian, or a combination of a white and colored Gaussian noise process, and θ is a random variable (r.v.) uniformly distributed over $[0, 2\pi]$. The amplitude and phase modulations, $f(t)$ and $\phi(t)$ respectively, are deterministic, with $f(t)$ assumed to satisfy

$$\int_0^T |f(t)|^2 \, dt = 1 \tag{3.2}$$

The case in which

$$n(t) = w(t) \tag{3.3}$$

where $w(t)$ is a white Gaussian random process, has been addressed extensively in the literature [Ref. 2] and the basic results have been presented earlier in Chapter 2. The basic performance equation in terms of ROC's, is given by Equation 2.13 and repeated here for completeness, namely

$$P_D = Q\left(\sqrt{\frac{2E_r}{N_0}}, \sqrt{2 \ln \frac{1}{P_F}}\right) \tag{3.4}$$

In the case where the additive Gaussian noise is other than white under both hypotheses, the receiver shown in Figure 3 on page 9 is no longer optimum and the performance of this receiver will no longer be given by Equation 3.4.

A. PROBLEM 1.

In this case the hypothesis testing problem is mathematicaly described as

$$\begin{aligned} H_1 &: r(t) = \sqrt{2E_r} f(t) \cos[\omega_c t + \phi(t) + \theta] + n_c(t) + w(t) \qquad 0 \le t \le T \\ H_0 &: r(t) = w(t) \end{aligned} \tag{3.5}$$

where E_r is the received signal energy, θ is a random variable (r.v.) uniformly distributed over $[0, 2\pi]$, and $n_c(t)$ and $w(t)$ are zero mean independent Gaussian random processes with PSD $S_{n_c}(\omega)$ (as yet unspecified) and $S_w(\omega) = N_0/2$, respectively. The performance of the receiver shown in Figure 3 on page 9, having input $r(t)$ given by Equation 3.5 is now evaluated.

The signal at the output of the receiver can be mathematically described as

$$L = L_c^2 + L_s^2 \tag{3.6}$$

where

$$L_c = \int_0^T \sqrt{2}\ r(t) f(t) \cos[\omega_c t + \phi(t)]\, dt \tag{3.7}$$

$$L_s = \int_0^T \sqrt{2}\ r(t) f(t) \sin[\omega_c t + \phi(t)]\, dt \tag{3.8}$$

In order for the performance to be evaluated, the probabilities P_D and P_F must be specified. To this end, the probability density function (p.d.f.) of the r.v. L at the output of the receiver, conditioned on both hypotheses, is required. This can be accomplished by observing that both L_c and L_s are conditionally Gaussian r.v.'s.

Using the notation $E\{\,.\,/\,.\,\}$ to denote conditional expectations, the conditioned means of the r.v.'s L_c and L_s can be obtained from

$$E\{L_c/H_1,\theta\} =$$

$$= E\left\{\int_0^T \sqrt{2}\left[\sqrt{2E_r}f(t)\cos[\omega_c t + \phi(t) + \theta] + w(t) + n_c(t)\right]f(t)\cos[\omega_c t + \phi(t)]dt\right\} \tag{3.9}$$

$$= \sqrt{E_r}\cos\theta$$

$$E\{L_s/H_1\ ,\ \theta\} =$$

$$= E\left\{\int_0^T \sqrt{2}\left[\sqrt{2E_r}f(t)\cos[\omega_c t + \phi(t) + \theta] + w(t) + n_c(t)\right]f(t)\sin[\omega_c t + \phi(t)]dt\right\} \tag{3.10}$$

$$= -\sqrt{E_r}\sin\theta$$

Obviously, since both $n_c(t)$ and $w(t)$ are assumed to be zero mean processes,

$$E\{L_c/H_0\} = E\{L_s/H_0\} = 0 \tag{3.11}$$

Bukofzer [Ref. 2] shows that, under the assumption of $\phi(t) \equiv 0$

$$Var\{L_c/H_1\ ,\ \theta\} = Var\{L_s/H_1\ ,\ \theta\} = \frac{N_0}{2} + \sigma_{n_c}^2 \tag{3.12}$$

where $\sigma_{n_c}^2$ is defined as

$$\sigma_{n_c}^2 \equiv \frac{1}{2\pi}\int_{-\infty}^{\infty} S_{n_c}(\omega)\,|F_c(\omega)|^2 d\omega \tag{3.13}$$

and $F_c(\omega)$ is the Fourier Transform of the $f_c(t)$, where

$$f_c(t) \equiv f(t)\cos\omega_c t \tag{3.14}$$

Under the hypothesis H_0, the conditional variances of L_c and L_s can be evaluated as

$$Var\{L_c/H_0\} = Var\{L_s/H_0\} = E\left\{\left[\int_0^T \sqrt{2}\ w(t) f(t) \cos[\omega_c t + \phi(t)]\, dt\right]^2\right\}$$

$$= 2\int_0^T \left[\int_0^T E\{w(t)w(\tau)\} f(t) f(\tau) \cos[\omega_c t + \phi(t)]\ \cos[\omega_c \tau + \phi(\tau)]\, dt\right] d\tau = \frac{N_0}{2} \tag{3.15}$$

Bukofzer [Ref. 2] shows that L_c and L_s are uncorrelated, and since the conditional r.v.'s are Gaussian, Whalen [Ref. 4] shows that the corresponding conditional p.d.f.'s can be written as

$$f_{l|H_1}(L/H_1) = \frac{1}{(N_0 + 2\sigma_{n_c}^2)} \exp\left(-\frac{L + E_r}{(N_0 + 2\sigma_{n_c}^2)}\right) I_0\left(\frac{\sqrt{E_r L}}{(\frac{N_0}{2} + \sigma_{n_c}^2)}\right) u(L)$$

$$f_{l|H_0}(L/H_0) = \frac{1}{N_0} \exp\left(-\frac{2L}{N_0}\right) u(L) \tag{3.16}$$

where $u(\,.\,)$ is the unit step function, $\sigma_{n_c}^2$ is defined in Equation 3.13 and $I_0(x)$ is the modified Bessel function of zero order, defined by Equation 2.12.

As a result of this, we can express the probabilities P_D and P_F as

$$P_D = \Pr\{l > \gamma/H_1\} = \int_\gamma^\infty f_{l|H_1}(L/H_1) dL$$

$$= \int_\gamma^\infty \frac{1}{N_0 + 2\sigma_{n_c}^2} \exp\left(-\frac{L + E_r}{(N_0 + 2\sigma_{n_c}^2)}\right) I_0\left(\frac{\sqrt{E_r L}}{(\frac{N_0}{2} + \sigma_{n_c}^2)}\right) u(L)\, dL$$

$$= \int_{\sqrt{\frac{\gamma}{N_0 + 2\sigma_{n_c}^2}}}^\infty x \exp\left[-\frac{x^2 + \alpha^2}{2}\right] I_0(\alpha x)\, dx \tag{3.17}$$

$$= Q\left(\alpha\ ,\ \sqrt{\frac{\gamma}{\frac{N_0}{2} + \sigma_{n_c}^2}}\right)$$

where

$$\alpha^2 \equiv \frac{E_r}{N_0/2 + \sigma_{n_c}^2} \tag{3.18}$$

and $Q(\alpha\ ,\ \beta)$ is the so-called Marcum's Q function.

Furthermore

$$\begin{aligned} P_F = \Pr\{l > \gamma / H_0\} &= \int_{\gamma}^{\infty} f_{l/H_0}(L/H_0) dL \\ &= \int_{\gamma}^{\infty} \frac{1}{N_0} \exp\left(- \frac{L}{N_0} \right) u(L)\, dL \\ &= \exp(- \frac{\gamma}{N_0}) \end{aligned} \tag{3.19}$$

Solving for γ yields

$$\gamma = N_0 \ln \frac{1}{P_F} \tag{3.20}$$

and a direct relationship between P_D and P_F can be obtained, namely

$$P_D = Q\left(\sqrt{\frac{E_r}{\frac{N_0}{2} + \sigma_{n_c}^2}}\ ,\ \sqrt{\frac{- N_0 \ln P_F}{\frac{N_0}{2} + \sigma_{n_c}^2}} \right) \tag{3.21}$$

This result specifies the performance of the receiver shown in Figure 3 on page 9, under the assumptions stated in Equation 3.5. In order for the P_D to be evaluated as a function of P_F and the parameters making up Equation 3.21, it is necessary to specify the type of signal envelope that is transmitted and the colored noise interference PSD with which to mask the reflected signal.

1. **Signal.**

A simple model is chosen to specify the signal envelope, that is

$$f(t) = \begin{cases} \frac{1}{\sqrt{T}} & 0 \le t \le T \\ 0 & \text{otherwise} \end{cases} \tag{3.22}$$

so that the transmitted waveform can be mathematically expressed as

$$f_c(t) = \begin{cases} \frac{1}{\sqrt{T}} \cos(\omega_c t) & 0 \le t \le T \\ 0 & \text{otherwise} \end{cases} \tag{3.23}$$

The Fourier Transform of the transmitted waveform $f_c(t)$, denoted $F_c(\omega)$, can be shown to have a magnitude squared given by

$$|F_c(\omega)|^2 = \frac{T}{2} \frac{\sin^2[(\omega - \omega_c)\frac{T}{2}]}{[(\omega - \omega_c)\frac{T}{2}]^2} + \frac{T}{2} \frac{\sin^2[(\omega + \omega_c)\frac{T}{2}]}{[(\omega + \omega_c)\frac{T}{2}]^2} \tag{3.24}$$

under the assumption that $\omega_c T \gg 1$.

2. **Noise.**

Since the noise power affecting the receiver performance (see Equation 3.21) depends on the PSD of the additive colored Gaussian noise, it is necessary to specify such ACGN PSD before performance evaluations are possible. Attempts to extremize P_D as a function of $\sigma_{n_c}^2$ have not proved succesful. Therefore, four different PSD's were chosen for $n_c(t)$ on the basis of simplicity and suitability as "useful" PSD shapes that could significantly degrade receiver performance. Therefore in Appendix A, the evaluation of Equation 3.13 for four different ACGN PSD shapes is presented, since as pointed out, it is apparent that the extremization of P_D for fixed P_F under a power constraint on $n_c(t)$, is not possible. Common to all those cases is the fact that the total power of $n_c(t)$ is constrained and set equal to P_{n_c}. The evaluation of Appendix A yield the general result

$$\sigma_{n_c}^2 = k\,T\,P_{n_c} \tag{3.25}$$

a. Bandlimited Constant Amplitude PSD

The bandlimited constant amplitude PSD is mathematically described as

$$S_{n_c}(\omega) = \begin{cases} \frac{T}{4\alpha} P_{n_c} & |\omega \pm \omega_c| \leq \alpha \frac{2\pi}{T} \\ 0 & \text{otherwise} \end{cases} \tag{3.26}$$

where α is a scalar. Based on the results of Appendix B for a similar case, k was evaluated for $\alpha = 1$, which results in the maximum effective noise power, yielding

$$k = 0.224 \tag{3.27}$$

b. Sinc Squared Shaped PSD

The PSD in this case can be mathematically described as

$$S_{n_c}(\omega) = \frac{TP_{n_c}}{2}\left[\frac{\sin^2[(\omega+\omega_c)\frac{T}{2\delta}]}{[(\omega+\omega_c)\frac{T}{2\delta}]^2} + \frac{\sin^2[(\omega-\omega_c)\frac{T}{2\delta}]}{[(\omega-\omega_c)\frac{T}{2\delta}]^2}\right] \quad -\infty \leq \omega \leq \infty \tag{3.28}$$

where δ is a scalar. For $\delta = 1$, which results in a noise bandwidth equal to the signal's main lobe width, k was evaluated as

$$k = 0.3333 \tag{3.29}$$

c. Butterworth Shaped PSD

The PSD in this case can be mathematically described as

$$S_{n_c}(\omega) = \frac{P_{n_c}(\beta\omega_s)}{(\beta\omega_s)^2 + (\omega+\omega_c)^2} + \frac{P_{n_c}(\beta\omega_s)}{(\beta\omega_s)^2 + (\omega-\omega_c)^2} \quad -\infty \leq \omega \leq \infty \tag{3.30}$$

where ω_s is half power point of the spectrum and β is a scalar. Based on the results of Appendix B for a similar case, k was evaluated for $\beta = 1$, which results in the maximum effective noise power, yielding

$$k = 0.304 \tag{3.31}$$

d. Triangular Shaped PSD

In this case the PSD is mathematically described as

$$S_{n_c}(\omega) = \begin{cases} \dfrac{P_{n_c}}{2\varepsilon\omega_0}\left(1 - \dfrac{|\omega - \omega_c|}{\varepsilon\omega_0}\right) & |\omega + \omega_c| \leq \varepsilon\omega_0 \\ \dfrac{P_{n_c}}{2\varepsilon\omega_0}\left(1 - \dfrac{|\omega + \omega_c|}{\varepsilon\omega_0}\right) & |\omega - \omega_c| \leq \varepsilon\omega_0 \end{cases} \tag{3.32}$$

where ε is a scalar. Based on the results of Appendix B for a similar case, k was evaluated for $\varepsilon = 1$, which results in the maximum effective noise power, yielding

$$k = 0.051 \tag{3.33}$$

Defining the Signal-to-Noise Ratio to be (the unitless quantity)

$$SNR = \frac{E_r}{N_0/2} \tag{3.34}$$

and the Jamming-to-Signal Ratio to be (the unitless quantity)

$$JSR = \frac{TP_{n_c}}{E_r} \tag{3.35}$$

the actual performance of the receiver operating under the four types of colored noise interference described above can now be specified. The results are all of the general form

$$\begin{aligned} P_D &= Q\left(\sqrt{\frac{E_r}{\frac{N_0}{2} + kTP_{n_c}}}\ ,\ \sqrt{\frac{-N_0 \ln P_F}{\frac{N_0}{2} + kTP_{n_c}}}\right) \\ &= Q\left(\sqrt{\frac{SNR}{1 + k\,SNR\,JSR}}\ ,\ \sqrt{\frac{-2\ln P_F}{1 + k\,SNR\,JSR}}\right) \end{aligned} \tag{3.36}$$

where the value of k is specified by Equations 3.27, 3.29, 3.31 and 3.33 for the four kinds of ACGN PSD shapes considered.

These results will be analyzed in more detail and presented via ROC's in Chapter 5.

IV. RECEIVER PERFORMANCE ANALYSIS BASED ON THE TARGET MODEL B.

The problem of discriminating between the two alternatives being addressed here, namely

H_1 : Signal is present

H_0 : Signal is not present

has been presented in Chapter 2, with the pertinent equations describing this problem given as Equations 2.50 to Equation 2.54.

Since the final goal is to mask the signal with an optimally shaped colored noise PSD, prior knowledge of the type of the receiver used for signal detection is very important. Depending on the type of additive Gaussian noise that is assumed to be present, there are two optimum receivers that can be used. The first one is a receiver designed to be optimum in the presence of additive white Gaussian noise, and which from now on will be referred to as *Receiver I* . On the other hand, the receiver can be designed to be optimum in the presence of additive colored Gaussian noise, which from now on will be referred to as *Receiver II* .

A. PERFORMANCE OF RECEIVER I.

For this case, the problem has been presented in Chapter 2, with the pertinent equations describing the problem given by Equations 2.42 through Equation 2.46.

The performance of the receiver shown in Figure 4 on page 16 and Figure 5 on page 17, which has been designed for the signal and noise model of Equation 2.42, can also be evaluated when the additive Gaussian noise process is colored, or a combination of white and a colored Gaussian noise process. It is obvious that these receivers are no longer optimum for the assumed signal and noise model. Depending on the colored noise PSD considered to be present, two cases are investigated below.

1. **Problem 1.**

The complex envelopes of the received signal under the two hypotheses are

$$\begin{aligned} H_1 &: \tilde{r}(t) = \sqrt{E_t}\ \tilde{b}\,\tilde{f}(t) + \tilde{n}(t) \qquad 0 \le t \le T \\ H_0 &: \tilde{r}(t) = \tilde{w}(t) \end{aligned} \tag{4.1}$$

where the additive noise $\tilde{n}(t)$ is a sample function from a zero mean nonwhite complex Gaussian process assumed to contain two statistically independent components, namely

$$\tilde{n}(t) = \tilde{n}_c(t) + \tilde{w}(t) \tag{4.2}$$

The covariance of $\tilde{n}(t)$ is again given by

$$E[\tilde{n}(t)\tilde{n}^*(u)] = \tilde{K}_{\tilde{n}}(t,u) = \tilde{K}_{\tilde{n}_c}(t,u) + N_0\delta(t-u) \qquad 0 \le t\,,\, u \le T \tag{4.3}$$

The receiver whose performance is to be evaluated under such conditions corresponds to the one shown in Figure 4 on page 16, and in Figure 5 on page 17 while this receiver is no longer optimum its performance can be evaluated by obtaining the probability density function of the r.v. at the receiver output conditioned on both hypotheses. The correlator output is a complex Gaussian r.v. whose probability density function can be mathematically expressed once the mean and variance of $\tilde{r}_1$ have been determined. Since

$$\begin{aligned} \tilde{r}_1 &= \int_0^T \tilde{r}(t)\tilde{f}^*(t)\ dt \\ &= \sqrt{E_t}\ \tilde{b} + \tilde{n}_1 \qquad \text{when } H_1 \text{ is true} \\ &= \tilde{w}_1 \qquad\qquad\quad \text{when } H_0 \text{ is true} \end{aligned} \tag{4.4}$$

where

$$\tilde{w}_1 = \int_0^T \tilde{w}(t)\tilde{f}^*(t)\,dt \tag{4.5}$$

and

$$\tilde{n}_1 = \int_0^T \tilde{n}(t)\tilde{f}^*(t)\,dt \tag{4.6}$$

Due to the fact that both $n_c(t)$ and $w(t)$ are assumed to be zero mean processes and $\tilde{b}$ is a zero mean Gaussian r.v.,

$$E\{\tilde{r}_1/H_0\} = E\{\tilde{r}_1/H_1\} = 0 \tag{4.7}$$

Denoting

$$Var\{\tilde{r}_1/H_0\} \equiv 2\sigma_{n_0}^2 \tag{4.8}$$

$$Var\{\tilde{r}_1/H_1\} \equiv 2\sigma_{n_1}^2 \tag{4.9}$$

the variances can be evaluated as

$$\begin{aligned} 2\sigma_{n_0}^2 = E\{|\tilde{r}_1|^2/H_0\} &= E\left\{\int_0^T\int_0^T \tilde{w}(t)\,\tilde{w}^*(u)\tilde{f}(t)\tilde{f}^*(u)\,dt\,du\right\} \\ &= \int_0^T\int_0^T N_0\delta(t-u)\tilde{f}(t)\tilde{f}^*(u)\,dt\,du = N_0 \end{aligned} \tag{4.10}$$

Also

$$2\sigma_{n_1}^2 = E\{|\tilde{r}_1|^2/H_1\} = E\left\{\left|\sqrt{E_t}\,\tilde{b}\int_0^T \tilde{f}(t)\tilde{f}^*(t)\,dt + \tilde{n}_1(t)\right|^2\right\}$$
$$= E_b\overline{|\tilde{b}|^2} + \overline{|\tilde{n}_1|^2} \tag{4.11}$$
$$= \overline{E}_r + N_0 + \sigma_{n_c}^2$$

where

$$\sigma_{n_c}^2 = \int_0^T\int_0^T \tilde{K}_{\tilde{n}_c}(t\ ,\ u)\tilde{f}(t)\tilde{f}^*(u)\,dt\,du \tag{4.12}$$

and using Parseval's Theorem, $\sigma_{n_c}^2$ can be expressed as

$$\sigma_{n_c}^2 = \frac{1}{2\pi}\int_{-\infty}^{\infty} \tilde{S}_{\tilde{n}_c}(\omega)\,\left|\tilde{F}(j\omega)\right|^2 d\omega \tag{4.13}$$

Since $\tilde{r}_1$ is a complex Gaussian r.v., the p.d.f.'s of $\tilde{r}_1$ conditioned on the two hypotheses can be written as

$$f_{\tilde{r}_1/H_1}(\tilde{R}_1/H_1) = \frac{1}{2\pi\sigma_{n_1}^2}\exp\left\{-\frac{|\tilde{R}_1|^2}{2\sigma_{n_1}^2}\right\} \tag{4.14}$$

$$f_{\tilde{r}_1/H_0}(\tilde{R}_1/H_0) = \frac{1}{2\pi\sigma_{n_0}^2}\exp\left\{-\frac{|\tilde{R}_1|^2}{2\sigma_{n_0}^2}\right\} \tag{4.15}$$

where

$$\tilde{R}_1 = R_c + jR_s \tag{4.16}$$

and R_c and R_s are zero mean, equal variance, uncorrelated Gaussian random variables. Using the transformation

$$M \equiv R_c^2 + R_s^2 = |\tilde{R}_1|^2 \tag{4.17}$$

the p.d.f.'s can be written as

$$f_{m/H_1}(M/H_1) = \frac{1}{2\sigma_{n_1}^2} \exp\left\{ -\frac{M}{2\sigma_{n_1}^2} \right\} u(m) \tag{4.18}$$

$$f_{m/H_0}(M/H_0) = \frac{1}{2\sigma_{n_0}^2} \exp\left\{ -\frac{M}{2\sigma_{n_0}^2} \right\} u(m) \tag{4.19}$$

Then the required probabilities can be expressed as

$$\begin{aligned} P_F &= \int_\gamma^\infty f_{m/H_0}(M/H_0)\, dm = 1 - \int_0^\gamma f_{m/H_0}(M/H_0)\, dm \\ &= 1 - (1 - \exp(-\frac{\gamma}{2\sigma_{n_0}^2})) \\ &= \exp(-\frac{\gamma}{2\sigma_{n_0}^2}) \end{aligned} \tag{4.20}$$

and furthermore

$$\begin{aligned} P_D &= \int_\gamma^\infty f_{m/H_1}(M/H_1)\, dm \\ &= \exp(-\frac{\gamma}{2\sigma_{n_1}^2}) \end{aligned} \tag{4.21}$$

A direct relationship between P_D and P_F can be obtained, namely

$$\begin{aligned} P_D &= (P_F)^{2\sigma_{n_0}^2/2\sigma_{n_1}^2} \\ &= (P_F)^{(\frac{N_0}{\bar{E}_r + N_0 + \sigma_{n_c}^2})} \end{aligned} \tag{4.22}$$

In this case the performance of the optimum receiver will be evaluated for four different kinds of noise interference.

a. Bandlimited Constant Amplitude PSD.

Assuming a single sided bandwidth of w, the colored noise PSD is given by

$$\tilde{S}_{\tilde{n}_c}(\omega) = \frac{\pi}{w} P_{n_c} \qquad -w \leq \omega \leq w \tag{4.23}$$

where P_{n_c} is the colored noise power. Then $\sigma^2_{n_c}$ can be evaluated as

$$\begin{aligned} \sigma^2_{n_c} &= \frac{1}{2\pi} \int_{-\infty}^{\infty} \tilde{S}_{\tilde{n}_c}(\omega) \left| \tilde{F}(\omega) \right|^2 d\omega \\ &= \frac{1}{2\pi} \frac{\pi}{w} P_{n_c} T \int_{-w}^{w} \frac{\sin^2(\omega \frac{T}{2})}{(\omega \frac{T}{2})^2} \, d\omega \\ &= 0.448 \, TP_{n_c} \end{aligned} \tag{4.24}$$

Therefore P_D can be written as

$$P_D = P_F^{\left(\frac{1}{1+SNR+0.448\, SNR\, JSR}\right)} \tag{4.25}$$

where

$$SNR = \frac{\bar{E}_r}{N_0} \tag{4.26}$$

$$JSR = \frac{TP_{n_c}}{\bar{E}_r} \tag{4.27}$$

b. Sinc Squared Shaped PSD.

In this case the colored noise PSD is mathematicaly described as

$$\tilde{S}_{\tilde{n}_c}(\omega) = TP_{n_c} \frac{\sin^2(\omega \frac{T}{2})}{(\omega \frac{T}{2})^2} \qquad -\infty < \omega < \infty \tag{4.28}$$

Then $\sigma_{n_c}^2$ can be evaluated as

$$\sigma_{n_c}^2 = \frac{1}{2\pi}\int_{-\infty}^{\infty} \tilde{S}_{\tilde{n}_c}(\omega)\left|\tilde{F}(j\omega)\right|^2 d\omega$$

$$= \frac{1}{2\pi} TP_{n_c}T\int_{-\infty}^{\infty}\left[\frac{\sin^2(\omega\frac{T}{2})}{(\omega\frac{T}{2})^2}\;\frac{\sin^2(\omega\frac{T}{2})}{(\omega\frac{T}{2})^2}\right]d\omega \qquad (4.29)$$

$$= 0.666\, TP_{n_c}$$

Therefore P_D can be written as

$$P_D = P_F^{\left(\frac{1}{1+SNR+0.666\,SNR\,JSR}\right)} \qquad (4.30)$$

c. Butterworth Shaped PSD.

In this case the colored noise PSD is mathematicaly described as

$$\tilde{S}_{\tilde{n}_c}(\omega) = 2P_{n_c}\frac{\alpha}{\alpha^2+\omega^2} \qquad -\infty < \omega < \infty \qquad (4.31)$$

where α is the half-power point of this spectrum. Then $\sigma_{n_c}^2$ can be evaluated as

$$\sigma_{n_c}^2 = \frac{1}{2\pi}\int_{-\infty}^{\infty} \tilde{S}_{\tilde{n}_c}(\omega)\left|\tilde{F}(j\omega)\right|^2 d\omega$$

$$= \frac{1}{2\pi} 2P_{n_c}T\int_{-\infty}^{\infty}\frac{\alpha}{\alpha^2+\omega^2}\;\frac{\sin^2(\omega\frac{T}{2})}{(\omega\frac{T}{2})^2}\,d\omega \qquad (4.32)$$

$$= 0.608\, TP_{n_c}$$

Therefore P_D can be written as

$$P_D = P_F^{\left(\frac{1}{1+SNR+0.608\,SNR\,JSR}\right)} \qquad (4.33)$$

d. Triangular Shaped PSD.

In this case the colored noise PSD can be mathematically described as

$$\tilde{S}_{\tilde{n}_c}(\omega) = \frac{P_{n_c}}{\omega_0}\left(1 - \frac{|\omega|}{\omega_0}\right) \qquad -\omega_0 \le \omega \le \omega_0 \tag{4.34}$$

where P_{n_c} is the available colored noise power. Then $\sigma^2_{n_c}$ can be evaluated as

$$\begin{aligned}\sigma^2_{n_c} &= \frac{1}{2\pi}\int_{-\infty}^{\infty} \tilde{S}_{\tilde{n}_c}(\omega)\left|\tilde{F}(\omega)\right|^2 d\omega \\ &= \frac{1}{2\pi}\frac{P_{n_c}}{\omega_0} T\int_{-\omega_0}^{\omega_0}\left(1 - \frac{|\omega|}{\omega_0}\right)\frac{\sin^2(\omega\frac{T}{2})}{(\omega\frac{T}{2})^2} d\omega \\ &= 0.103\, TP_{n_c}\end{aligned} \tag{4.35}$$

Therefore P_D can be written as

$$P_D = P_F^{\left(\frac{1}{1+SNR+0.103\,SNR\,JSR}\right)} \tag{4.36}$$

2. Problem 2.

The problem addressed here is described by the Equation 2.50 in Chapter 2.

Due to the similarities of this case to the problem previously investigated, use may be made of the development of Equations 4.7 through Equation 4.22. The difference between the present case and that previously considered is that the variance of the correlator output is given by

$$2\sigma_{n_0}^2 = E\{|\tilde{r}_1|^2/H_0\} = E\left\{\int_0^T\int_0^T \tilde{n}(t)\,\tilde{n}^*(u)\tilde{f}(t)\tilde{f}^*(u)\,dt\,du\right\}$$

$$= \int_0^T\int_0^T \tilde{K}_{\tilde{n}}(t,u)\tilde{f}(t)\tilde{f}^*(u)\,dt\,du \qquad (4.37)$$

$$= \sigma_{n_c}^2 + N_0$$

and

$$2\sigma_{n_1}^2 = E\{|\tilde{r}_1|^2/H_1\} = E\left\{\left[\sqrt{E_t}\,\tilde{b}\int_0^T \tilde{f}(t)\tilde{f}^*(t)\,dt + \tilde{n}_1(t)\right]\right\}$$

$$= E_b\overline{|\tilde{b}|^2} + \overline{|\tilde{n}_1|^2} \qquad (4.38)$$

$$= \overline{E}_r + N_0 + \sigma_{n_c}^2$$

where $\sigma_{n_c}^2$ is defined in Equation 4.13. The performance now is obtained as

$$P_D = (P_F)^{2\sigma_{n_0}^2/2\sigma_{n_1}^2}$$

$$= (P_F)^{\Theta} \qquad (4.39)$$

where

$$\Theta \equiv \frac{N_0 + \sigma_{n_c}^2}{\overline{E}_r + N_0 + \sigma_{n_c}^2} \qquad (4.40)$$

From Equation 4.39 it is obvious that as Θ increases, P_D always decreases. Observe furthermore that Θ is a monotonically increasing function of $\sigma_{n_c}^2$ as can be seen from the fact that

$$\frac{d\Theta}{d(\sigma_{n_c}^2)} = \frac{\overline{E}_r + N_0 + \sigma_{n_c}^2 - N_0 - \sigma_{n_c}^2}{(\overline{E}_r + N_0 + \sigma_{n_c}^2)^2}$$
$$= \frac{\overline{E}_r}{(\overline{E}_r + N_0 + \sigma_{n_c}^2)^2} \geq 0 \tag{4.41}$$

This means that as $\sigma_{n_c}^2$ increases, P_D always decreases for fixed P_F.

Using Equation 4.13 and the Cauchy-Schwarz inequality, we have that

$$\int_{-\infty}^{\infty} \tilde{S}_{\tilde{n}_c}(\omega) \left|\tilde{F}(\omega)\right|^2 d\omega \leq \left[\int_{-\infty}^{\infty} \tilde{S}_{\tilde{n}_c}^2(\omega)\, d\omega\right]^{\frac{1}{2}} \left[\int_{-\infty}^{\infty} \left|\tilde{F}(\omega)\right|^4 d\omega\right]^{\frac{1}{2}} \tag{4.42}$$

with equality if and only if

$$\tilde{S}_{\tilde{n}_c}(\omega) = \rho \left|\tilde{F}(\omega)\right|^2 \tag{4.43}$$

where ρ is an arbitrary constant.

Integrating both sides of of Equation 4.43, yields

$$\int_{-\infty}^{\infty} \tilde{S}_{\tilde{n}_c}(\omega)\, d\omega \equiv P_{n_c} = \rho \int_{-\infty}^{\infty} \left|\tilde{F}(\omega)\right|^2 d\omega \tag{4.44}$$

so that

$$\rho = \frac{P_{n_c}}{\int_{-\infty}^{\infty} \left|\tilde{F}(\omega)\right|^2 d\omega} \tag{4.45}$$

and the optimum solution for $\tilde{S}_{\tilde{n}_c}(\omega)$, which satisfies both the minimization of P_D and the power constraint of the noise interference, denoted as $\tilde{S}_{n_c}^{o}(\omega)$, can be written as

$$\tilde{S}^{o}_{n_c}(\omega) = \frac{P_{n_c}\left|\tilde{F}(\omega)\right|^2}{\int_{-\infty}^{\infty}\left|\tilde{F}(\omega)\right|^2 d\omega} \tag{4.46}$$

This means that the optimum noise interference PSD, depends on the envelope $\tilde{f}(t)$ that is transmitted.

Assuming that the complex envelope of the transmitted signal is given by Equation 3.22 the corresponding Fourier Transform can be written as

$$\tilde{F}(\omega) = \sqrt{T}\ \frac{\sin(\omega\frac{T}{2})}{(\omega\frac{T}{2})}\ \exp(-j\omega\frac{T}{2}) \rightarrow \tilde{f}(t) \tag{4.47}$$

and

$$\left|\tilde{F}(\omega)\right|^2 = T\,\frac{\sin^2(\omega\frac{T}{2})}{(\omega\frac{T}{2})^2} \tag{4.48}$$

The optimum noise interference PSD, can be specified as

$$\tilde{S}^{o}_{n_c}(\omega) = \frac{P_{n_c}T\dfrac{\sin^2(\omega\frac{T}{2})}{(\omega\frac{T}{2})^2}}{\int_{-\infty}^{\infty}\left|\tilde{F}(\omega)\right|^2 d\omega} \tag{4.49}$$

Since

$$\int_0^T\left|\tilde{f}(t)\right|^2 dt = \frac{1}{2\pi}\int_{-\infty}^{\infty}\left|\tilde{F}(\omega)\right|^2 d\omega = 1 \tag{4.50}$$

the optimum noise interference PSD is simply given by

$$\tilde{S}^{o}_{n_c}(\omega) = P_{n_c}T\frac{\sin^2(\omega\frac{T}{2})}{(\omega\frac{T}{2})^2} \tag{4.51}$$

so that

$$\sigma_{n_c}^2 = \frac{1}{2\pi}\int_{-\infty}^{\infty} \tilde{S}_{\tilde{n}_c}(\omega)\left|\tilde{F}(\omega)\right|^2 d\omega$$

$$= \frac{1}{2\pi} TP_{n_c} T \int_{-\infty}^{\infty} \frac{\sin^2(\omega\frac{T}{2})}{(\omega\frac{T}{2})^2} \frac{\sin^2(\omega\frac{T}{2})}{(\omega\frac{T}{2})^2} d\omega \qquad (4.52)$$

$$= 0.666\, TP_{n_c}$$

Therefore the performance of the receiver under signal and interference conditions described above, is given in terms of P_D and P_F as

$$P_D = P_F^{\left(\frac{1+0.666\,SNR\,JSR}{1+SNR+0.666\,SNR\,JSR}\right)} \qquad (4.53)$$

where SNR and JSR are defined in Equation 4.26 and Equation 4.27, respectively.

These results will be analyzed in more detail and presented graphically as ROS's in Chapter 5.

B. PERFORMANCE OF RECEIVER II.

The problem addressed here, has been mathematically described by the Equations 4.1 to Equation 4.3.

The optimum threshold test has been given in Chapter 2 by Equations 2.53 and 2.54 and the performance of the receiver that implements this test is given by Equations 2.48 and 2.56. The so-called SPLOT problem introduced in Chapter 2 yields a simpler solution for the optimum receiver and its performance as given by Equations 2.55 and 2.56. Specific performance evaluations can be carried out for the SPLOT problem under the assumption that the signal envelope takes the mathematical form given by Equation 3.22.

Now, based on the type of additive Gaussian noise PSD considered to be present under the two hypotheses, two cases are investigated below.

1. **Problem 1.**

The performance of the receiver shown in Figure 6 on page 20, and Figure 7 on page 21, which has been designed for the signal and noise model of Equation 4.1, can be evaluated when the additive noise is different under the two hypothesis, namely ACGN under the H_1 hypothesis and AWGN under the H_0 hypothesis. It is obvious that these receivers are no longer optimum for the now assumed signal and noise model.

In this case, the complex envelopes of the received waveform under the two hypotheses can be mathematically described as

$$\begin{aligned} H_1 &: \tilde{r}(t) = \sqrt{E_t}\,\tilde{b}\,\tilde{f}(t) + \tilde{n}(t) \qquad 0 \le t \le T \\ H_0 &: \tilde{r}(t) = \tilde{w}(t) \end{aligned} \tag{4.54}$$

where $\tilde{b}$ is a complex Gaussian random variable, which models the target and whose moments are given by Equation 2.23 and Equation 2.24, $\tilde{f}(t)$ is the complex envelope of the transmitted waveform, $\tilde{n}(t)$ is a zero mean Gaussian random process defined in Equation 4.2, and $\tilde{w}(t)$ is a zero mean white Gaussian process, independent of the colored noise $\tilde{n}_c(t)$.

In order to evaluate the performance of the receiver shown in Figure 6 on page 20, and Figure 7 on page 21, the probability density function of the signal at the receiver output conditioned on both hypotheses must be determined.

The correlator output is a complex Gaussian random variable, which defined by Equations 4.4 through Equation 4.6.

Obviously, since both $n_c(t)$ and $w(t)$ are assumed to be zero mean processes, and recalling that $\tilde{b}$ is a zero mean Gaussian r.v.,

$$E\{\tilde{r}_1/H_0\} = E\{\tilde{r}_1/H_1\} = 0 \tag{4.55}$$

and using the definitions introduced by Equations 4.8 and 4.9 the appropriate variances can be evaluated as

$$2\sigma_{n_0}^2 = E\left\{|\tilde{w}_1|^2/H_0\right\} = E\left\{\int_0^T\int_0^T \tilde{w}(t)\,\tilde{w}^*(u)\tilde{g}(t)\,\tilde{g}^*(u)\,dt\,du\right\}$$
$$= N_0\int_0^T |g(t)|^2\,dt \tag{4.56}$$

and since

$$E\{|\tilde{n}_1|^2\} = E\left\{\int_0^T\int_0^T \tilde{n}(t)\,\tilde{n}^*(u)\tilde{g}(t)\,\tilde{g}^*(u)\,dt\,du\right\}$$
$$= \int_0^T\int_0^T \tilde{K}_{\tilde{n}}(t\,,\,u)\tilde{g}(t)\,\tilde{g}^*(u)\,dt\,du$$
$$= \int_0^T \tilde{g}^*(t)\left[\int_0^T \tilde{K}_{\tilde{n}}(t\,,\,u)\,\tilde{g}(u)du\right]dt \tag{4.57}$$
$$= \int_0^T \tilde{f}(t)\,\tilde{g}^*(t)\,dt$$

then

$$2\sigma_{n_1}^2 = E\{|\tilde{r}_1|^2/H_1\} = E\left\{\left|\sqrt{E_t}\,\tilde{b}\int_0^T \tilde{f}(t)\tilde{g}^*(t)\,dt + \tilde{n}_1(t)\right|^2\right\}$$

$$= E_t|\tilde{b}|^2\left|\int_0^T \tilde{f}(t)\tilde{g}^*(t)\,dt\right|^2 + \int_0^T \tilde{f}(t)\tilde{g}^*(t)\,dt \qquad (4.58)$$

$$= E_r\left|\int_0^T \tilde{f}(t)\tilde{g}^*(t)\,dt\right|^2 + \int_0^T \tilde{f}(t)\tilde{g}^*(t)\,dt$$

Since $\tilde{r}_1$ is a complex Gaussian r.v., the p.d.f.'s of $\tilde{r}_1$ conditioned on the two hypotheses can be written as

$$f_{\tilde{r}_1/H_1}(\tilde{R}_1/H_1) = \frac{1}{2\pi\sigma_{n_1}^2}\exp\left\{-\frac{|\tilde{R}_1|^2}{2\sigma_{n_1}^2}\right\} \qquad (59)$$

$$f_{\tilde{r}_1/H_0}(\tilde{R}_1/H_0) = \frac{1}{2\pi\sigma_{n_0}^2}\exp\left\{-\frac{|\tilde{R}_1|^2}{2\sigma_{n_0}^2}\right\} \qquad (4.60)$$

The procedure carried out in Equations 4.14 to Equation 4.19 can be utilized here to obtain alternative expressions to the above p.d.f.'s. This yields

$$f_{m/H_1}(M/H_1) = \frac{1}{2\sigma_{n_1}^2}\exp\left\{-\frac{M}{2\sigma_{n_1}^2}\right\}u(m) \qquad (4.61)$$

$$f_{m/H_0}(M/H_0) = \frac{1}{2\sigma_{n_0}^2}\exp\left\{-\frac{M}{2\sigma_{n_0}^2}\right\}u(m) \qquad (4.62)$$

where the r.v. m is defined by Equation 4.17. Similar to the steps carried out by Equations 4.20 to 4.22, we obtain

$$P_F = \exp(-\frac{\gamma}{2\sigma_{n_0}^2})$$

and

$$P_D = \exp(-\frac{\gamma}{2\sigma_{n_1}^2})$$

so that

$$P_D = (P_F)^{2\sigma_{n_0}^2/2\sigma_{n_1}^2} \tag{4.65}$$

Using Equation 4.56 and Equation 4.58, the exponent of Equation 4.65 can be written as

$$\Gamma \equiv \frac{2\sigma_{n_0}^2}{2\sigma_{n_1}^2} = \frac{N_0 \int_0^T |\tilde{g}(t)|^2 \, dt}{\bar{E}_r \left[\int_0^T \tilde{f}(t)\, \tilde{g}^*(t)\, dt \right]^2 + \int_0^T \tilde{f}(t)\, \tilde{g}^*(t)\, dt} \tag{4.66}$$

From Equation 4.65 and Equation 4.66, we observe that as Γ increases P_D decreases for fixed P_F so that the analysis of ROC's can be equivalently replaced by analyzing the behavior of Γ.

Therefore the performance in terms of the parameter Γ of the receiver shown in Figure 6 on page 20 and Figure 7 on page 21, for the SPLOT problem and under the above stated hypotheses will be evaluated for four kinds of colored noise interference PSDs.

a. Bandlimited Constant Amplitude PSD.

In this case the jamming noise PSD is given in Equation 4.23. Then $\tilde{G}_\infty(j\omega)$ from Equation 2.55, becomes

$$\tilde{G}_{\infty}(\omega) = \frac{\left[\sqrt{T}\ \frac{\sin(\omega\frac{T}{2})}{(\omega\frac{T}{2})}\ \exp(-j\omega\frac{T}{2})\right]}{\left[N_0 + \frac{\pi}{w} P_{n_c}\right]} \qquad -w \le \omega \le w$$

$$= \frac{\left[\sqrt{T}\ \frac{\sin(\omega\frac{T}{2})}{(\omega\frac{T}{2})}\ \exp(-j\omega\frac{T}{2})\right]}{N_0} \qquad \omega < -w\ ,\ \omega > w \tag{4.67}$$

The Inverse Fourier Transform of $\tilde{G}_{\infty}(\omega)$ is obtained from

$$\tilde{g}(t) = \frac{\sqrt{T}}{N_0 + \frac{\pi}{w} P_{n_c}} \frac{1}{2\pi} \int_{-w}^{w} \frac{\sin(\omega\frac{T}{2})}{(\omega\frac{T}{2})} \exp[j\omega(t-\frac{T}{2})]\ d\omega +$$

$$+ \frac{\sqrt{T}}{2\pi N_0} \int_{-\infty}^{-w} \frac{\sin(\omega\frac{T}{2})}{(\omega\frac{T}{2})} \exp[j\omega(t-\frac{T}{2})]\ d\omega + \tag{4.68}$$

$$+ \frac{\sqrt{T}}{2\pi N_0} \int_{w}^{\infty} \frac{\sin(\omega\frac{T}{2})}{(\omega\frac{T}{2})} \exp[j\omega(t-\frac{T}{2})]\ d\omega$$

Since

$$\frac{T}{2\pi} \int_{-\infty}^{\infty} \left[\frac{\sin(\omega\frac{T}{2})}{(\omega\frac{T}{2})} \exp[j\omega(t-\frac{T}{2})] \right] d\omega = 1 \qquad 0 \le t \le T \tag{4.69}$$

$\tilde{g}(t)$ becomes

$$\tilde{g}(t) = \frac{1}{N_0\sqrt{T}}\,[u(t) - u(t-T)] -$$

$$-\frac{\sqrt{T}}{2\pi}\,\frac{P_{n_c}}{N_0(\frac{w}{\pi}N_0 + P_{n_c})}\int_{-w}^{w}\frac{\sin(\omega\frac{T}{2})}{(\omega\frac{T}{2})}\exp[j\omega(t-\frac{T}{2})]d\omega \tag{4.70}$$

so that

$$\int_0^T \tilde{f}(t)\tilde{g}^*(t)dt = \frac{1}{N_0}\,\frac{1}{\sqrt{T}}\,\frac{1}{\sqrt{T}}\int_0^T dt -$$

$$-\frac{\sqrt{T}}{2\pi}\,\frac{P_{n_c}}{N_0(\frac{w}{\pi}N_0 + P_{n_c})}\int_0^T\left[\int_{-w}^{w}\frac{1}{\sqrt{T}}\,\frac{\sin(\omega\frac{T}{2})}{(\omega\frac{T}{2})}\exp[-j\omega(t-\frac{T}{2})]d\omega\right]dt \tag{4.71}$$

$$= \frac{1}{N_0} - \frac{1}{2\pi}\,\frac{P_{n_c}}{N_0(\frac{w}{\pi}N_0 + P_{n_c})}\,T\int_{-w}^{w}\frac{\sin^2(\omega\frac{T}{2})}{(\omega\frac{T}{2})}\,d\omega$$

Defining now the normalized frequency w as

$$w \equiv \alpha\,\frac{2\pi}{T} \tag{4.72}$$

where α is a scalar, and changing variables, the integral in Equation 4.71 becomes

$$\int_{-w}^{w}\frac{\sin^2(\omega\frac{T}{2})}{(\omega\frac{T}{2})}\,d\omega = \frac{2\pi}{T}\int_{-\alpha}^{\alpha}\left[\frac{\sin\pi x}{\pi x}\right]^2 dx = \frac{2\pi}{T}\,n(\alpha) \tag{4.73}$$

where

$$n(\alpha) = \int_{-\alpha}^{\alpha}\left[\frac{\sin\pi x}{\pi x}\right]^2 dx \tag{4.74}$$

therefore

$$\int_0^T \tilde{f}(t)\tilde{g}^*(t)\,dt = \frac{1}{N_0} - \frac{P_{n_c} n(\alpha)}{N_0(\frac{w}{\pi} N_0 + P_{n_c})} = \frac{1}{N_0}\left[1 - n(\alpha)\,\frac{SNR\,JSR}{2\alpha + SNR\,JSR}\right] \tag{4.75}$$

Since the problem being analyzed assumes a long observation time, use of the approximation

$$\int_0^T |\tilde{g}(t)|^2\,dt \approx \int_0^\infty |\tilde{g}(t)|^2\,dt \tag{4.76}$$

is made so that by Parseval's Theorem, the integral in the numerator of Equation 4.66 can be evaluated

$$\int_0^T |\tilde{g}(t)|^2\,dt \approx \frac{T}{\left[N_0 + \frac{\pi}{w} P_{n_c}\right]^2}\,\frac{1}{2\pi}\int_{-w}^{w} \frac{\sin^2(\omega\frac{T}{2})}{(\omega\frac{T}{2})^2}\,d\omega + \frac{T}{2\pi N_0^2}\left[\int_{-\infty}^{-w} \frac{\sin^2(\omega\frac{T}{2})}{(\omega\frac{T}{2})^2}\,d\omega + \int_{w}^{\infty} \frac{\sin^2(\omega\frac{T}{2})}{(\omega\frac{T}{2})^2}\,d\omega\right] = \frac{1}{N_0^2}\left[(1 - n(\alpha)) + n(\alpha)\left(\frac{2\alpha}{2\alpha + SNR\,JSR}\right)^2\right] \tag{4.77}$$

Therefore

$$\Gamma = \frac{(1 - n(\alpha)) + n(\alpha)\left(\frac{2\alpha}{2\alpha + SNR\,JSR}\right)^2}{SNR\left(1 - n(\alpha)\,\frac{SNRJSR}{2\alpha + SNR\,JSR}\right)^2 + \left(1 - n(\alpha)\,\frac{SNR\,JSR}{2\alpha + SNR\,JSR}\right)} \tag{4.78}$$

As shown in Appendix B, the worst receiver performance occurs for $\alpha = 1$, so that evaluating Equation 4.78 with $\alpha = 1$ results in

$$\Gamma = \frac{0.1 + 0.9\left(\frac{2}{2 + SNR\,JSR}\right)^2}{SNR\left(1 - 0.9\,\frac{SNR\,JSR}{2 + SNR\,JSR}\right)^2 + \left(1 - 0.9\,\frac{SNR\,JSR}{2 + SNR\,JSR}\right)} \tag{4.79}$$

b. Sinc Squared Shaped PSD.

In this case the jamming noise PSD is given in Equation 4.28. As a result of this

$$\tilde{G}_{\infty}(\omega) = \frac{\sqrt{T}\,\frac{\sin(\omega\frac{T}{2})}{(\omega\frac{T}{2})}\,\exp(-j\omega\frac{T}{2})}{N_0 + TP_{n_c}\,\frac{\sin^2(\omega\frac{T}{2})}{(\omega\frac{T}{2})^2}} \tag{4.80}$$

Evaluating now the Inverse Fourier Transform of $\tilde{G}_{\infty}(\omega)$ results in

$$\tilde{g}(t) = \frac{\sqrt{T}}{2\pi}\int_{-\infty}^{\infty}\left[\frac{\frac{\sin(\omega\frac{T}{2})}{(\omega\frac{T}{2})}\,\exp[j\omega(t-\frac{T}{2})]}{N_0 + TP_{n_c}\,\frac{\sin^2(\omega\frac{T}{2})}{(\omega\frac{T}{2})^2}}\right]d\omega \qquad 0 \le t \le T \tag{4.81}$$

Therefore

$$\int_0^T \tilde{f}(t)\tilde{g}^*(t)dt =$$

$$= \frac{\sqrt{T}}{2\pi} \int_0^T \frac{1}{\sqrt{T}} \left[\int_{-\infty}^{\infty} \frac{\frac{\sin(\omega \frac{T}{2})}{(\omega \frac{T}{2})} \exp[j\omega(t - \frac{T}{2})]}{N_0 + TP_{n_c} \frac{\sin^2(\omega \frac{T}{2})}{(\omega \frac{T}{2})^2}} d\omega \right] dt \tag{4.82}$$

$$= \frac{T}{2\pi} \int_{-\infty}^{\infty} \frac{\left[\frac{\sin(\omega \frac{T}{2})}{(\omega \frac{T}{2})} \right]^2}{N_0 + TP_{n_c} \frac{\sin^2(\omega \frac{T}{2})}{(\omega \frac{T}{2})^2}} d\omega$$

A change of variables results in

$$\int_0^T \tilde{f}(t)\tilde{g}^*(t)dt = \frac{1}{N_0} D_2 \tag{4.83}$$

where

$$D_2 = \int_{-\infty}^{\infty} \left[\frac{\frac{\sin^2(\pi x)}{(\pi x)^2}}{1 + SNR\ JSR\ \frac{\sin^2(\pi x)}{(\pi x)^2}} \right] dx \tag{4.84}$$

and SNR and JSR are given in Equation 4.26 and Equation 4.27, respectively.

Using Parseval's Theorem and the approximation of Equation 4.76 yields

$$\int_0^T |\tilde{g}(t)|^2 \, dt \approx \frac{1}{N_0^2} \int_{-\infty}^{\infty} \left[\frac{\frac{\sin \pi x}{\pi x}}{1 + SNR\, JSR \frac{\sin^2 \pi x}{\pi x^2}} \right]^2 dx \tag{4.85}$$

$$= \frac{1}{N_0^2} N_2$$

where

$$N_2 = \int_{-\infty}^{\infty} \left[\frac{\frac{\sin(\pi x)}{\pi x}}{1 + SNR\, JSR \frac{\sin^2(\pi x)}{(\pi x)^2}} \right]^2 dx \tag{4.86}$$

so that

$$\Gamma = \frac{\frac{1}{N_0} N_2}{\frac{\overline{E}_r}{N_0^2} D_2^2 + \frac{1}{N_0} D_2} = \frac{N_2}{SNR\, D_2^2 + D_2} \tag{4.87}$$

c. Butterworth Shaped PSD.

In this case the jamming noise PSD is given in Equation 4.31. As a result of this

$$\tilde{G}_\infty(\omega) = \frac{\left[\sqrt{T} \frac{\sin(\omega \frac{T}{2})}{(\omega \frac{T}{2})} \exp(-j\omega \frac{T}{2}) \right]}{\left[N_0 + \frac{2 P_{n_c} \alpha}{\alpha^2 + \omega^2} \right]} \tag{4.88}$$

and via inverse Fourier Transformation

$$\tilde{g}(t) = \frac{\sqrt{T}}{2\pi} \int_{-\infty}^{\infty} \left[\frac{\frac{\sin(\omega \frac{T}{2})}{(\omega \frac{T}{2})} \exp[j\omega(t - \frac{T}{2})]}{N_0 + \frac{2 P_{n_c} \alpha}{\alpha^2 + \omega^2}} \right] d\omega \qquad 0 \le t \le T \quad (4.89)$$

Therefore

$$\int_0^T \tilde{f}(t)\tilde{g}^*(t)dt =$$

$$= \frac{1}{2\pi} \int_{-\infty}^{\infty} \left[\frac{\left(\frac{\sin(\omega \frac{T}{2})}{(\omega \frac{T}{2})} \exp(j\omega \frac{T}{2}) \right)}{\left(N_0 + \frac{2 P_{n_c} \alpha}{\alpha^2 + \omega^2} \right)} \left[\int_0^T \exp(-j\omega t)\, dt \right] \right] d\omega$$

$$= \frac{1}{N_0} \int_{-\infty}^{\infty} \left[\frac{\left(\frac{\sin^2(\pi x)}{(\pi x)^2} \right)}{\left(1 + SNR\, JSR\, \frac{1}{T} \frac{2\alpha}{\alpha^2 + \frac{4\pi^2}{T^2} x^2} \right)} \right] dx \quad (4.90)$$

$$= \frac{1}{N_0} \int_{-\infty}^{\infty} \frac{\frac{\sin^2(\pi x)}{(\pi x)^2}}{1 + \frac{1}{\pi}\, SNR\, JSR\, \frac{\beta}{\beta^2 + x^2}} dx$$

$$= \frac{1}{N_0} D_3$$

where

$$\alpha \equiv \beta \frac{2\pi}{T} \quad (4.91)$$

and β is a scalar, SNR and JSR are defined in Equation 4.26 and Equation 4.27, respectively and

$$D_3 = \int_{-\infty}^{\infty} \frac{\dfrac{\sin^2(\pi x)}{(\pi x)^2}}{1 + \frac{1}{\pi} SNR\, JSR\, \dfrac{\beta}{\beta^2 + x^2}}\, dx \tag{4.92}$$

Using Parseval's Theorem and the approximation of Equation 4.76 yields

$$\begin{aligned} \int_0^T \left|\tilde{g}(t)\right|^2 dt &\approx \frac{1}{N_0^2} \int_{-\infty}^{\infty} \frac{\dfrac{\sin^2(\pi x)}{(\pi x)^2}}{\left(1 + \frac{1}{\pi} SNR\, JSR\, \dfrac{\beta}{\beta^2 + x^2}\right)}\, dx \\ &= \frac{1}{N_0^2} N_3 \end{aligned} \tag{4.93}$$

where

$$N_3 = \int_{-\infty}^{\infty} \frac{\dfrac{\sin^2(\pi x)}{(\pi x)^2}}{\left[1 + \frac{1}{\pi} SNR\, JSR\, \dfrac{\beta}{\beta^2 + x^2}\right]^2}\, dx \tag{4.94}$$

Therefore

$$\Gamma = \frac{\frac{1}{N_0} N_3}{\frac{\bar{E}_r}{N_0^2} D_3^2 + \frac{1}{N_0} D_3} = \frac{N_3}{SNR\, D_3^2 + D_3} \tag{4.95}$$

d. Triangular Shaped PSD.

In this case the jamming noise PSD is given in Equation 4.34. Then

$$\tilde{G}_{\infty}(\omega) = \frac{\sqrt{T}\ \dfrac{\sin(\omega\frac{T}{2})}{(\omega\frac{T}{2})}\ \exp(-j\omega\frac{T}{2})}{N_0 + \dfrac{P_{n_c}}{\omega_0}\left(1 - \dfrac{|\omega|}{\omega_0}\right)} \qquad -w \le \omega \le w$$

$$= \frac{\sqrt{T}\ \dfrac{\sin(\omega\frac{T}{2})}{(\omega\frac{T}{2})}\ \exp(-j\omega\frac{T}{2})}{N_0} \qquad \omega \le -w\ ,\ \omega \ge w \tag{4.96}$$

and via inverse Fourier Transformation, we obtain

$$\tilde{g}(t) = \frac{\sqrt{T}}{2\pi}\int_{-\omega_0}^{\omega_0}\left[\frac{\dfrac{\sin(\omega\frac{T}{2})}{(\omega\frac{T}{2})}\ \exp[j\omega(t-\frac{T}{2})]}{N_0 + \dfrac{P_{n_c}}{\omega_0}\left(1 - \dfrac{|\omega|}{\omega_0}\right)}\right]d\omega +$$

$$+ \frac{\sqrt{T}}{2\pi N_0}\int_{-\infty}^{-\omega_0}\frac{\sin(\omega\frac{T}{2})}{(\omega\frac{T}{2})}\ \exp[j\omega(t-\frac{T}{2})]\ d\omega + \tag{4.97}$$

$$+ \frac{\sqrt{T}}{2\pi N_0}\int_{\omega_0}^{\infty}\frac{\sin(\omega\frac{T}{2})}{(\omega\frac{T}{2})}\ \exp[j\omega(t-\frac{T}{2})]\ d\omega$$

From Equation 4.69, $\tilde{g}(t)$ becomes

$$\tilde{g}(t) = \frac{1}{N_0\sqrt{T}}[u(t) - u(t-T)] +$$

$$+ \frac{\sqrt{T}}{2\pi}\int_{-\omega_0}^{\omega_0} \frac{\left(\frac{\sin(\omega\frac{T}{2})}{(\omega\frac{T}{2})} \exp[j\omega(t-\frac{T}{2})]\right)}{\left[N_0 + \frac{P_{n_c}}{\omega_0}\left(1 - \frac{|\omega|}{\omega_0}\right)\right]} d\omega \qquad (4.98)$$

$$- \frac{\sqrt{T}}{2\pi N_0}\int_{-\omega_0}^{\omega_0}\left[\frac{\sin(\omega\frac{T}{2})}{(\omega\frac{T}{2})} \exp[j\omega(t-\frac{T}{2})]\right] d\omega$$

Therefore

$$\int_0^T \tilde{f}(t)\,\tilde{g}^*(t)\,dt =$$

$$= \frac{1}{N_0}\,\frac{1}{\sqrt{T}}\,\frac{1}{\sqrt{T}}\int_0^T dt +$$

$$+ \frac{\sqrt{T}}{2\pi}\int_0^T\left[\int_{-\omega_0}^{\omega_0}\frac{1}{\sqrt{T}}\,\frac{\left(\frac{\sin(\omega\frac{T}{2})}{(\omega\frac{T}{2})} \exp[-j\omega(t-\frac{T}{2})]\right)}{\left[N_0 + \frac{P_{n_c}}{\omega_0}\left(1 - \frac{|\omega|}{\omega_0}\right)\right]} d\omega\right] dt \qquad (4.99)$$

$$- \frac{\sqrt{T}}{2\pi}\int_0^T\left[\int_{-\omega_0}^{\omega_0}\frac{1}{\sqrt{T}}\left[\frac{\sin(\omega\frac{T}{2})}{(\omega\frac{T}{2})} \exp[-j\omega(t-\frac{T}{2})]\right] d\omega\right] dt$$

$$= \frac{1}{N_0} + \frac{2}{\pi N_0} D_3$$

where

$$D_3 = \int_0^T \left[\frac{SNR\,JSR\,(\frac{x}{\varepsilon} - 1)}{2\pi\varepsilon + SNR\,JSR\,(1 - \frac{x}{\varepsilon})} \frac{\sin^2(\pi x)}{(\pi x)^2} \right] dx$$

ε is a scalar related to ω_0 according to

$$\omega_0 \equiv \varepsilon \frac{2\pi}{T} \tag{4.101}$$

and SNR and JSR have been defined by Equations 4.26 and 4.27 respectively.

Again, from the approximation of Equation 4.76 and using Parseval's Theorem to evaluate the appropriate integral, we obtain

$$\begin{aligned}
\int_0^T |\tilde{g}(t)|^2\, dt \approx \frac{1}{2\pi} \int_{-w}^{w} & \frac{\left[T \frac{\sin^2(\omega \frac{T}{2})}{(\omega \frac{T}{2})^2} \right]}{\left[N_0 + \frac{P_{n_c}}{\omega_0} \left(1 - \frac{|\omega|}{\omega_0} \right) \right]^2} d\omega + \\
& + \frac{1}{2\pi N_0^2} \int_{-\infty}^{-w} T \frac{\sin^2(\omega \frac{T}{2})}{(\omega \frac{T}{2})^2} d\omega + \\
& + \frac{1}{2\pi N_0^2} \int_{w}^{\infty} T \frac{\sin^2(\omega \frac{T}{2})}{(\omega \frac{T}{2})^2} d\omega \\
& = \frac{1}{N_0^2} [1 - n(\varepsilon)] + \frac{1}{N_0^2} N_3
\end{aligned} \tag{4.102}$$

where

$$N_3 = \int_{-\varepsilon}^{\varepsilon} \frac{\frac{\sin^2 \pi x}{\pi x^2}}{\left[1 + \frac{1}{2\pi\varepsilon} SNR\,JSR \left(1 - \frac{|x|}{\varepsilon} \right) \right]^2} dx \tag{4.103}$$

and $n(\,.\,)$ is defined in Equation 4.74.

Therefore

$$\Gamma = \frac{\frac{1}{N_0}[1 - n(\varepsilon) + N_3]}{\frac{\bar{E}_r}{N_0^2}\left[1 + \frac{2}{\pi} D_3\right]^2 + \frac{1}{N_0}\left[1 + \frac{2}{\pi} D_3\right]} \tag{4.104}$$

$$= \frac{[1 - n(\varepsilon) + N_3]}{SNR\left[1 + \frac{2}{\pi} D_3\right]^2 + \left[1 + \frac{2}{\pi} D_3\right]}$$

As shown in Appendix B, the worst receiver performance occurs for $\varepsilon = 1$ and therefore Equation 4.104 becomes

$$\Gamma = \frac{(0.1 + N_3)}{SNR[1 + 0.636D_3]^2 + [1 + 0.636D_3]}$$

2. Problem 2.

The problem which is mathematically described in Equation 4.1 and the corresponding performance of the receiver shown in Figure 6 on page 20 and Figure 7 on page 21, specified by Equation 2.48 and Equation 2.56, is now evaluated for four different kinds of colored noise PSD.

a. Bandlimited Constant Amplitude PSD.

Using the results in Equation 4.75, Δ becomes

$$\Delta = \frac{\bar{E}_r}{N_0} - n(\alpha) \frac{P_{n_c} \bar{E}_r}{N_0(\frac{w}{\pi} N_0 + P_{n_c})}$$

$$= \frac{\bar{E}_r}{N_0} - n(\alpha) \frac{\bar{E}_r}{N_0} \frac{SNR\, JSR}{\frac{\alpha}{\pi}\frac{2\pi}{T} T + SNR\, JSR} \tag{4.106}$$

$$= SNR - n(\alpha) \frac{JSR\,(SNR)^2}{2\alpha + JSR\, SNR}$$

where SNR and JSR are defined in Equation 4.26 and Equation 4.27, respectively.

Appendix B is devoted to investigating how Δ behaves as a function of α. It is demonstrated there that when $\alpha = 1$ Δ is minimized, which results in the worst receiver performance. Therefore evaluating Δ when $\alpha = 1$ results in

$$\Delta = SNR - 0.9 \frac{JSR\,(SNR)^2}{2 + JSR\,SNR} \tag{4.107}$$

Furthermore, it can be proved that P_D is a non-increasing function of JSR. That is

$$P_D = (P_F)^{\left(\frac{1}{1+\Delta}\right)} \tag{4.108}$$

and taking the first derivative we have

$$\begin{aligned}
\frac{dP_D}{d(JSR)} &= \frac{d\Delta(JSR)}{d(JSR)} (P_F)^{\frac{1}{1+\Delta}} \ln(P_F) \frac{d\left(\frac{1}{1+\Delta}\right)}{d\Delta} \\
&= 0.9 \frac{(SNR)^2(2 + JSRSNR) - JSR(SNR)^3}{(2 + JSR\,SNR)^2} (P_F)^{\frac{1}{1+\Delta}} \ln(P_F) \frac{1}{(1+\Delta)^2} \\
&= \ln(P_F) \left\{ \frac{1.8(SNR)^2}{(2 + JSR\,SNR)^2} (P_F)^{\frac{1}{1+\Delta}} \frac{1}{(1+\Delta)^2} \right\}
\end{aligned} \tag{4.109}$$

For $0 \le P_F \le 1$, $\ln(P_F) \le 0$, and $(P_F)^{\frac{1}{1+\Delta}} \ge 0$, this demonstrates that

$$\frac{dP_D}{d(JSR)} \le 0 \tag{4.110}$$

so that indeed P_D is a non-increasing function of JSR, which means that as JSR grows, P_D can at best remain constant, but is most likely to decrease. This clearly shows that increasing the colored noise power transmitted by the noise makers, the performance of the receiver is degraded.

b. Sinc Squared Shaped PSD.

Using the result in Equation 4.83, Δ can be evaluated as

$$\Delta = SNR \int_{-\infty}^{\infty} \frac{\frac{\sin^2(\pi x)}{(\pi x)^2}}{1 + SNR\, JSR\, \frac{\sin^2(\pi x)}{(\pi x)^2}}\, dx \tag{4.111}$$

where SNR and JSR have been defined in Equation 4.26 and Equation 4.27, respectively. The mathematical form of Δ and its dependence on JSR make it simple to prove that P_D is a non-increasing function of JSR.

Using Equation 4.108 and 4.111, and taking the first derivative we have

$$\frac{dP_D}{d(JSR)} = \frac{d\Delta(JSR)}{d(JSR)} (P_F)^{\frac{1}{1+\Delta}} \ln(P_F) \frac{d\left(\frac{1}{1+\Delta}\right)}{d\Delta}$$

$$= SNR \int_{-\infty}^{\infty} \left[\frac{-SNR\, \frac{\sin^4(\pi x)}{(\pi x)^4}}{\left(1 + JSR\, SNR\, \frac{\sin^2(\pi x)}{(\pi x)^2}\right)^2} \right] dx (P_F)^{\frac{1}{1+\Delta}} \ln(P_F) \frac{-1}{(1+\Delta)^2} \tag{4.112}$$

$$= \ln(P_F) \left\{ (SNR)^2 \int_{-\infty}^{\infty} \frac{\frac{\sin^4(\pi x)}{(\pi x)^4}}{\left(1 + JSR\, SNR\, \frac{\sin^2(\pi x)}{(\pi x)^2}\right)^2} dx\, (P_F)^{\frac{1}{1+\Delta}} \frac{1}{(1+\Delta)^2} \right\}$$

It is obvious however that

$$\int_{-\infty}^{\infty} \frac{\pi\, \frac{\sin^4(\pi x)}{(\pi x)^4}}{\left[1 + JSR\, SNR\, \frac{\sin^2(\pi x)}{(\pi x)^2}\right]^2} > 0 \tag{4.113}$$

Since $(P_F)^{\frac{1}{1+\Delta}} > 0$ and $\ln(P_F) \leq 0$ for $0 \leq P_F \leq 1$, it can be seen that

$$\frac{dP_D}{d(JSR)} \leq 0 \tag{4.114}$$

and therefore P_D is a non-increasing function of JSR. This clearly shows that increasing the colored noise power transmitted by the noise makers, the performance of the receiver is degraded.

c. *Butterworth Shaped PSD.*

Using Equation 4.90, Δ can be evaluated as

$$\Delta = SNR \int_{-\infty}^{\infty} \frac{\dfrac{\sin^2(\pi x)}{(\pi x)^2}}{1 + \dfrac{1}{\pi}\, SNR\, JSR\, \dfrac{\beta}{\beta^2 + x^2}}\, dx \tag{4.115}$$

In Appendix B the behavior of Δ as a function of β is investigated. It is shown therein that for $\beta = 1$, Δ is minimized and therefore the receiver performance becomes worst. so that evaluation of P_D as a function of P_F is carried out for $\beta = 1$. Furthermore, it is now proved that P_D is a non-increasing function of JSR. Taking the first derivative we have,

$$\frac{dP_D}{d(JSR)} = \frac{d\Delta(JSR)}{d(JSR)} (P_F)^{\frac{1}{1+\Delta}} \ln(P_F) \frac{d\left(\dfrac{1}{1+\Delta}\right)}{d\Delta}$$

$$= SNR \int_{-\infty}^{\infty} \frac{-\dfrac{1}{\pi} SNR \dfrac{\sin^2(\pi x)}{(\pi x)^2} \dfrac{\beta}{\beta^2 + x^2}}{\left[1 + \dfrac{1}{\pi} JSR\, SNR \dfrac{\beta}{\beta^2 + x^2}\right]^2} dx\, (P_F)^{\frac{1}{1+\Delta}} \ln(P_F) \frac{-1}{(1+\Delta)^2} \tag{4.116}$$

$$= \ln(P_F) \left\{ (SNR)^2 \int_{-\infty}^{\infty} \frac{\dfrac{1}{\pi} \dfrac{\sin^2(\pi x)}{(\pi x)^2} \dfrac{\beta}{\beta^2 + x^2}}{\left[1 + \dfrac{1}{\pi} JSR\, SNR \dfrac{\beta}{\beta^2 + x^2}\right]^2} dx\, (P_F)^{\frac{1}{1+\Delta}} \frac{1}{(1+\Delta)^2} \right\}$$

Since

$$\int_{-\infty}^{\infty} \frac{\frac{1}{\pi}\,\frac{\sin^2(\pi x)}{(\pi x)^2}\,\frac{\beta}{\beta^2 + x^2}}{\left[1 + \frac{1}{\pi} JSR\, SNR \frac{\beta}{\beta^2 + x^2}\right]^2} dx > 0 \qquad (4.117)$$

and $(P_F)^{\frac{1}{1+\Delta}} > 0$ while $\ln(P_F) \leq 0$ for $0 \leq P_F \leq 1$, results in

$$\frac{dP_D}{d(JSR)} \leq 0 \qquad (4.118)$$

Therefore P_D is a non-increasing function of JSR. This clearly shows that increasing the colored noise power transmitted by the noise makers, the performance of the receiver is degraded.

d. Triangular Shaped PSD.

Using the result in Equation 4.99, Δ can be evaluated as

$$\Delta = SNR + 2\,SNR \int_0^{\varepsilon} \left[\frac{SNR\, JSR\,(\frac{x}{\varepsilon} - 1)}{2\pi\varepsilon + SNR\, JSR\,(1 - \frac{x}{\varepsilon})} \frac{\sin^2(\pi x)}{(\pi x)^2} \right] dx \qquad (4.119)$$

The behavior of Δ as a function of ε is investigated in Appendix B. As before, performance will be evaluated for $\varepsilon = 1$, which is shown to minimize Δ and therefore yields the worst receiver performance. Furthermore, the next few steps prove that P_D is a non-increasing function of JSR, by evaluating

$$\frac{dP_D}{d(JSR)} = \frac{d\Delta(JSR)}{d(JSR)} (P_F)^{\frac{1}{1+\Delta}} \ln(P_F) \frac{d\left(\frac{1}{1+\Delta}\right)}{d\Delta}$$

$$= 2(SNR)^2 \int_0^{\varepsilon} \left[\frac{-2\pi\varepsilon[(1-\frac{x}{\varepsilon\pi}) \frac{\sin^2(\pi x)}{(\pi x)^2}]}{[2\varepsilon\pi - SNR\, JSR(1-\frac{x}{\varepsilon})]^2} \right] dx (P_F)^{\frac{1}{1+\Delta}} \ln(P_F) \frac{1}{(1+\Delta)^2} \qquad (4.120)$$

$$= \ln(P_F) \left\{ \frac{2}{\pi} (SNR)^2 \int_0^{\varepsilon} \left[\frac{2\pi\varepsilon[(1-\frac{x}{\varepsilon}) \frac{\sin^2(\pi x)}{(\pi x)^2}]}{[2\pi\varepsilon - SNR\, JSR(1-\frac{x}{\varepsilon})]^2} \right] dx (P_F)^{\frac{1}{1+\Delta}} \frac{1}{(1+\Delta)^2} \right\}$$

Since

$$\int_0^{\varepsilon} \left[\frac{2\pi\varepsilon[(1-\frac{x}{\varepsilon}) \frac{\sin^2(\pi x)}{(\pi x)^2}]}{[2\pi\varepsilon - SNR\, JSR\,(1-\frac{x}{\varepsilon})]^2} \right] dx \; > 0 \qquad (4.121)$$

whereas $(P_F)^{(\frac{1}{1+\Delta})} > 0$ and $\ln(P_F) \leq 0$ for $0 \leq P_F \leq 1$, results in

$$\frac{dP_D}{d(JSR)} \leq 0 \qquad (4.122)$$

so that P_D is a non-increasing function of JSR. This clearly shows that increasing the colored noise power transmitted by the noise makers, the performance of the receiver is degraded.

These results will be analyzed in more detail and presented graphically as ROC's in Chapter 5.

V. RESULTS

A. TARGET MODEL A.

1. Problem 1.

Given that P_D as a function of P_F is given by Equation 3.36, the ROC's for the suboptimum receiver can be obtained, using numerical methods.

In Figure 8 on page 64, Figure 9 on page 65, Figure 10 on page 66, and Figure 11 on page 67, the ROC's are presented for four different values of SNR, the Signal-to-Noise Ratio, namely 0dB, 5dB, 10 dB and 15 dB, respectively. In each figure, the ROC's are plotted for three different values of JSR, the Jamming-to-Signal Ratio, namely 0, 0dB and 10 dB. The first value of JSR, corresponds to the absence of noise interference for comparison purposes.

Observe that for low to moderate values of SNR, any amount of jamming noise power actually improves the performance of the receiver. As the Signal-to-Noise Ratio increases (Figure 10 on page 66), some amount of performance degradation is achieved, but again as JSR is increased, which corresponds to more target generated noise power at the input of the receiver, the performance is improved. The limited amount of performance degradation achieved is more evident for higher values of SNR (as demonstrated by Figure 10 on page 66), for which SNR takes a value of 15 dB. Therefore, there are cases where an optimum value of JSR exists that achieves the maximum possible receiver performance degradation, for given values of SNR and P_F. However, even in the case where is some performance degradation is achieved, the receiver still operates with a relatively high value of P_D with corresponding values of P_F in the order of 10^{-3}, which is still high for a radar receiver.

Since the noise interference power that is needed in order to degrade the performance of the receiver is a function of both P_F and SNR, and the target attempting to generate this noise interference has no prior knowledge of those values, it is apparent that this form of receiver performance degradation is not very effective or practical.

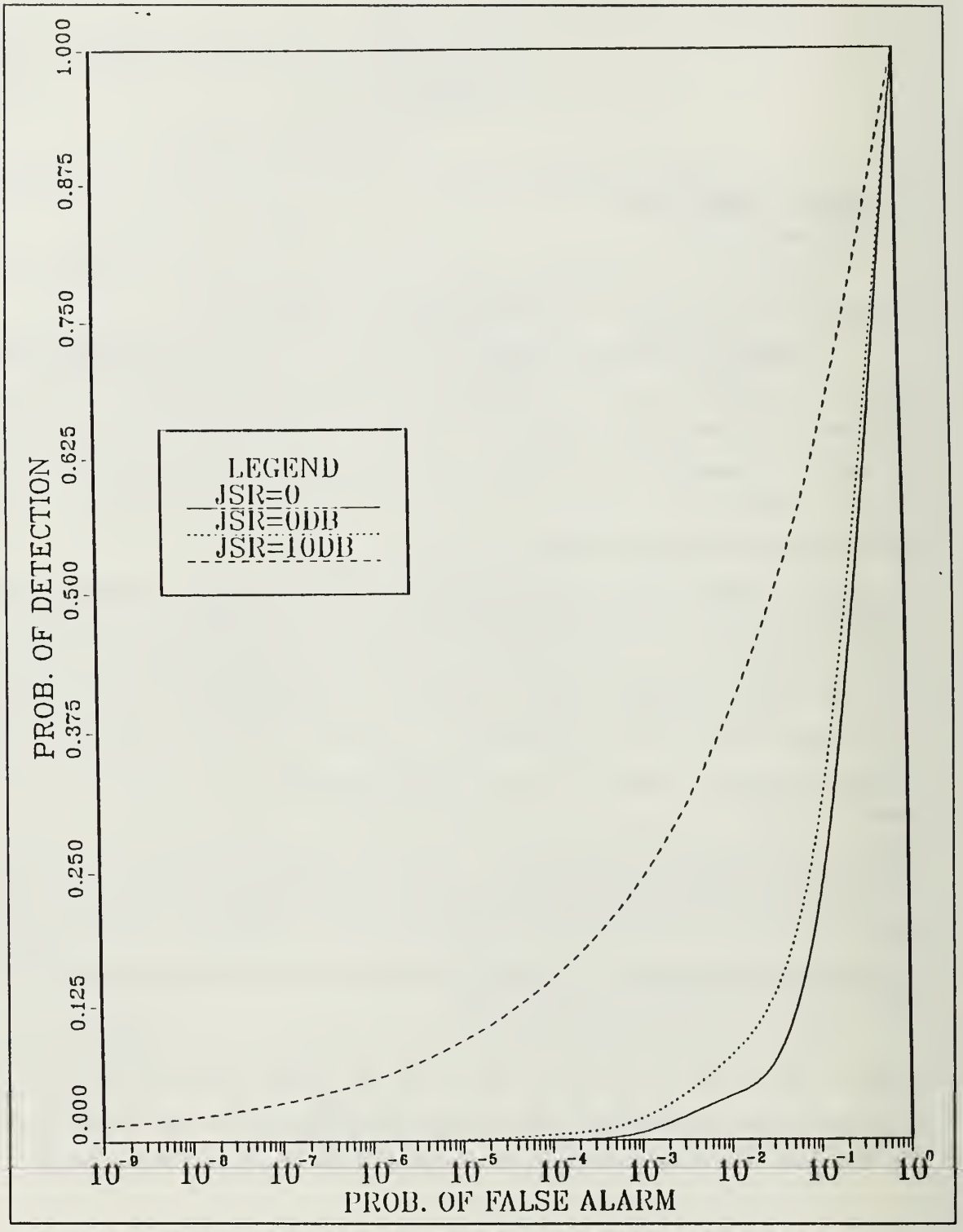

Figure 8. Optimum White Receiver, H_1 Colored H_0 White SNR = 0 dB.

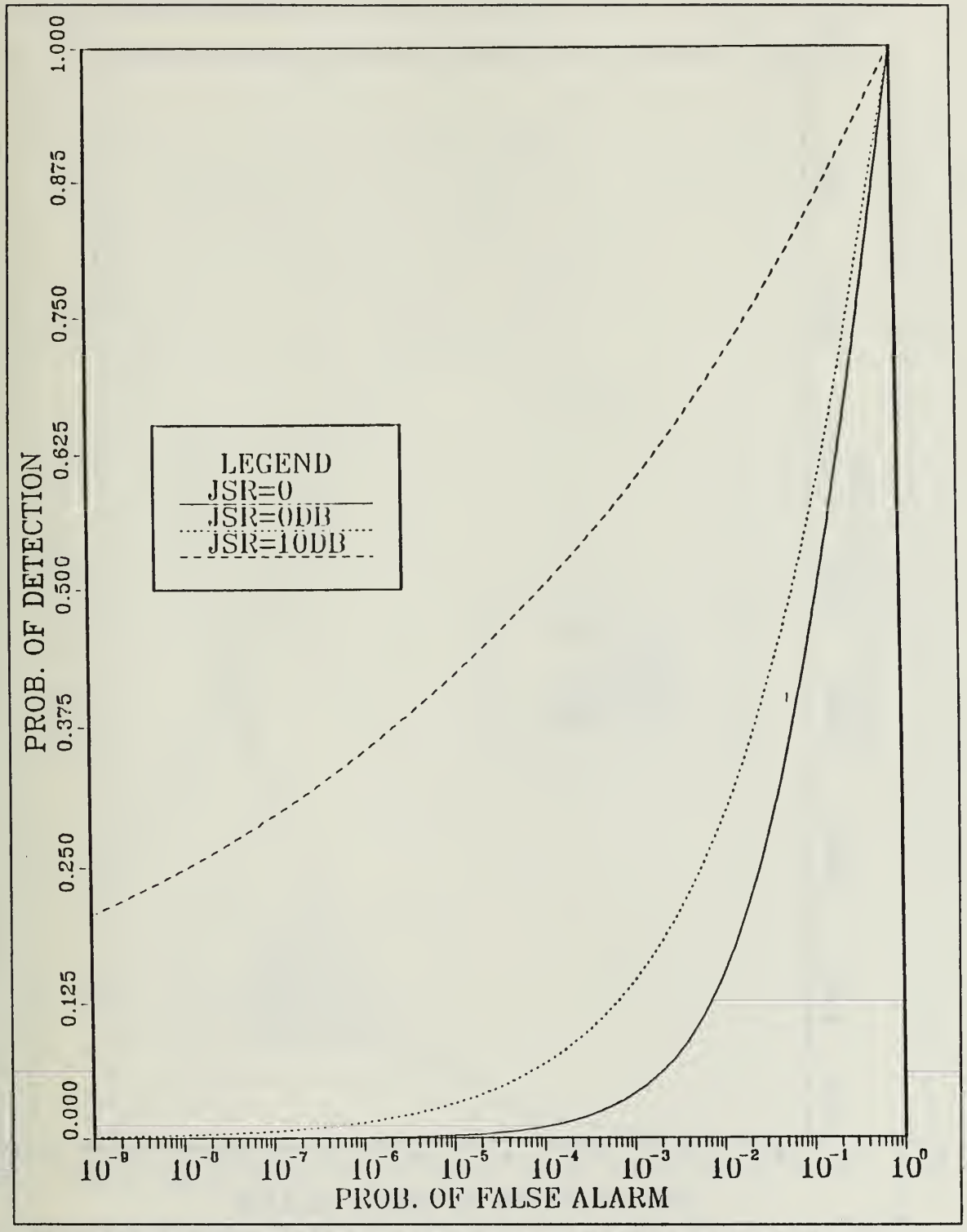

Figure 9. Optimum White Receiver, H_1 Colored H_0 White SNR = 5 dB.

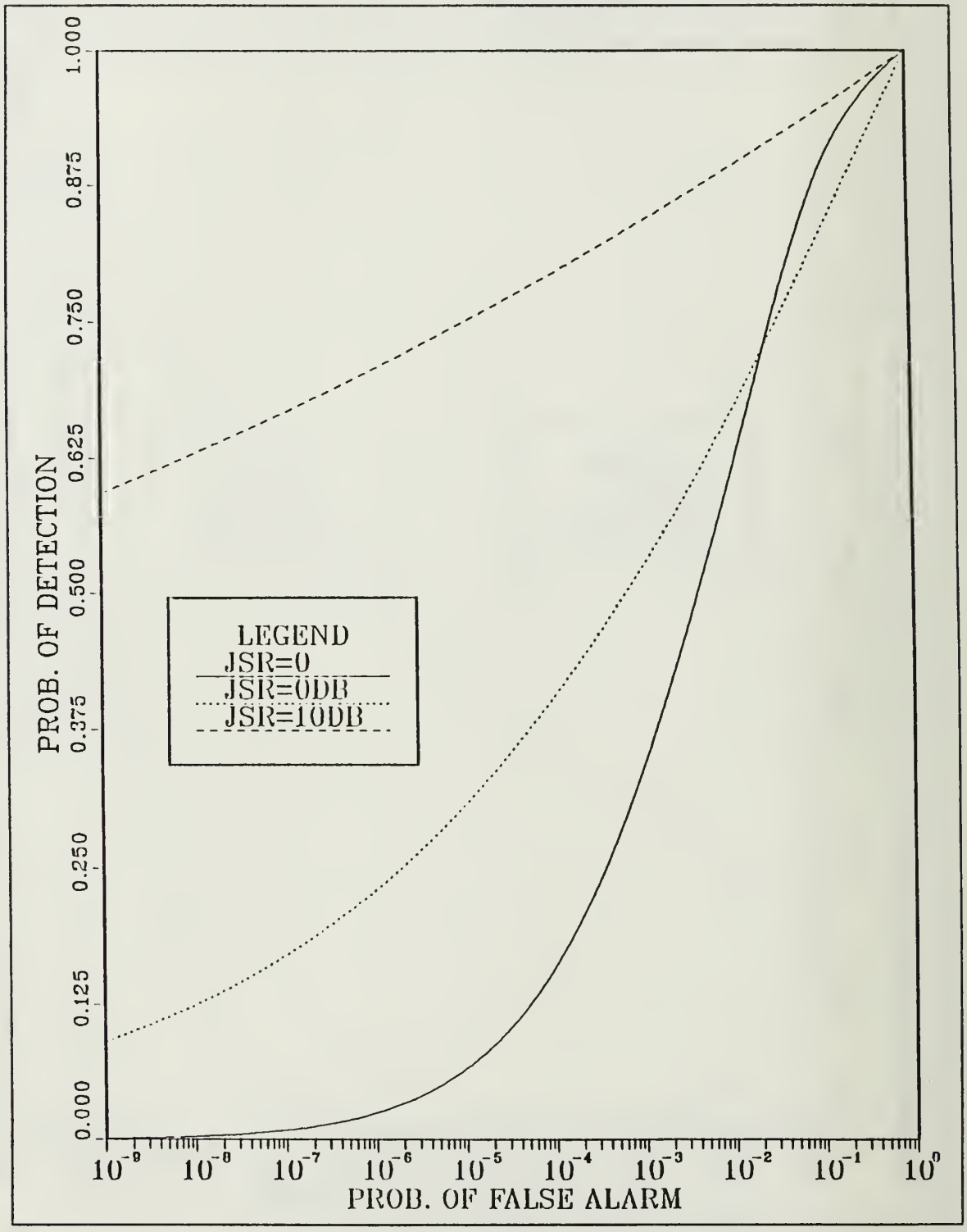

Figure 10. Optimum White Receiver, H_1 Colored H_0 White SNR = 10 dB.

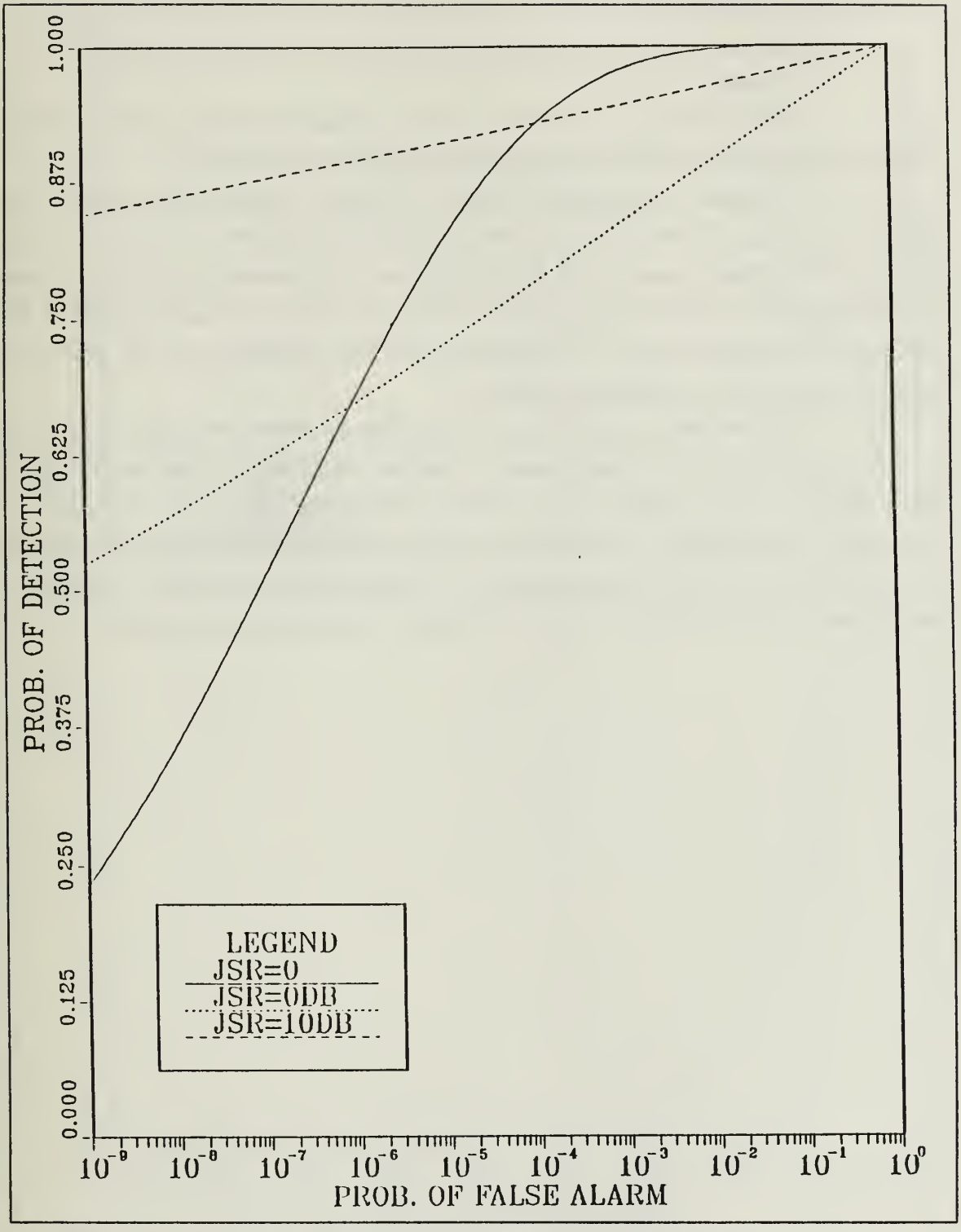

Figure 11. Optimum White Receiver, H_1 Colored H_0 White SNR = 15 dB.

B. TARGET MODEL B.

1. Receiver I.

a. Problem 1.

Given that P_D as a function of P_F is given by Equation 4.30, the ROC's for the suboptimum receiver can be evaluated using numerical methods.

In Figure 12 on page 69, Figure 13 on page 70, Figure 14 on page 71, and Figure 15 on page 72, the ROC's are presented for four different values of SNR, the Signal-to-Noise Ratio, namely 0 dB, 5 dB, 10 dB and 15 dB, respectively. In each figure, the performance is shown for three different values of JSR, the Jamming-to-Signal Ratio, namely 0, 0 dB and 10 dB. The first value of JSR, corresponds to the absence of noise interference for comparison purposes.

Observe from the plots that the addition of colored Gaussian noise interference always improves the performance of the receiver. Since the receiver is designed to be optimum in the presence of just white noise interference, this performance improvement occurs because the colored noise becomes associated with the target reflected signal rather than the noise, and therefore the colored noise is seen by the receiver as a reinforcement of the reflected signal rather than as additive noise interference.

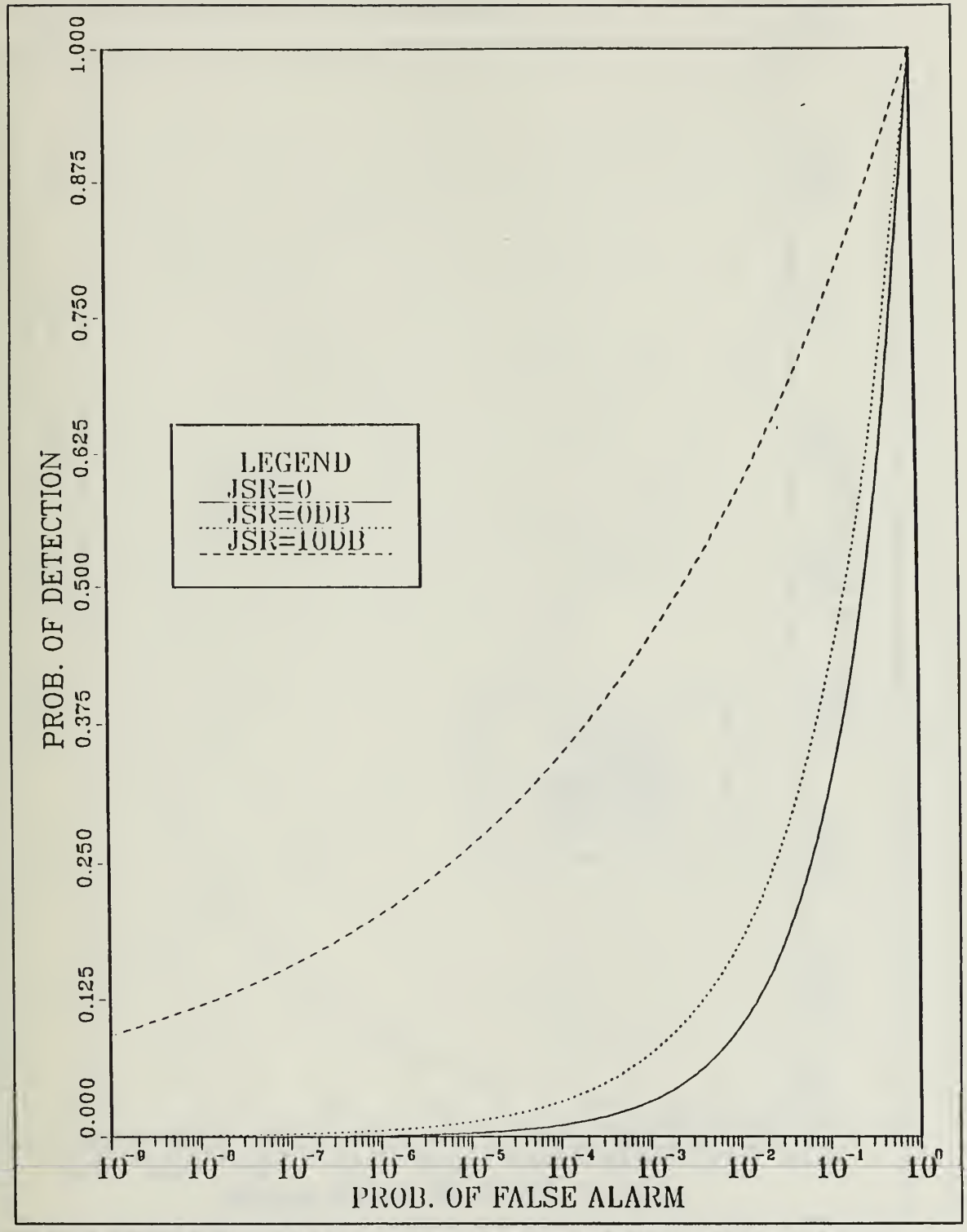

Figure 12. Optimum White Receiver, H_1 Colored H_0 White SNR = 0 dB.

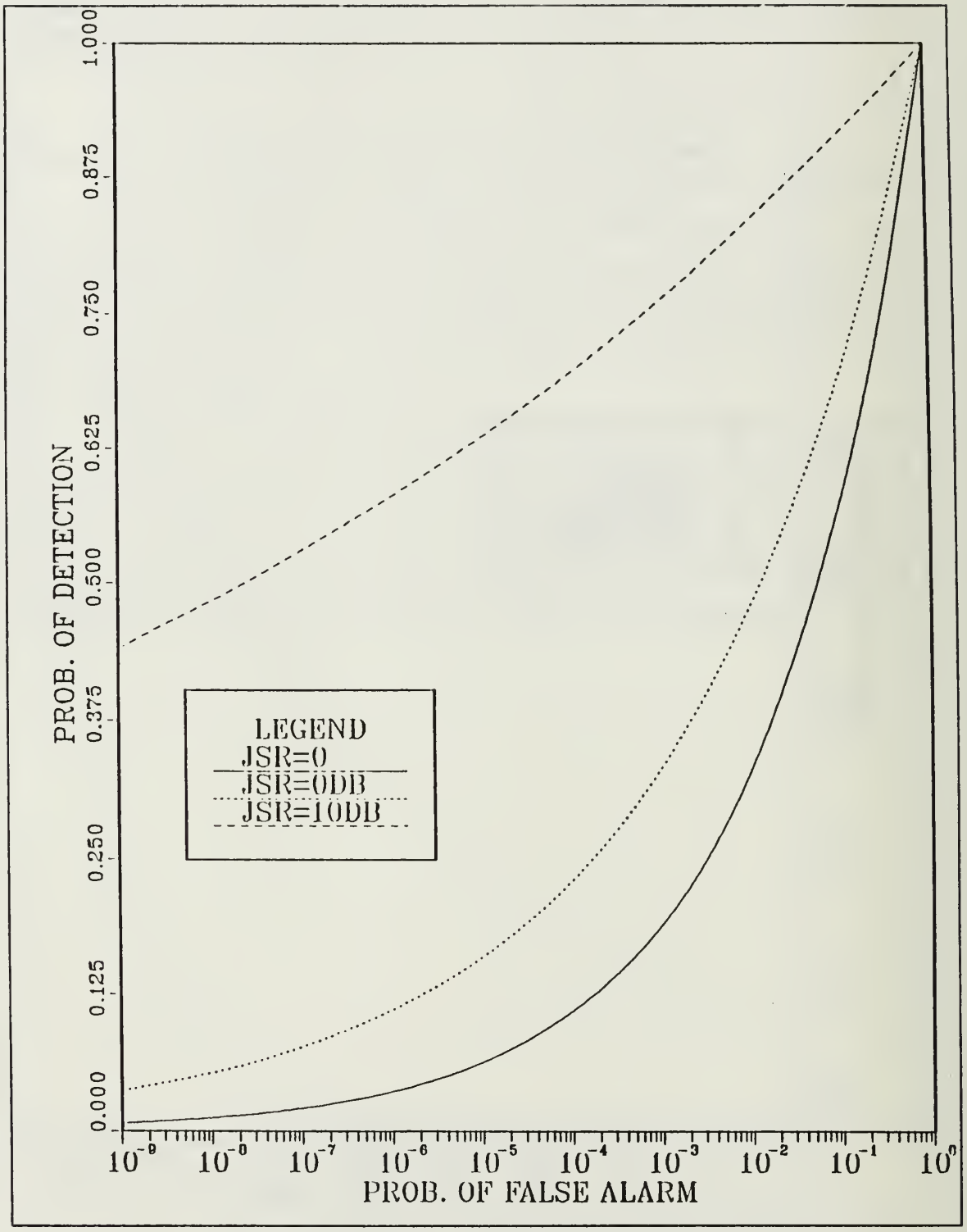

Figure 13. Optimum White Receiver, H_1 Colored H_0 White SNR = 5 dB.

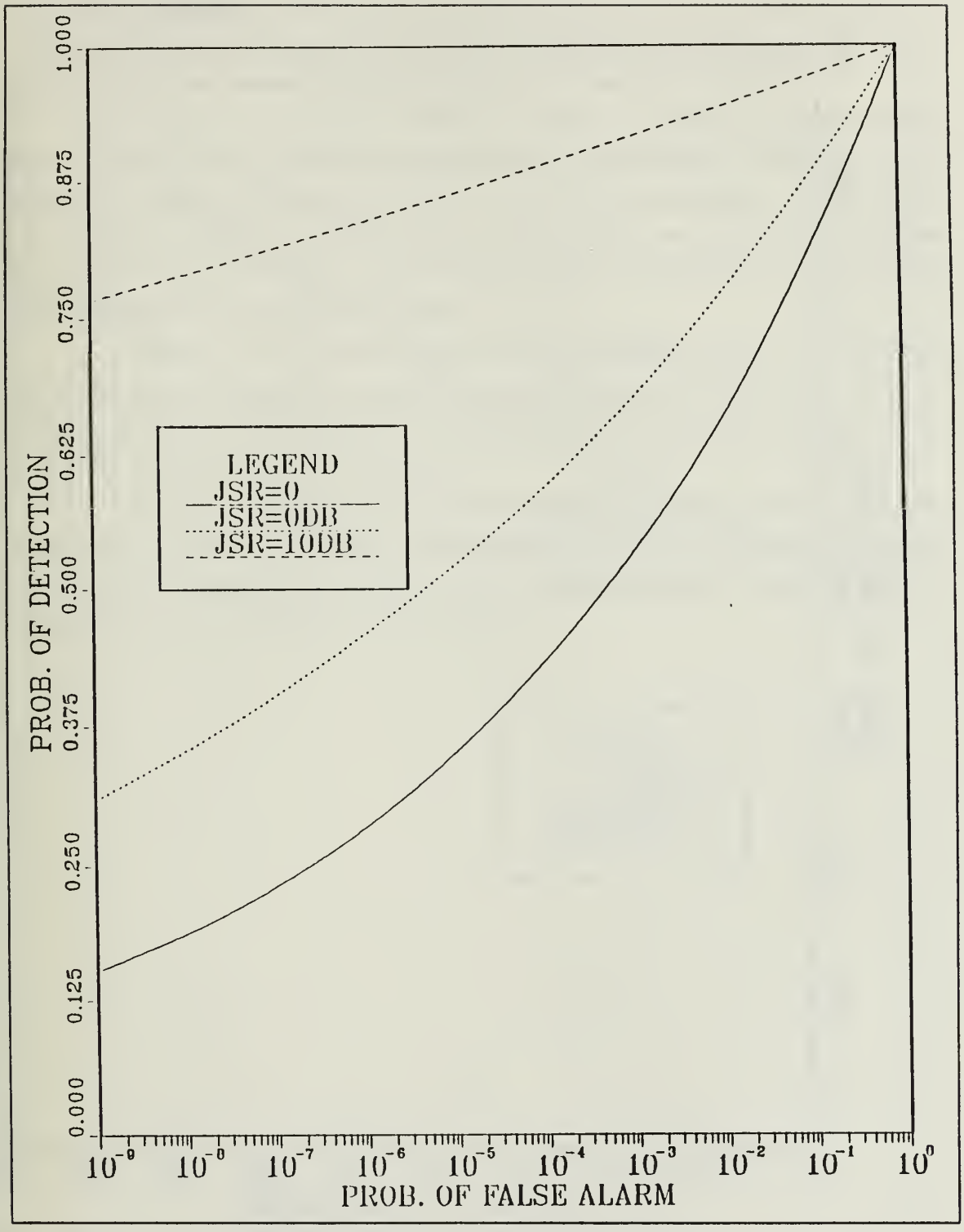

Figure 14. Optimum White Receiver, H_1 Colored H_0 White SNR = 10 dB.

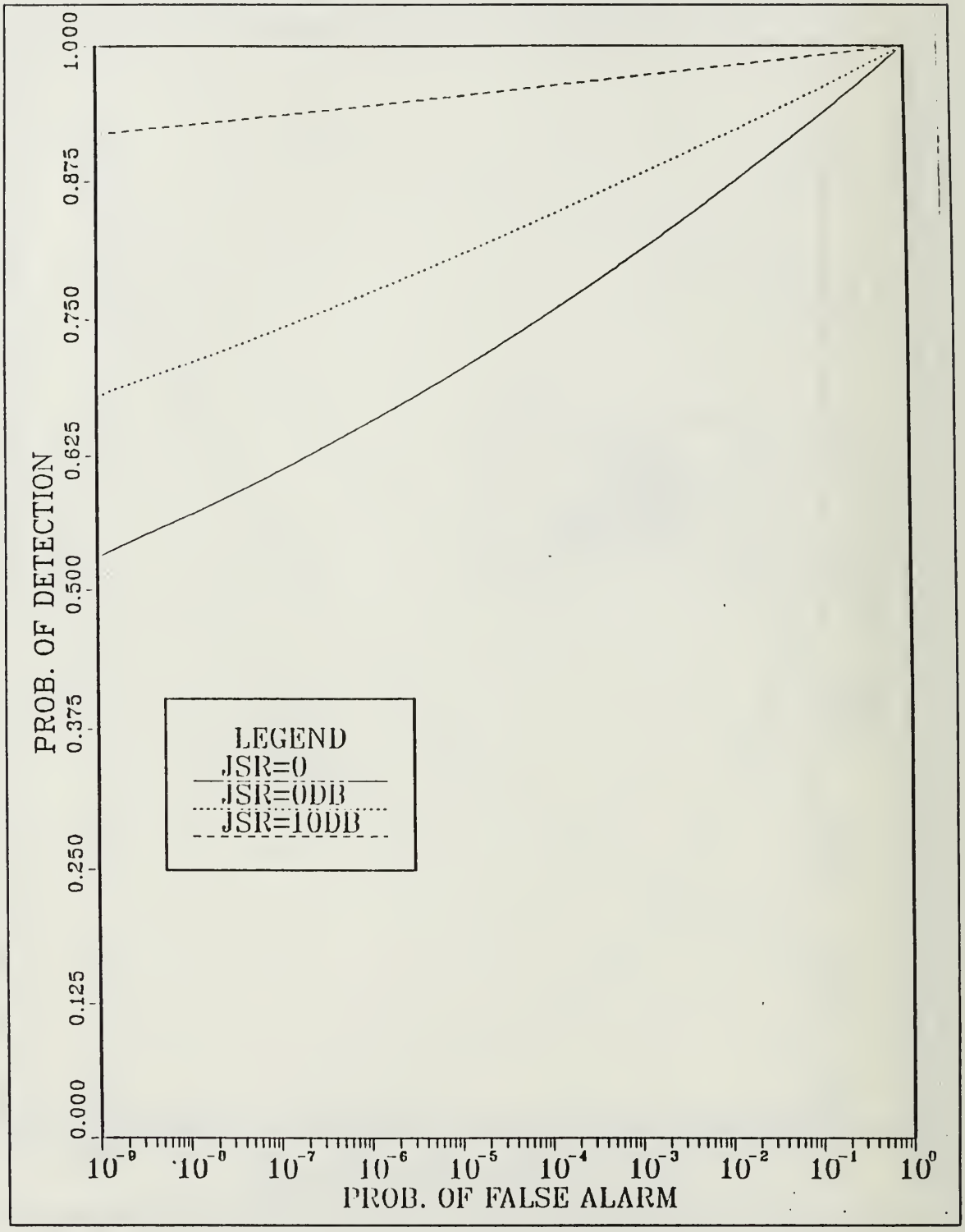

Figure 15. Optimum White Receiver, H_1 Colored H_0 White SNR = 15 dB.

b. Problem 2.

Given that P_D as a function of P_F is given by Equation 4.53, the ROC's for the suboptimum receiver can be evaluated, using numerical methods.

In Figure 16 on page 74, Figure 17 on page 75, Figure 18 on page 76, and Figure 19 on page 77, the ROC's are presented for four different values of SNR, the Signal-to-Noise Ratio, namely 0 dB, 5 dB, 10 dB and 15 dB, respectively. In each figure, the performance is shown for three different values of JSR, the Jamming-to-Signal Ratio, namely 0, 0 dB and 10 dB. The first value of JSR, corresponds to the absence of noise interference for comparison purposes.

Observe that, for every value of SNR considered, there is a significant amount of receiver performance degradation corresponding to the amount of noise interference present (as determined by the JSR value), and is quite large for high values of SNR (as shown in Figure 19 on page 77).

This case considered, demonstrates significant receiver performance degradation which is achieved under the assumption that the ability to generate and transmit colored noise interference continuously (under both hypotheses), when the target is within the radar detection range, is indeed valid.

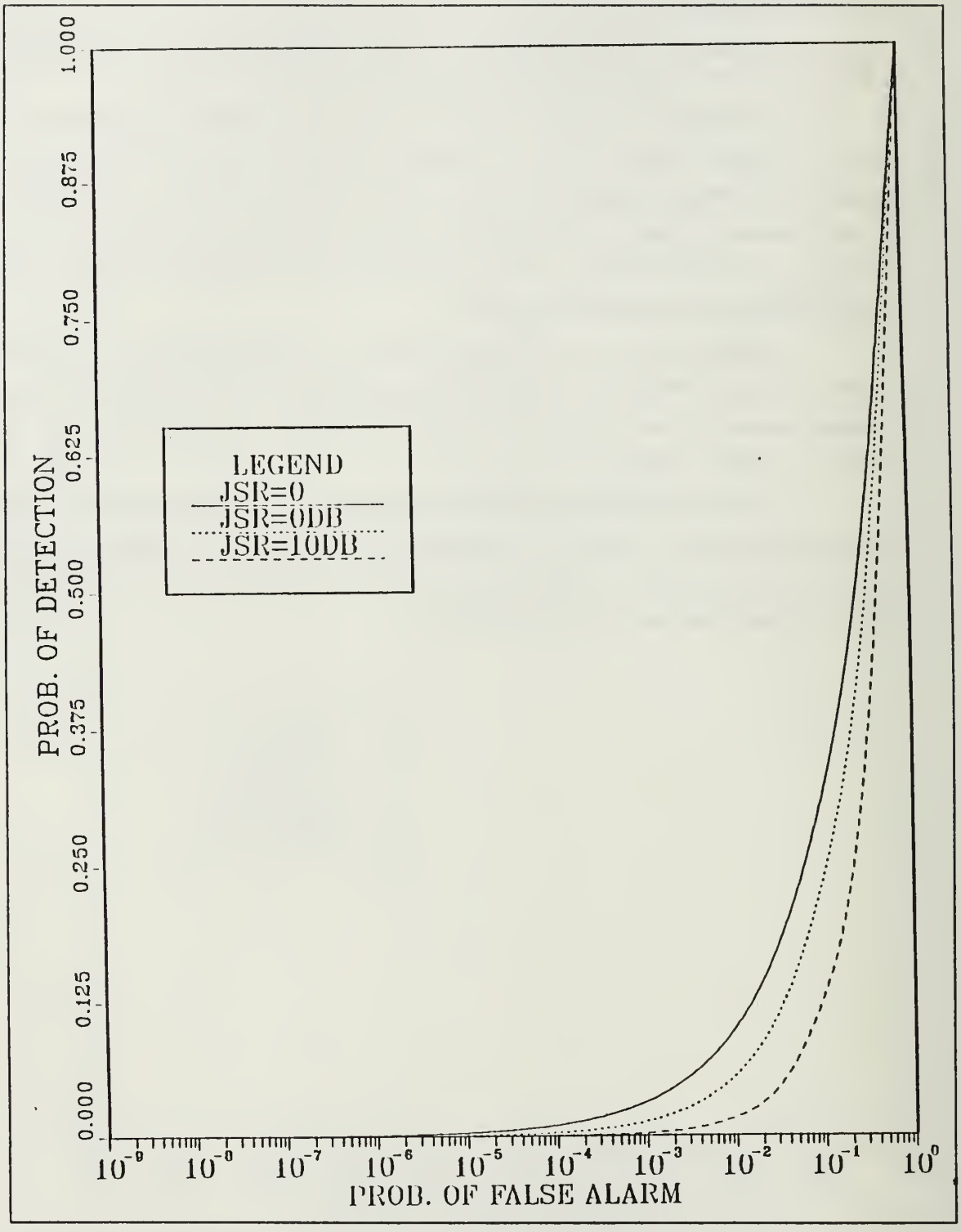

Figure 16. Optimum White Receiver, H_1 Colored H_0 Colored SNR = 0 dB.

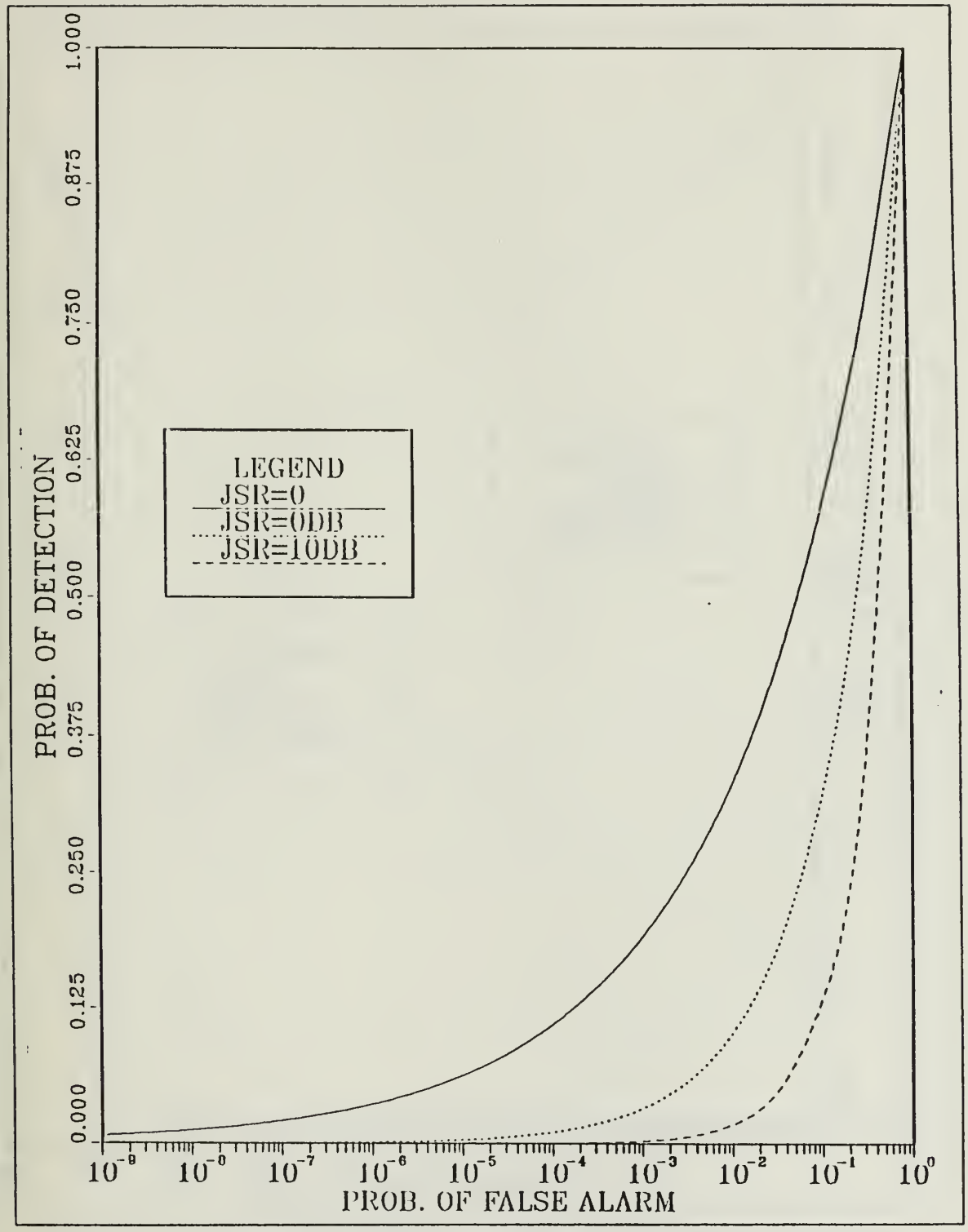

Figure 17. Optimum White Receiver, H_1 Colored H_0 Colored SNR = 5 dB.

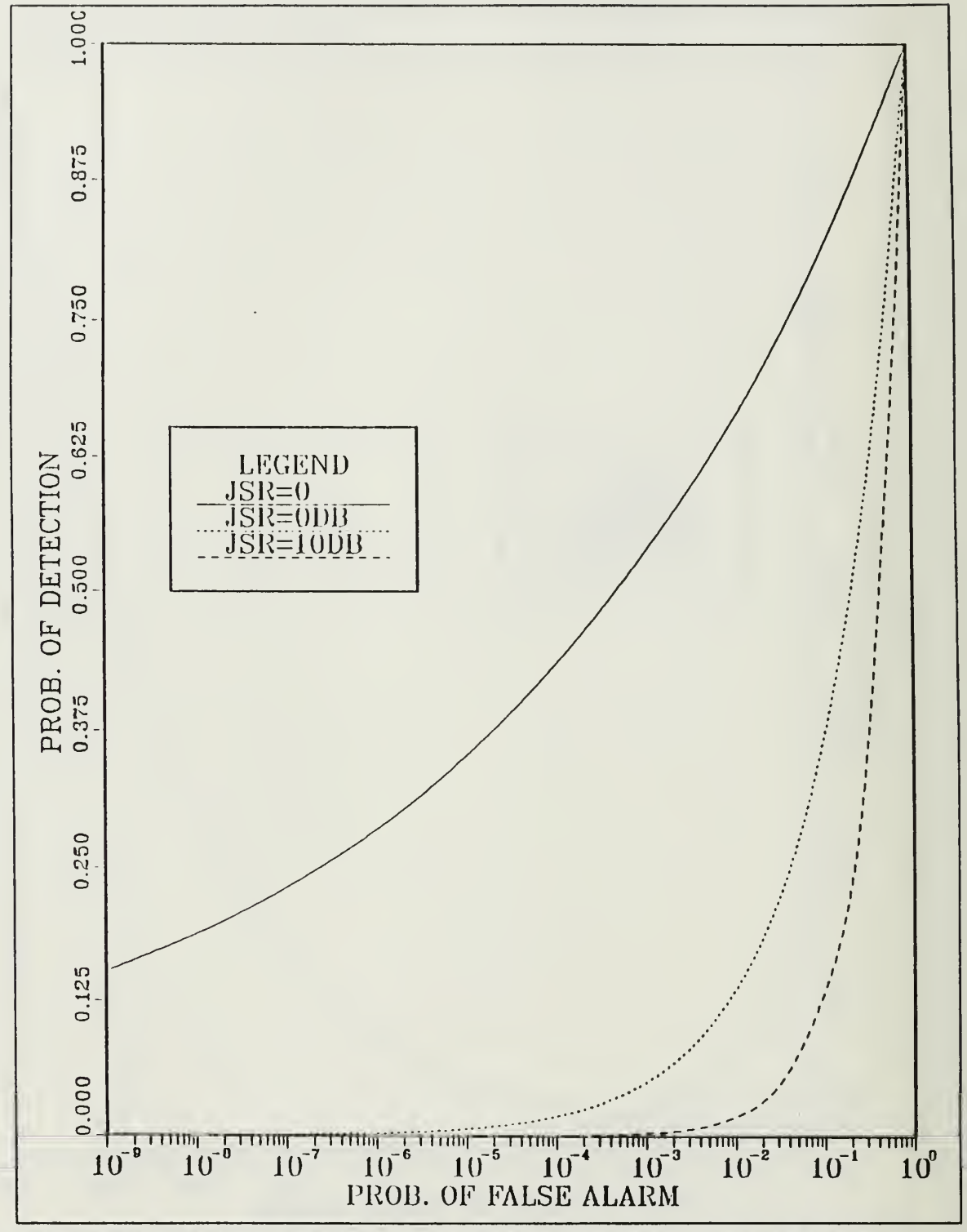

Figure 18. Optimum White Receiver, H_1 Colored H_0 Colored SNR = 10 dB.

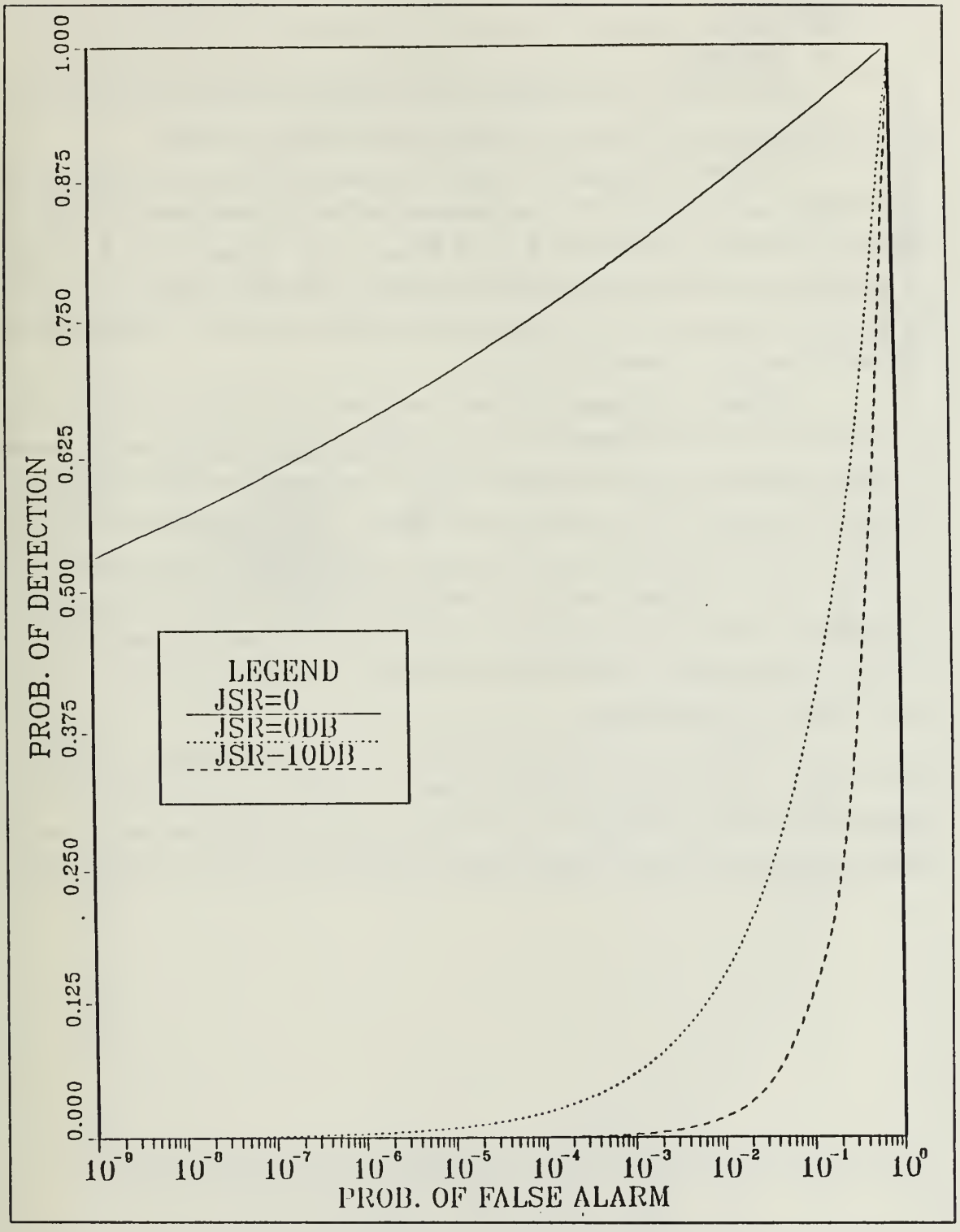

Figure 19. Optimum White Receiver, H_1 Colored H_0 Colored SNR = 15 dB.

2. Receiver II.

a. Problem 1.

Given that P_D as a function of P_F is given by Equation 4.87, the ROC's for the suboptimum receiver can be evaluated, using numerical methods.

In Figure 20 on page 79, Figure 21 on page 80, Figure 22 on page 81, and Figure 23 on page 82, the ROC's are presented for four different values of SNR, the Signal-to-Noise Ratio, namely 0 dB, 5 dB, 10 dB and 15 dB, respectively. In each figure, the performance is shown for three different values of JSR, the Jamming-to-Signal Ratio, namely 0, 0 dB and 10 dB. The first value of JSR, corresponds to the absence of noise interference for comparison purposes.

In Figure 20 on page 79, which corresponds to an SNR value of 0 dB, there is a clear performance improvement for any amount of noise interference power present. A somewhat similar occurence is visible in Figure 21 on page 80, which has been plotted with an SNR value of 5 dB. For JSR = 10 dB there is a slight performance degradation, however for JSR = 0 dB, there is an actual receiver performance improvement. This means that there is a unique value of JSR, which for a specific value of SNR, yields the largest receiver performance improvement. Clearly, the noise generating target must not only avoid producing such a JSR value at the receiver, but it must attempt to cause the largest performance degradation.

In Figure 22 on page 81, and Figure 23 on page 82, which correspond to SNR values of 10 and 15 dB, respectively, there is a significant amount of receiver performance degradation in relation to the amount of noise interference power present. This performance degradation increases with increasing SNR values as the figures show.

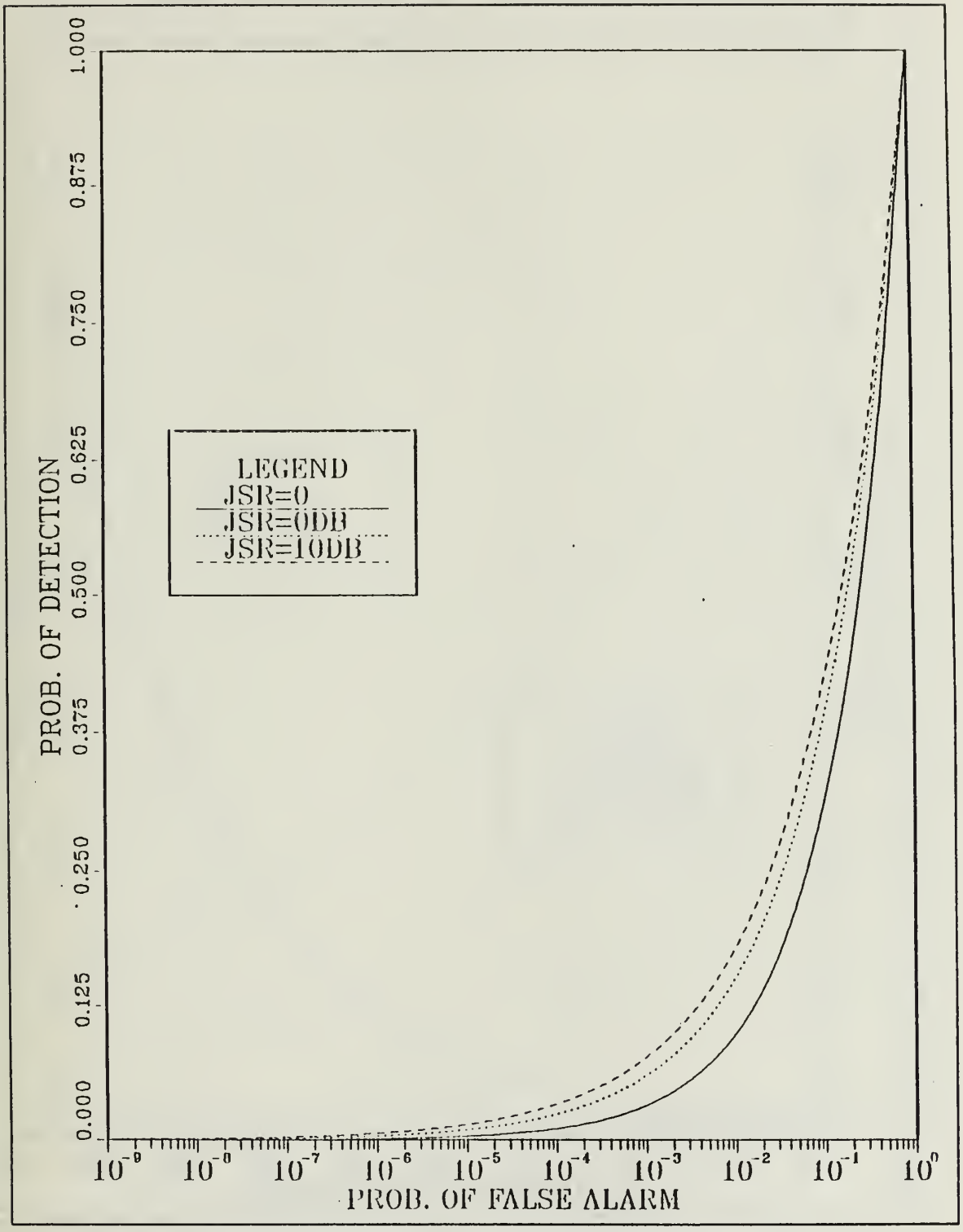

Figure 20. Optimum Colored Receiver, H_1 Colored H_0 White SNR = 0 dB.

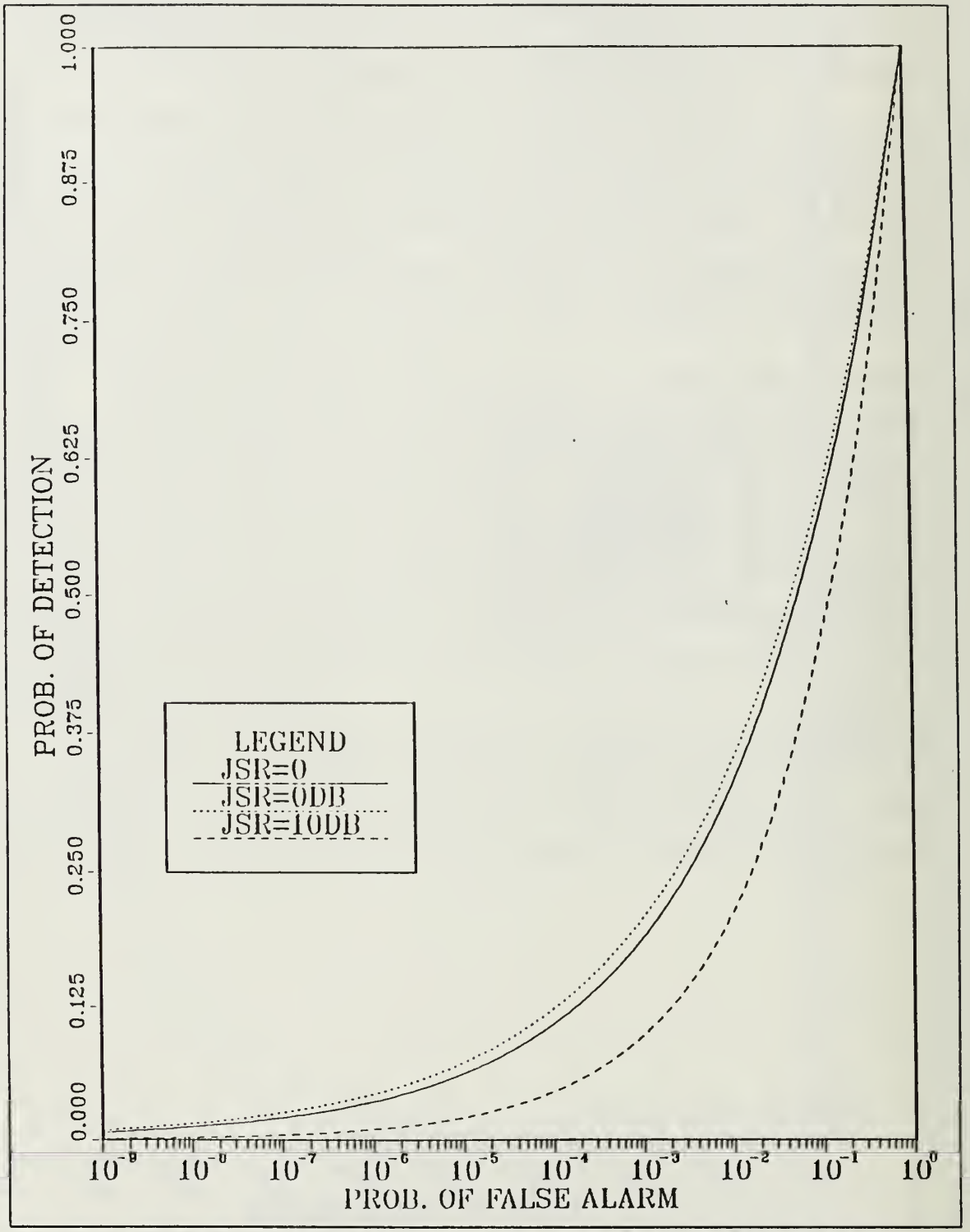

Figure 21. Optimum Colored Receiver, H_1 Colored H_0 White SNR = 5 dB.

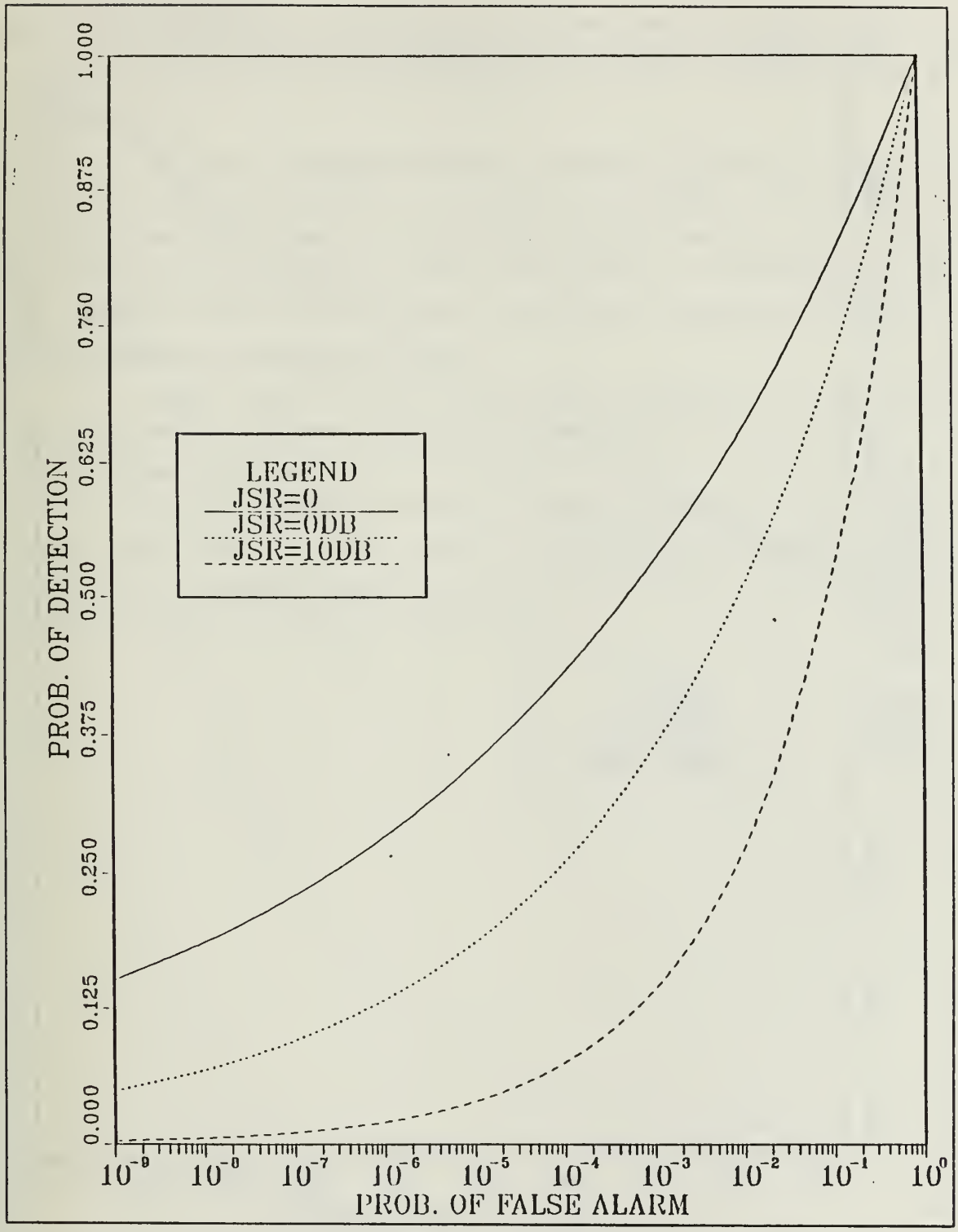

Figure 22. Optimum Colored Receiver, H_1 Colored H_0 White SNR = 10 dB.

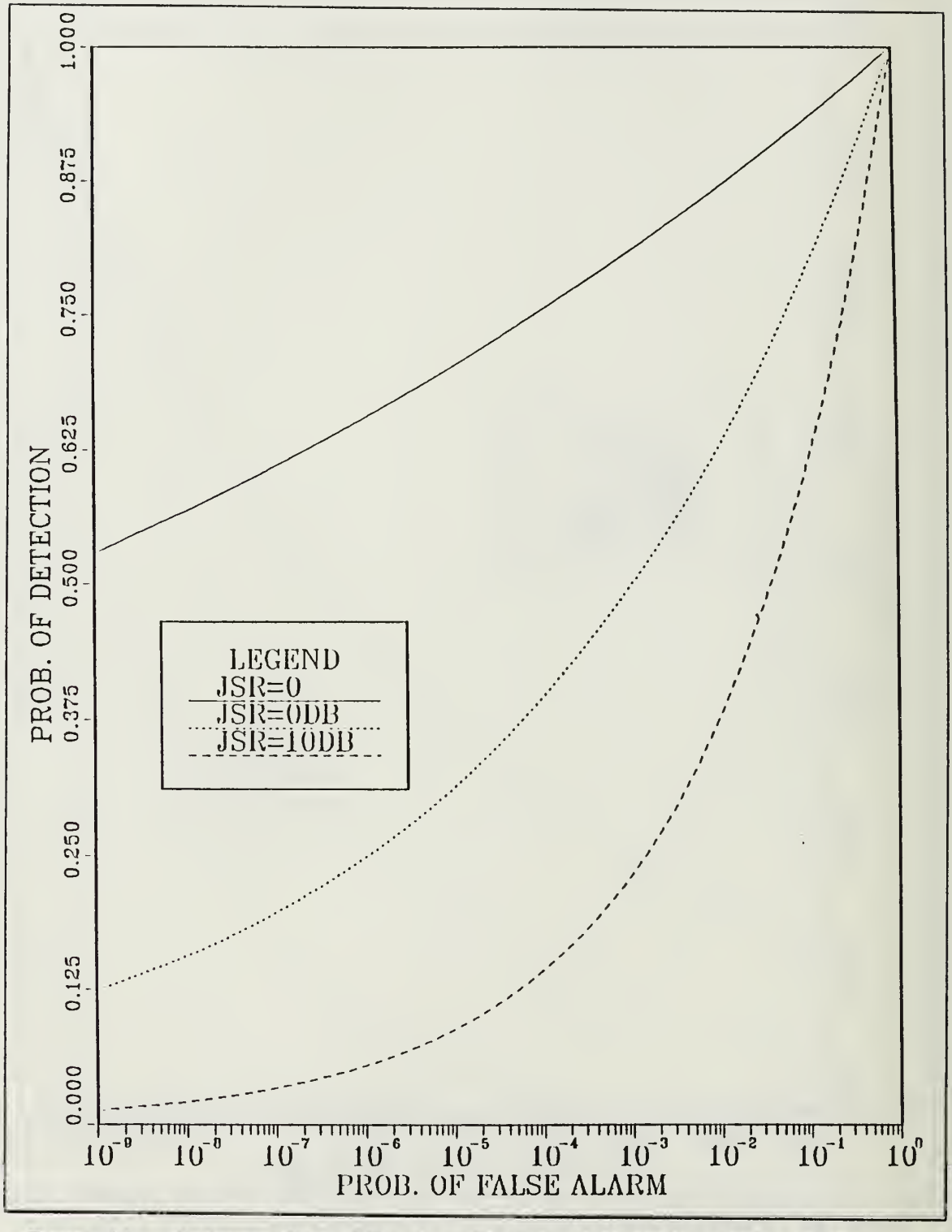

Figure 23. Optimum Colored Receiver, H_1 Colored H_0 White SNR = 15 dB.

b. Problem 2.

Given that P_D as a function of P_F is given by Equation 4.108 and Equation 4.111, the ROC's for the suboptimum receiver can be evaluated, using numerical methods.

In Figure 24 on page 84, Figure 25 on page 85, Figure 26 on page 86, and Figure 27 on page 87, the ROC's are presented for four different values of SNR, the Signal-to-Noise Ratio, namely 0 dB, 5 dB, 10 dB and 15 dB, respectively. In each figure, the performance is shown for three different values of JSR, the Jamming-to-Signal Ratio, namely 0, 0 dB and 10 dB. The first value of JSR, corresponds to the absence of noise interference for comparison purposes.

Observe that, for every value of SNR considered there is a significant amount of receiver performance degradation corresponding to the amount of noise interference present (as determined by the JSR value).

This case considered, demonstrates significant receiver performance degradation which is achieved under the assumption that the ability to generate and transmit colored noise interference continuously (under both hypotheses), when the target is within the radar detection range, is indeed valid.

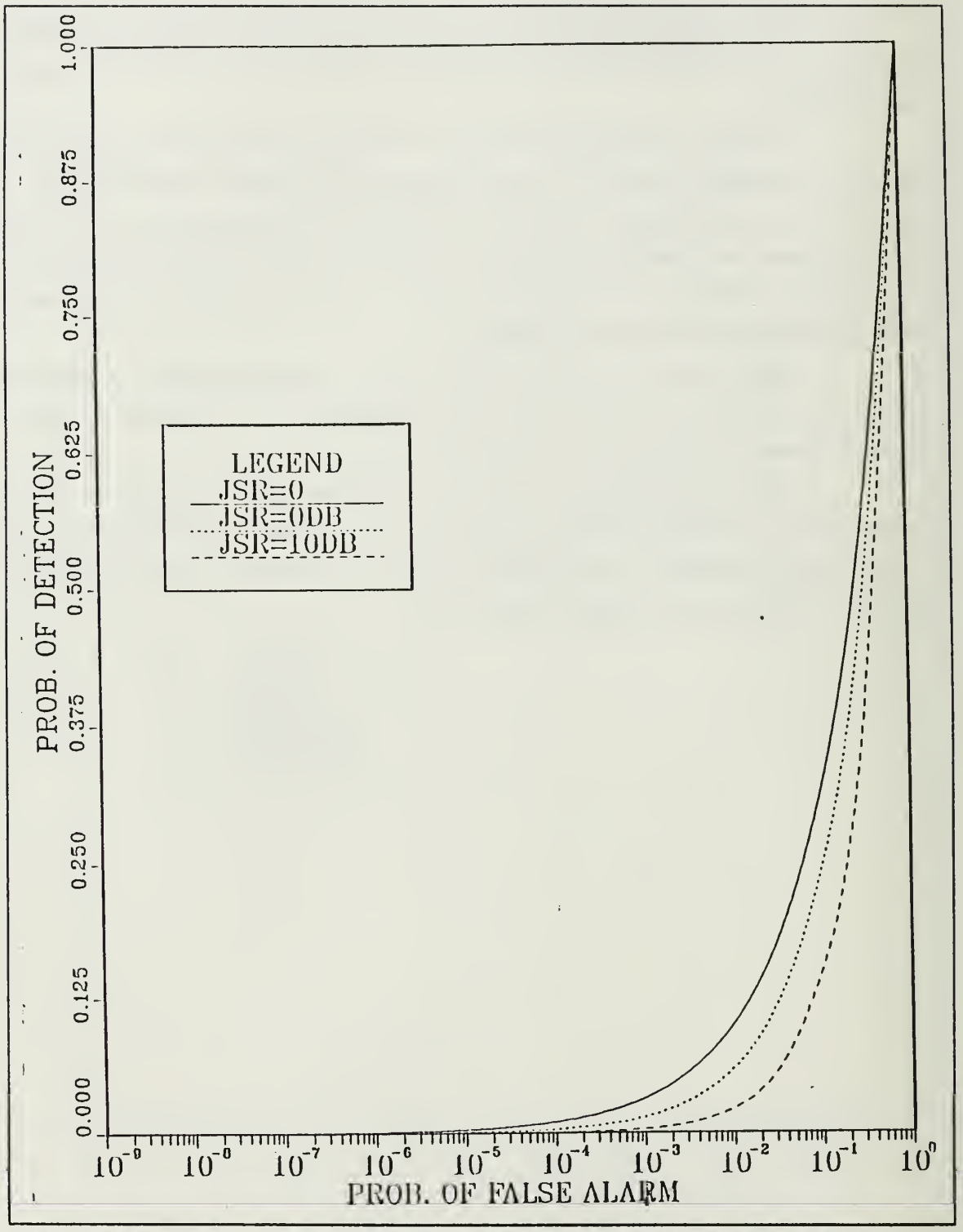

Figure 24. Optimum Colored Receiver, H_1 Colored H_0 Colored SNR = 0 dB.

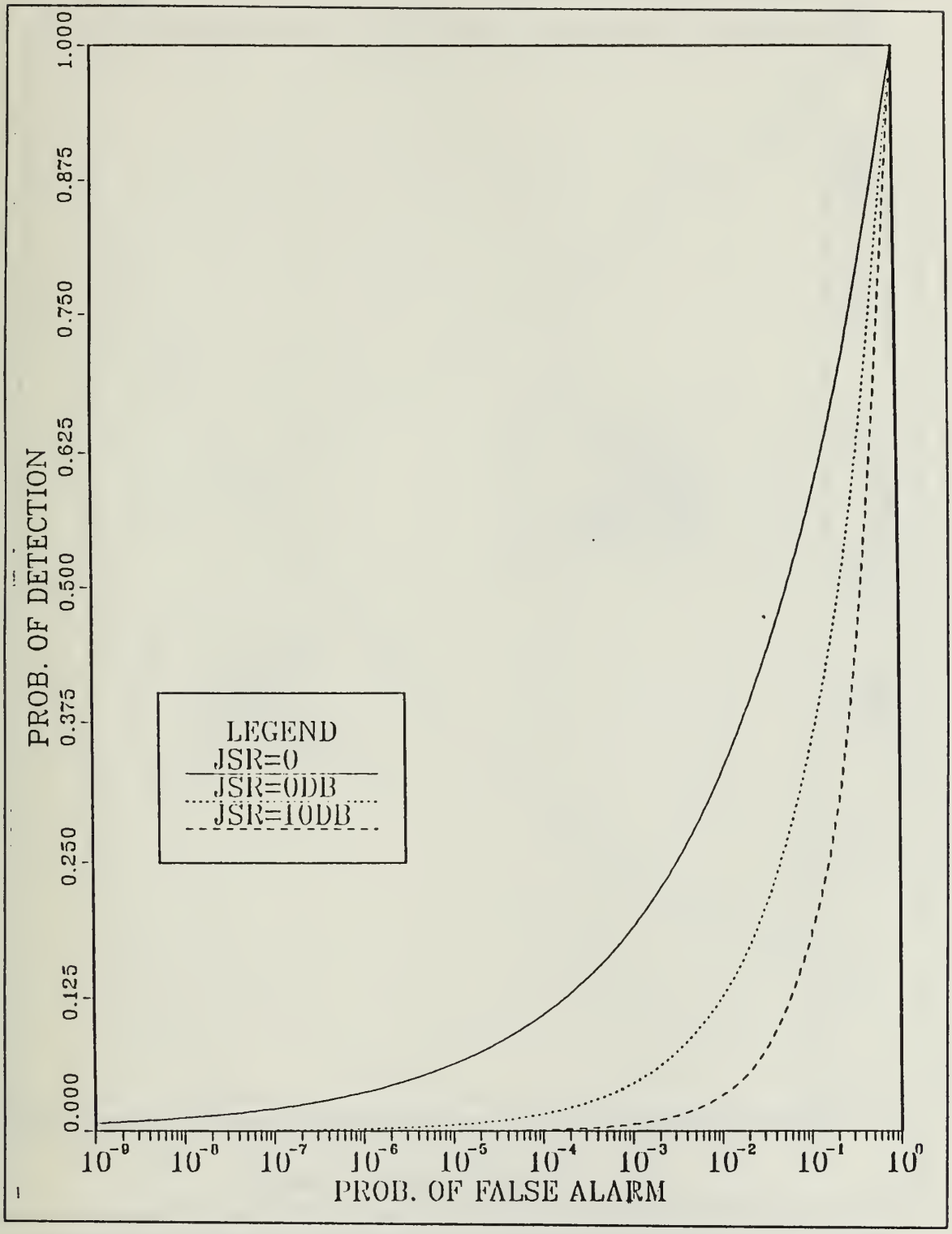

Figure 25. Optimum Colored Receiver, H_1 Colored H_0 Colored SNR = 5 dB.

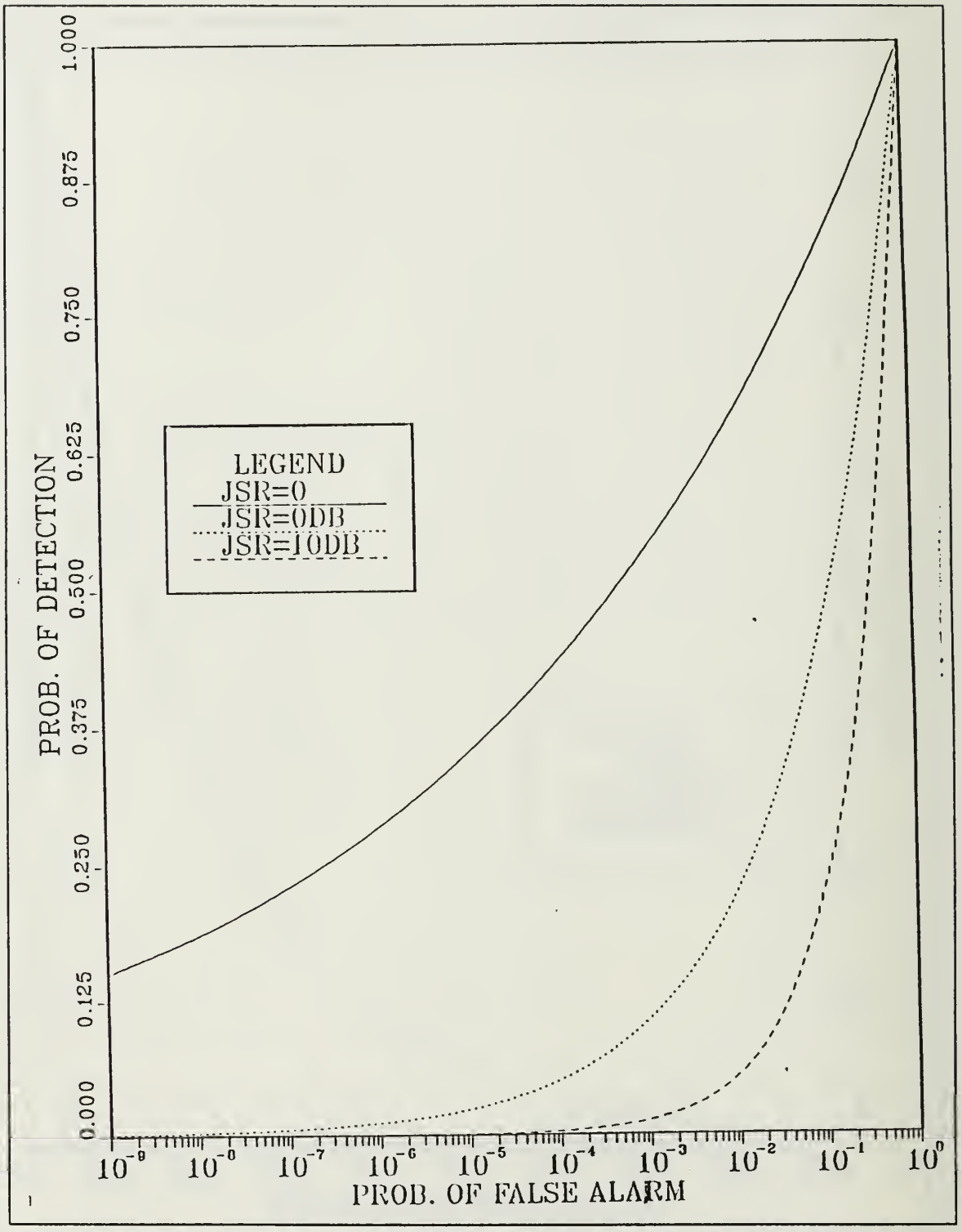

Figure 26. Optimum Colored Receiver, H_1 Colored H_0 Colored SNR = 10 dB.

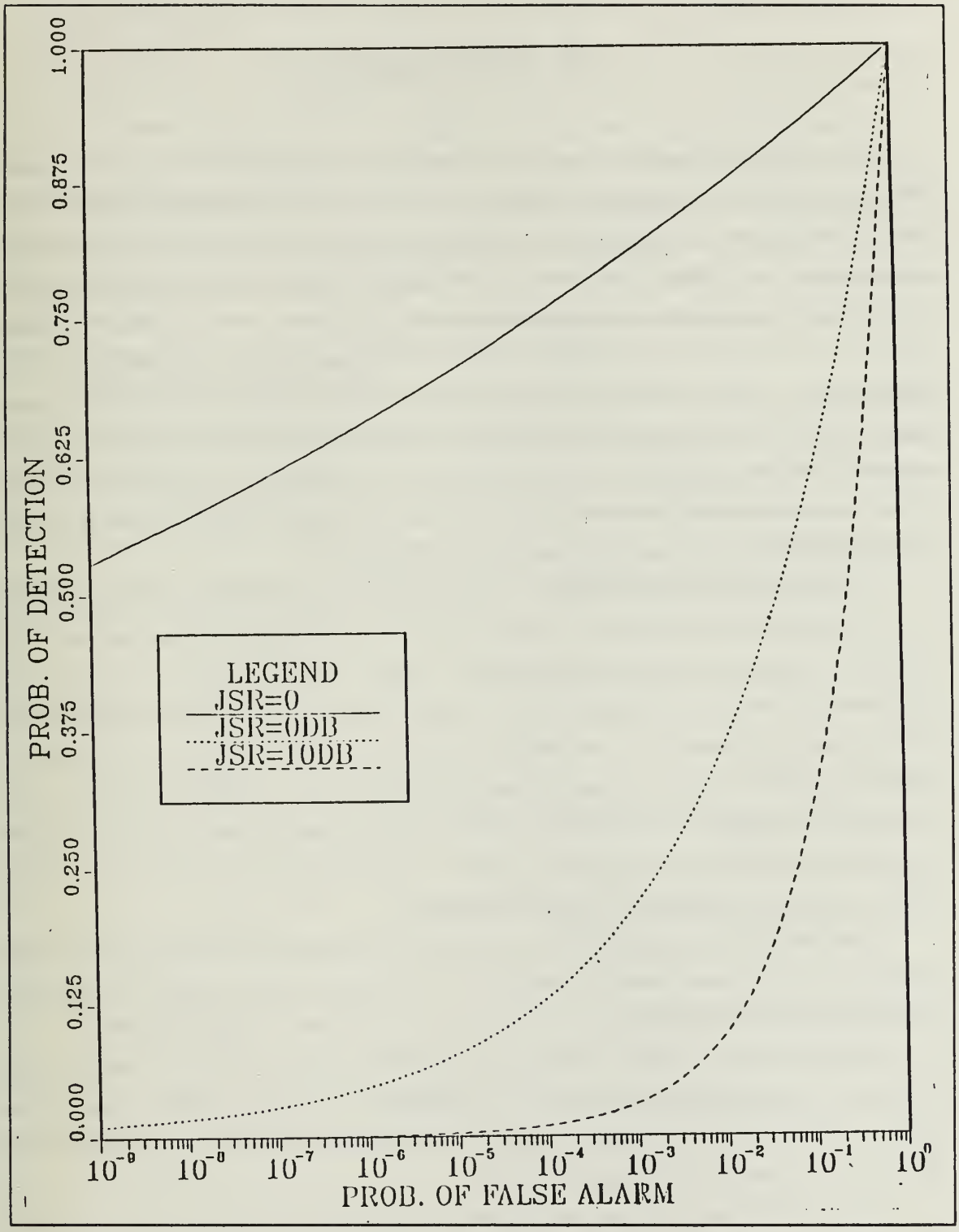

Figure 27. Optimum Colored Receiver, H_1 Colored H_0 Colored SNR = 15 dB.

VI. CONCLUSIONS

The problem of masking a radar signal return by selecting the power spectral density (PSD) of an externally generated power constrained noise interference has been considered under two sets of assumptions. In the first one, the radar receiver is assumed to have no prior knowledge of the actual noise present, and thus it has been designed to be optimum when additive white Gaussian noise (AWGN) is the only source of interference. In the second one the radar receiver is assumed to have prior knowledge of the noise present, so that it has been designed to be optimum in the presence of the actual noise, which will be assumed to be additive colored Gaussian noise (ACGN) that contains an AWGN component. In both these cases, the external noise interference is assumed to be generated and transmitted by either the target itself or by noise making devices present in the area being penetrated by the target.

Using first a simple target model, that is assumed to only introduce a random phase to the transmitted sinusoid upon reflection whenever the target generates and transmits the noise interference while illuminated by a radar, a modest amount of receiver performance degradation was shown to be achievable. Such performance degradation was demonstrated to depend on the specific values of JSR and P_F, and to yield only a moderate decrease in the receiver's probability detection, P_D. Taking into account the fact that any performance degradation effects depend on parameters over which the target has no control, one must conclude that target generated interference is not an effective method for masking the radar signal return.

Using the second target model which takes into account the reflectivity of the target so that the radar signal return is modeled as a Gaussian random process, the performance degradation results depend on the type of receiver that is being analyzed.

If the radar receiver used is designed to be optimum in the presence of only AWGN interference, then any noise interference transmitted by the target (when it realizes that it has been illuminated by a radar) is added to the reflected signal and consequently helps the receiver to identify the target's presence.

On the other hand, if noise making devices used to generate and transmit ACGN, the results clearly show a receiver performance degradation that is proportional to the amount of noise interference present.

If the radar receiver used is designed to be optimum in the presence of ACGN that contains an AWGN component, (this would imply that the receiver has prior knowledge of the kind of noise being generated either by the target or the noise making devices), the use of noise making devices to generate and transmit noise interference causes a significant receiver performance degradation. The same receiver undergoes limited performance degradation when the noise interference is transmitted by the target itself. At low values of Signal-to-Noise Ratio, the receiver performance is actually improved. Since the receiver performance degradation is a function of SNR, a parameter over which the target has no control, it appears that again, target generated interference is not an effective way of masking the radar signal return.

From the cases investigated, it is clear that the choice of PSD shape associated with the colored noise interference generated, strongly depends on the type of signal transmitted by the radar. Furthermore, such ACGN interference is best generated by friendly noise making devices present in the area that the target penetrates. This appears to be the only effective method of significantly degrading the radar receiver performance, thus allowing a target to penetrate an area with low probability for being detected.

APPENDIX A. EVALUATION OF $\sigma_{n_c}^2$ FOR FOUR PSD CASES.

Equation 3.13, defines $\sigma_{n_c}^2$, which is repeated here for convenience

$$\sigma_{n_c}^2 = \frac{1}{2\pi}\int_{-\infty}^{\infty} S_{n_c}(\omega)\,|\,F_c(\omega)\,|^2 d\omega \tag{A.1}$$

where $S_{n_c}(\omega)$ is the PSD of the colored noise $n_c(t)$, and $|\,F_c(\omega)\,|^2$ is defined in Equation 3.24.

The quantity $\sigma_{n_c}^2$ can be evaluated under a total power constraint on $n_c(t)$ for four different PSD shapes of $S_{n_c}(\omega)$.

A. BANDLIMITED CONSTANT AMPLITUDE PSD.

The PSD of the bandlimited white noise is mathematically described as

$$S_{n_c}(\omega) = \begin{cases} c & |\,\omega \pm \omega_c\,| \le \frac{2\pi}{T} \\ 0 & \text{otherwise} \end{cases} \tag{A.2}$$

Assuming that the power of $n_c(t)$ is P_{n_c}, then c must satisfy

$$\frac{1}{2\pi}\int_{-\omega_c-\frac{2\pi}{T}}^{-\omega_c+\frac{2\pi}{T}} c\,d\omega + \frac{1}{2\pi}\int_{\omega_c-\frac{2\pi}{T}}^{\omega_c+\frac{2\pi}{T}} c\,d\omega = P_{n_c} \tag{A.3}$$

therefore

$$c = \frac{T}{4} P_{n_c} \tag{A.4}$$

and

$$S_{n_c}(\omega) = \begin{cases} \frac{T}{4} P_{n_c} & |\,\omega \pm \omega_c\,| \le \frac{2\pi}{T} \\ 0 & \text{otherwise} \end{cases} \tag{A.5}$$

As a result of this, we obtain

$$\sigma_{n_c}^2 = \frac{1}{2\pi}\int_{-\infty}^{\infty} S_{n_c}(\omega)\,|\,F_c(\omega)\,|^2 d\omega$$

$$= \frac{T^2 P_{n_c}}{16\pi}\left[\int_{\omega_c - \frac{2\pi}{T}}^{\omega_c + \frac{2\pi}{T}} \frac{\sin^2[(\omega-\omega_c)\frac{T}{2}]}{[(\omega-\omega_c)\frac{T}{2}]^2}\,d\omega + \int_{-\omega_c - \frac{2\pi}{T}}^{-\omega_c + \frac{2\pi}{T}} \frac{\sin^2[(\omega+\omega_c)\frac{T}{2}]}{[(\omega+\omega_c)\frac{T}{2}]^2}\,d\omega\right] \quad (A.6)$$

Changing variables we obtain

$$\begin{aligned}\sigma_{n_c}^2 &= \frac{TP_{n_c}}{8\pi}\left[\int_{-\pi}^{\pi}\frac{\sin^2 x}{x^2}\,dx + \int_{-\pi}^{\pi}\frac{\sin^2 y}{y^2}\,dy\right] \\ &= 1.42\,\frac{TP_{n_c}}{2\pi} \\ &= 0.227\,T\,P_{n_c}\end{aligned} \quad (A.7)$$

B. SINC SQUARED SHAPED PSD.

The PSD in this case can be mathematically described as

$$S_{n_c}(\omega) = c\,\frac{\sin^2[(\omega+\omega_c)\frac{T}{2})}{[(\omega+\omega_c)\frac{T}{2}]^2} + c\,\frac{\sin^2[(\omega-\omega_c)\frac{T}{2})}{[(\omega-\omega_c)\frac{T}{2}]^2} \qquad -\infty < \omega < \infty \quad (A.8)$$

Under a similar power constraint, c can be evaluated as

$$\frac{c}{2\pi}\int_{-\infty}^{\infty}\left[\frac{\sin^2[(\omega+\omega_c)\frac{T}{2}]}{[(\omega+\omega_c)\frac{T}{2}]^2} + \frac{\sin^2[(\omega-\omega_c)\frac{T}{2}]}{[(\omega-\omega_c)\frac{T}{2}]^2}\right]d\omega = P_{n_c} \quad (A.9)$$

therefore

$$c = \frac{T\,P_{n_c}}{2} \quad (A.10)$$

Assuming that $\omega_c T$ is sufficiently large so that

$$\frac{\sin^2[(\omega-\omega_c)\frac{T}{2}]}{[(\omega-\omega_c)\frac{T}{2}]^2}\,\frac{\sin^2[(\omega+\omega_c)\frac{T}{2}]}{[(\omega+\omega_c)\frac{T}{2}]^2} \approx 0 \qquad (A.11)$$

and since

$$S_{n_c}(\omega) = \frac{TP_{n_c}}{2}\left[\frac{\sin^2[(\omega+\omega_c)\frac{T}{2}]}{[(\omega+\omega_c)\frac{T}{2}]^2} + \frac{\sin^2[(\omega-\omega_c)\frac{T}{2}]}{[(\omega-\omega_c)\frac{T}{2}]^2}\right] \quad -\infty \le \omega \le \infty \qquad (A.12)$$

we obtain

$$\begin{aligned}\sigma_{n_c}^2 &= \frac{1}{2\pi}\int_{-\infty}^{\infty} S_{n_c}(\omega)\,|\,F_c(\omega)\,|^2 d\omega \\ &= \frac{T^2 P_{n_c}}{8\pi}\left[\int_{-\infty}^{\infty}\frac{\sin^4[(\omega+\omega_c)\frac{T}{2}]}{[(\omega+\omega_c)\frac{T}{2}]^4}\,d\omega + \int_{-\infty}^{\infty}\frac{\sin^4[(\omega-\omega_c)\frac{T}{2}]}{[(\omega+\omega_c)\frac{T}{2}]^2}\right]d\omega\end{aligned} \qquad (A.13)$$

and changing variables

$$\begin{aligned}\sigma_{n_c}^2 &= \frac{TP_{n_c}}{2\pi}\int_{-\infty}^{\infty}\frac{\sin^4 x}{x^4}\,dx \\ &= 0.333\,T\,P_{n_c}\end{aligned} \qquad (A.14)$$

C. BUTTERWORTH SHAPED PSD.

The Butterworth shaped PSD can be mathematically described as

$$S_{n_c}(\omega) = \frac{c}{\alpha^2+(\omega+\omega_c)^2} + \frac{c}{\alpha^2+(\omega-\omega_c)^2} \quad -\infty \le \omega \le \infty \qquad (A.15)$$

and under a similar power constraint, c can be evaluated as

$$\frac{1}{2\pi}\int_{-\infty}^{\infty}\left[\frac{c}{\alpha^2+(\omega+\omega_c)^2}+\frac{c}{\alpha^2+(\omega-\omega_c)^2}\right]d\omega = P_{n_c} \tag{A.16}$$

so that

$$c = \alpha P_{n_c} \tag{A.17}$$

thus

$$S_{n_c}(\omega)=\frac{\alpha P_{n_c}}{\alpha^2+(\omega+\omega_c)^2}+\frac{\alpha P_{n_c}}{\alpha^2+(\omega-\omega_c)^2} \qquad -\infty \le \omega \le \infty \tag{A.18}$$

and as a result of this

$$\begin{aligned}\sigma_{n_c}^2 &= \frac{1}{2\pi}\int_{-\infty}^{\infty} S_{n_c}(\omega)\,|\,F_c(\omega)\,|^2 d\omega \\ &= \frac{TP_{n_c}}{4\pi}\int_{-\infty}^{\infty}\left[\frac{\alpha}{\alpha^2+(\omega-\omega_c)^2}\right]\frac{\sin^2[(\omega-\omega_c)\frac{T}{2}]}{[(\omega-\omega_c)\frac{T}{2}]^2}\,d\omega \\ &+ \frac{TP_{n_c}}{4\pi}\int_{-\infty}^{\infty}\left[\frac{\alpha}{\alpha^2+(\omega+\omega_c)^2}\right]\frac{\sin^2[(\omega+\omega_c)\frac{T}{2}]}{[(\omega+\omega_c)\frac{T}{2}]^2}\,d\omega\end{aligned} \tag{A.19}$$

Changing variables yields

$$\begin{aligned}\sigma_{n_c}^2 &= \frac{TP_{n_c}}{2}\int_{-\infty}^{\infty}\frac{\left(\frac{\sin^2 x}{x^2}\right)}{(\pi^2+x^2)}\,dx \\ &= 0.304\,T\,P_{n_c}\end{aligned} \tag{A.20}$$

D. TRIANGULAR SHAPED PSD.

In this case the PSD is mathematically described as

$$S_{n_c}(\omega) = \begin{cases} \dfrac{P_{n_c}}{2\omega_0}\left(1 - \dfrac{|\,\omega - \omega_c\,|}{\omega_0}\right) & |\,\omega + \omega_c\,| \leq \omega_0 \\ \dfrac{P_{n_c}}{2\omega_0}\left(1 - \dfrac{|\,\omega + \omega_c\,|}{\omega_0}\right) & |\,\omega - \omega_c\,| \leq \omega_0 \end{cases} \tag{A.21}$$

so that

$$\sigma_{n_c}^2 = \frac{1}{2\pi}\int_{-\infty}^{\infty} S_{n_c}(\omega)\,|\,F_c(\omega)\,|^2 d\omega$$

$$= \frac{TP_{n_c}}{8\pi\omega_0}\int_{-\omega_c-\omega_0}^{-\omega_c+\omega_0}\left(1 - \frac{|\,\omega+\omega_c\,|}{\omega_0}\right)\frac{\sin^2[(\omega+\omega_c)\frac{T}{2}]}{[(\omega+\omega_c)\frac{T}{2}]^2}\,d\omega \tag{A.22}$$

$$+ \frac{TP_{n_c}}{8\pi\omega_0}\int_{\omega_c-\omega_0}^{\omega_c+\omega_0}\left(1 - \frac{|\,\omega-\omega_c\,|}{\omega_0}\right)\frac{\sin^2[(\omega-\omega_c)\frac{T}{2}]}{[(\omega-\omega_c)\frac{T}{2}]^2}\,d\omega$$

Assuming $\omega_0 = \dfrac{2\pi}{T}$ and changing variables

$$\sigma_{n_c}^2 = \frac{TP_{n_c}}{4\pi^2}\int_{-\pi}^{\pi}\left(1 - \frac{|\,x\,|}{\pi}\right)\frac{\sin^2 x}{x^2}\,dx \tag{A.23}$$

$$= 0.051\,T\,P_{n_c}$$

APPENDIX B. BEHAVIOR OF Δ AS A FUNCTION OF NOISE BANDWIDTHS.

In this Appendix the behavior of Δ as a function of the interference noise bandwidth for various types of noise PSD shapes is investigated.

A. BANDLIMITED CONSTANT AMPLITUDE PSD.

It is shown in Chapter 4, Equation 4.106 that

$$\Delta = SNR - \frac{JSR\,(SNR)^2}{2\alpha + JSR\,SNR} \int_{-\alpha}^{\alpha} \frac{\sin^2(\pi x)}{(\pi x)^2}\, dx \qquad (B.1)$$

In Figure 28 on page 96 and Figure 29 on page 97, Δ has been plotted as a function of α for JSR = 0 dB and JSR = 10 dB respectively. SNR values of 0 dB, 10 dB and 15 dB have been chosen in each plot.

From the pictures it is clear that the smaller Δ , which yields the worst receiver performance, corresponds to $\alpha = 1$.

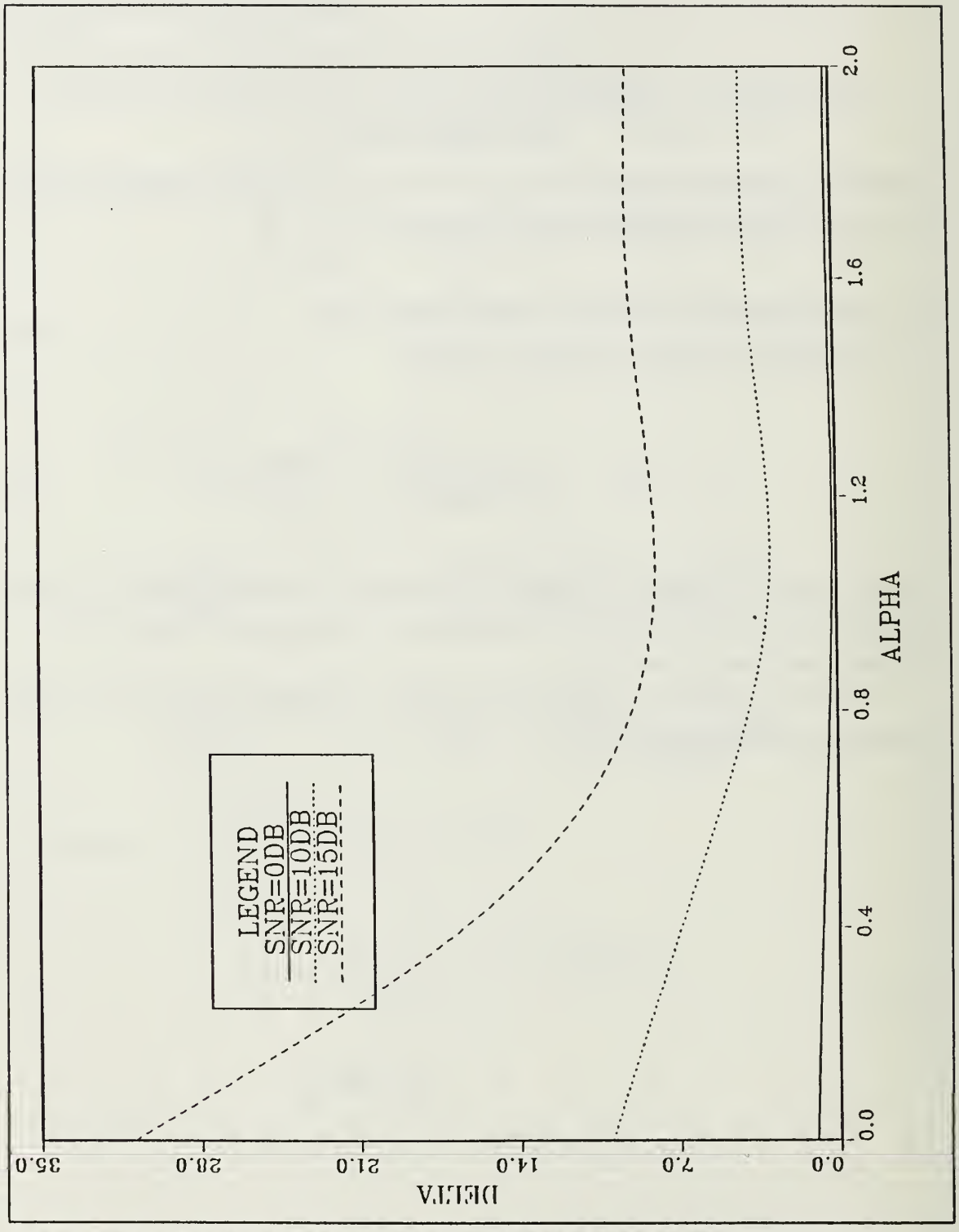

Figure 28. Bandlimited Constant Amplitude PSD, JSR = 0 dB

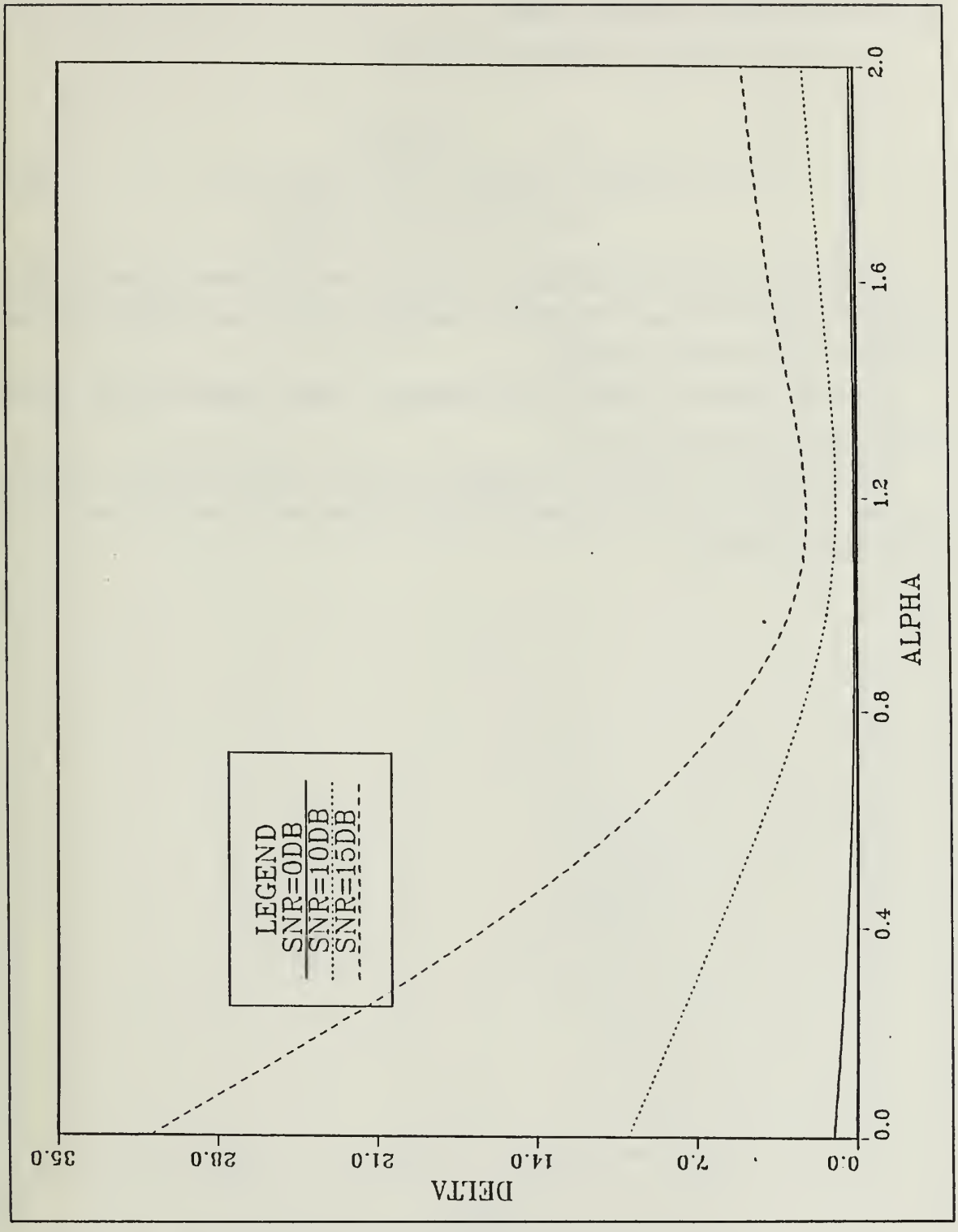

Figure 29. Bandlimited Constant Amplitude PSD, JSR = 10dB

B. BUTTERWORTH SHAPED PSD.

It is shown in Chapter 4, Equation 4.115, that

$$\Delta = SNR \int_{-\infty}^{\infty} \frac{\dfrac{\sin^2(\pi x)}{(\pi x)^2}}{1 + \dfrac{1}{\pi}\, SNR\, JSR\, \dfrac{\beta}{\beta^2 + x^2}}\, dx \qquad (B.2)$$

In Figure 30 on page 99 and Figure 31 on page 100, Δ has been plotted as a function of β for JSR = 0 dB and JSR = 10 dB respectively. SNR values of 0 dB, 10 dB and 15 dB have been chosen in each plot.

From the pictures it is clear that the smaller Δ , which yields the worst receiver performance, corresponds to $\beta = 1$.

The overshooting in Figure 31 on page 100 resulting in slightly negative values for Δ is due to limitations in the computer plotting package used, rather than due to erroneous numerical results.

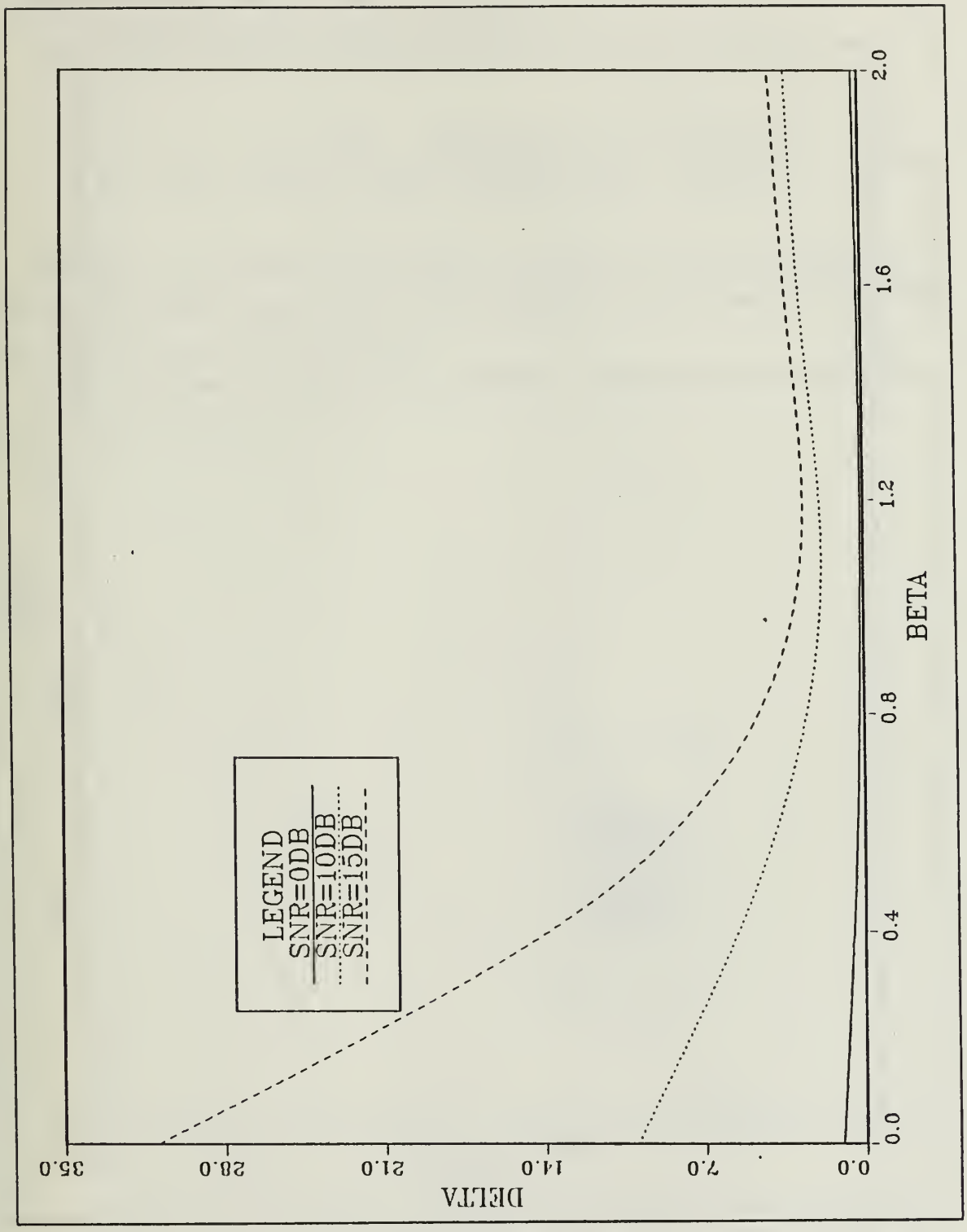

Figure 30. Butterworth Shaped PSD, JSR = 0 dB

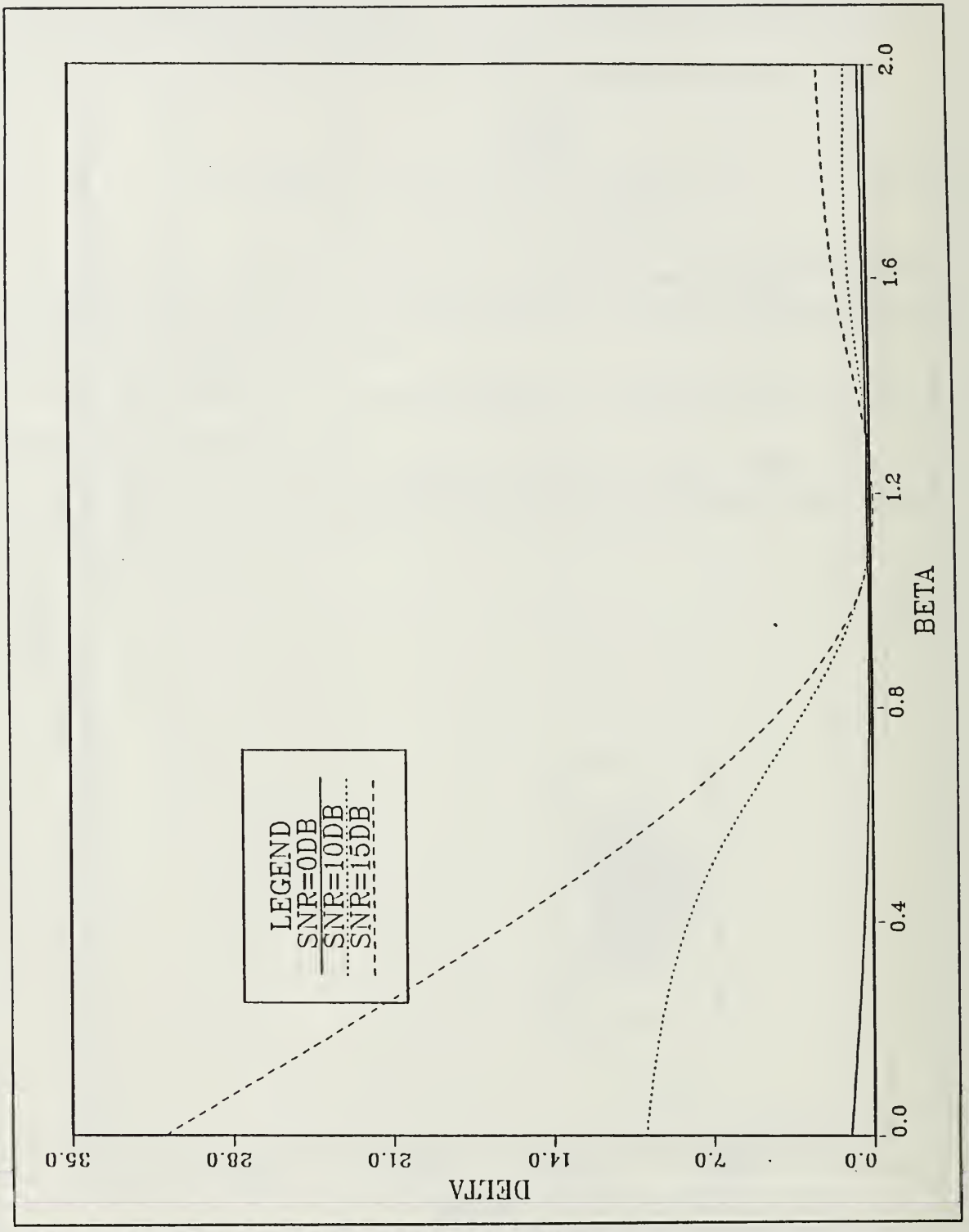

Figure 31. Butterworth Shaped PSD, JSR = 10dB

C. TRIANGULAR SHAPED PSD.

It is shown in Chapter 4, Equation 4.99, that

$$\Delta = SNR + 2SNR \int_0^{\varepsilon} \left[\frac{SNR\, JSR\, (\frac{x}{\varepsilon} - 1)}{2\pi\varepsilon + SNR\, JSR\, (1 - \frac{x}{\varepsilon})} \; \frac{\sin^2(\pi x)}{(\pi x)^2} \right] dx \qquad (B.3)$$

In Figure 32 on page 102 and Figure 33 on page 103, Δ has been plotted as a function of ε for JSR = 0 dB and JSR = 10 dB respectively. SNR values of 0 dB, 10 dB and 15 dB have been chosen in each plot.

From the pictures it is clear that the smaller Δ , which yields the worst receiver performance, corresponds to $\varepsilon = 1$.

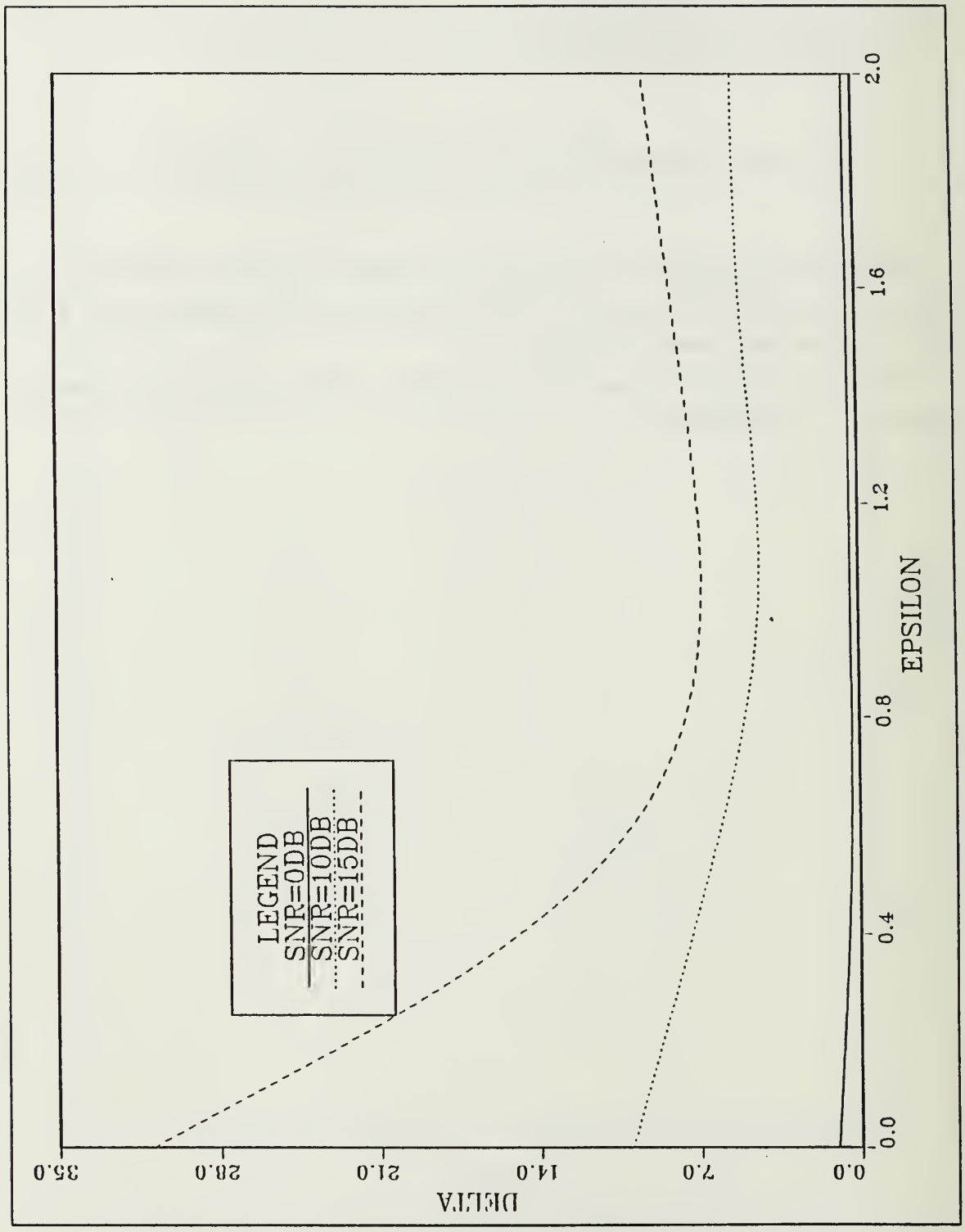

Figure 32. Triangular Shaped PSD, JSR = 0 dB

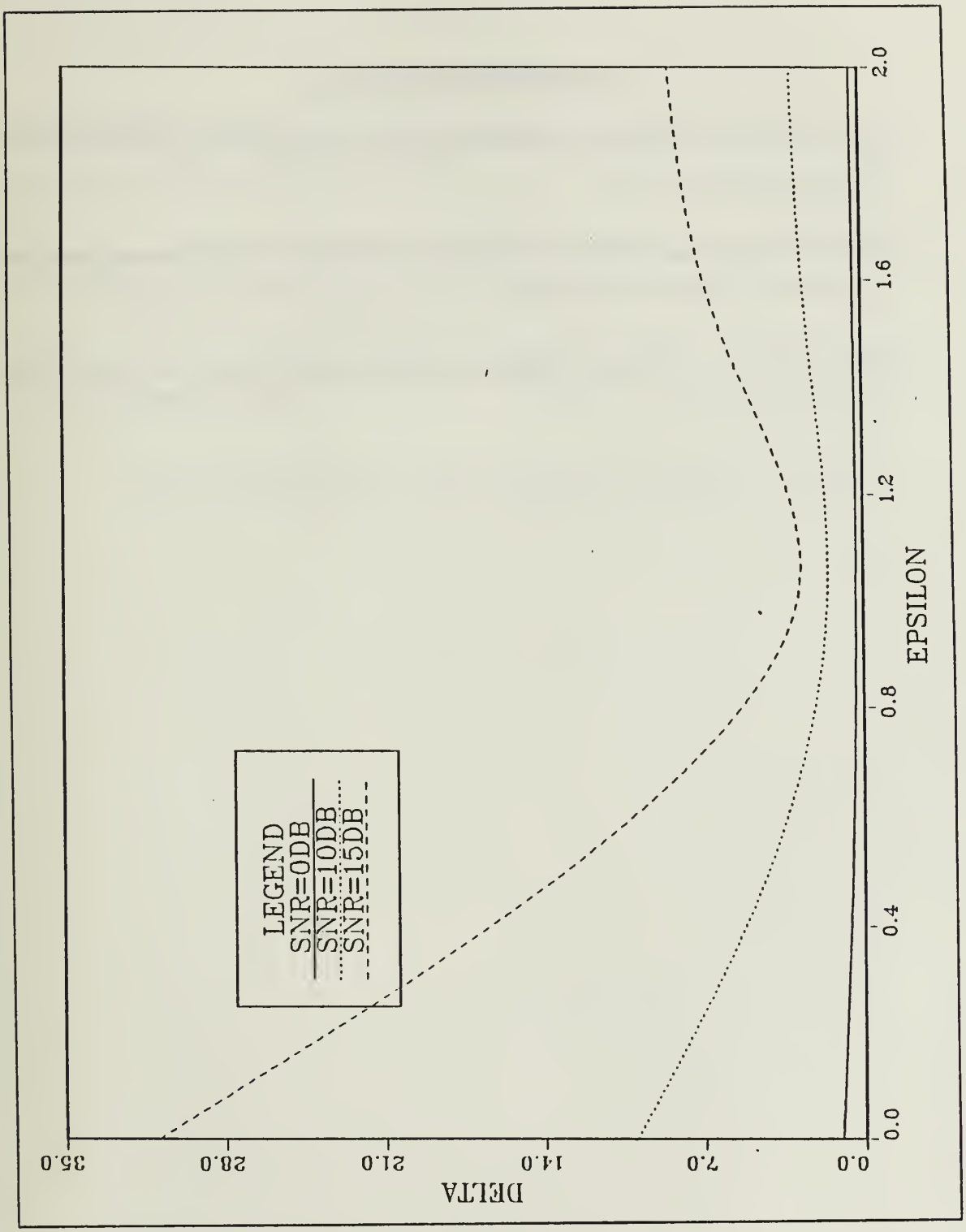

Figure 33. Triangular Shaped PSD, JSR = 10 dB

LIST OF REFERENCES

1. Van Trees, H.L. *Detection, Estimation, and Modulation Theory, Part III*, John Wiley & Sons, Inc., 1968.

2. Bukofzer, D.C., *Solutions to the Radar Signal Return Masking Problem*, paper presented at the Radar-87 Conference, London, England, 19-21 October 87.

3. Van Trees, H.L. *Detection, Estimation,and Modulation Theory, Part I*, John Wiley & Sons, Inc., 1968.

4. Whalen, A.D., *Detection of Signals in Noise*, Academic Press, Inc., 1971.

BIBLIOGRAPHY

Cooper, G.R., McGillem, C.D., *Probabilistic Methods of Signals and System Analysis,* Holt, Rinehart and Winston, 1986.

Papoulis, A., *Probability, Random Variables and Stochastic Process,* McGraw-Hill, Inc., 1984.

Peebles, P.Z. Jr., *Probability, Random Variables and Random Signal Principles,* McGraw-Hill, Inc., 1987.

INITIAL DISTRIBUTION LIST

		No. Copies
1.	Defense Technical Information Center Cameron Station Alexandria, VA 22304-6145	2
2.	Library, Code 0142 Naval Postgraduate School Monterey, CA 93943-5002	2
3.	Chairman, Code 62 Electrical and Computer Engineering Department Naval Postgraduate School Monterey, CA 93943-5000	1
4.	Professor Daniel Bukofzer, Code 62Bh Electrical and Computer Engineering Department Naval Postgraduate School Monterey, CA 93943-5000	5
5.	Professor Ralph Hippenstiel, Code 62Hi Electrical and Computer Engineering Department Naval Postgraduate School Monterey, CA 93943-5000	1
6.	Mavropoulos Panagiotis Ag. Nectariou 30 14122 N.Iraklio GREECE	2
8.	Army General Staff DDB/5 EG STG 1020 Athens, GREECE	1
9.	Electronics and Communicications School STHAD STG 1020 Athens, GREECE	1